EUROPEAN ORGANISATION FOR NUCLEAR RESEARCH (CERN)

Submitted to: EPJC

CERN-EP-2025-252
4th December 2025

Performance and efficiency of a transformer-based quark/gluon jet tagger in the ATLAS experiment

The ATLAS Collaboration

A deep-learning approach based on the transformer architecture is developed to distinguish between jets originating from quarks and gluons. The algorithm operates on jets with transverse momentum $p_{\mathrm{T}} > 20$ and pseudorapidity $|\eta| < 4.5$ and takes as input several properties derived from the jet constituents, using information from the ATLAS detector's tracker and calorimeter. The algorithm's performance is evaluated by analyzing dijet data events from proton–proton collisions at $\sqrt{s} = 13$ and 13.6 TeV during Run 2 and Run 3 of the Large Hadron Collider. Two methods are used to obtain distributions from quark- or gluon-initiated jets in data: a matrix method fully based on Monte Carlo simulation and a new approach named 'jet topics' which has less dependence on the modelling of the physics process under study. The quark and gluon identification efficiencies measured in data for the 50% quark-identification-efficiency working point vary from the simulated ones for quark-initiated (gluon-initiated) jets by factors of 0.88–1.30 (0.61–1.05) with uncertainties of 10%–70% (10%–95%). The uncertainties estimated with the jet topics method are smaller than those estimated with the matrix method, with up to 20% less systematic uncertainty in some phase-space regions. The advances in jet identification reported here provide a robust tool for precision Standard Model measurements and searches for new physics at the LHC.

Contents

1 Introduction

Collisions at the Large Hadron Collider (LHC) [1] produce high-energy quarks and gluons that hadronize into collimated sprays of particles called jets. Theoretical studies have shown it is possible to label jets according to the type of parton that initiated their formation in an infrared- and collinear-safe manner [2, 3]. Moreover, it was observed that jet labelling is independent of the production process under consideration [4]. Once a labelling algorithm is chosen, jets labelled as originating from light quarks (quark jets) and the ones labelled as originating from gluons (gluon jets) can be studied, where gluon jets are seen to have a wider radiation pattern and be made of more particles with a lower average energy than quark jets [5]. These differences can be exploited to build algorithms (q/g taggers) that infer the jet label and distinguish between the two jet types. Given the process-independence of jet labelling, such taggers can be built to perform consistently across different physics analyses. The precise definition of the jet labelling algorithm used in this analysis is given in Section 4.

Distinguishing between quark and gluon jets is crucial for a variety of applications. For instance, many electroweak processes and new-physics scenarios predict signatures with quark jets [6–9], while specific searches benefit from gluon jet identification [10, 11]. Measurements of Higgs boson properties exploit final states with quark jets produced by the vector-boson fusion process, and gluon jets arising from the gluon–gluon fusion process [12, 13]. Furthermore, an accurate q/g tagger can refine jet energy calibrations by using the different calorimeter responses to quark and gluon jets [14].

In the past, ATLAS has employed q/g taggers based on variables associated with jets as a whole (high-level jet variables), such as the number of charged-particle tracks or the jet width [15, 16]. More recent approaches have explored variables sensitive to energy and angular correlations between jet constituents [17] and even a convolutional neural-network approach using full jet images [18]. ATLAS's most recent calibrated q/g tagger was based on a Boosted Decision Tree architecture [19], taking high-level jet variables as input. This paper presents a new q/g tagger, trained using modern deep-learning techniques that directly process variables derived from jet constituents, building upon and extending an approach outlined in Ref. [20]. The presented DeParT model, based on the ParT [21] and Transformer [22] architectures, is applied across the full jet phase space reconstructed by ATLAS, consisting of jets with transverse momentum $p_{\mathrm{T}} > 20$ GeV and pseudorapidity $|\eta| < 4.5$.

The performance of the new q/g tagger is evaluated using data from dijet events produced in proton–proton (pp) collisions at $\sqrt{s} = 13$ TeV and 13.6 TeV during Run 2 and Run 3 of the LHC and recorded by ATLAS. The tagger score distributions for quark and gluon jets are extracted from data using two methods: the jet topics method [23–25], used to obtain the primary result of this paper, and the matrix method [16], used in a previous ATLAS publication [19] and taken as a reference. Both methods exploit forward- and central-jet samples with different q/g fractions to statistically demix them into samples of quark and gluon jets. Jet topics is a novel technique that is expected to rely less on Monte Carlo (MC) simulations and provide a more precise evaluation of the q/g tagger's performance. The quark- and gluon-jet-tagging identification efficiencies are measured in data and compared with MC simulation predictions, at a fixed q/g tagger working point. Scale factors defined as the ratio of the measured identification efficiency to the expected identification efficiency are derived as a function of the jet p_{T} and $|\eta|$.

This paper is organized as follows. The ATLAS detector is described in Section 2. Section 3 introduces the data sets used in the present publication. Details of the reconstruction and identification of physical objects are provided in Section 4. The DeParT model is presented in Section 5. Section 6 describes the extraction of quark and gluon samples from data. The scale factors are defined in Section 7 and Section 8 discusses their associated uncertainties. The tagger's performance is summarized in Section 9, and Section 10 concludes the paper.

2 ATLAS detector

The ATLAS detector [26, 27] at the LHC covers nearly the entire solid angle around the collision point.[1] It consists of an inner tracking detector surrounded by a thin superconducting solenoid, electromagnetic and hadronic calorimeters, and a muon spectrometer incorporating three large superconducting air-core toroidal magnets.

The inner-detector system is immersed in a 2 T axial magnetic field and provides charged-particle tracking in the range $|\eta| < 2.5$. The high-granularity silicon pixel detector covers the interaction region and typically

[1] ATLAS uses a right-handed coordinate system with its origin at the nominal interaction point (IP) in the centre of the detector and the z-axis along the beam pipe. The x-axis points from the IP to the centre of the LHC ring, and the y-axis points upwards. Polar coordinates (r, ϕ) are used in the transverse plane, ϕ being the azimuthal angle around the z-axis. The pseudorapidity is defined in terms of the polar angle θ as $\eta = -\ln\tan(\theta/2)$ and is equal to the rapidity $y = (1/2)[(E + p_z)/(E - p_z)]$ in the relativistic limit. Angular distance is measured in units of $\Delta R \equiv \sqrt{(\Delta y)^2 + (\Delta\phi)^2}$.

provides four measurements per track, the first hit generally being in the insertable B-layer. It is followed by the silicon microstrip detector, which usually provides eight measurements per track. These silicon detectors are complemented by the transition radiation tracker (TRT), which enables radially extended track reconstruction up to $|\eta| = 2.0$. The TRT also provides electron identification information based on the fraction of hits (typically 30 in total) above a higher energy-deposit threshold corresponding to transition radiation.

The calorimeter system covers the pseudorapidity range $|\eta| < 4.9$. Within the region $|\eta| < 3.2$, electromagnetic calorimetry is provided by barrel and endcap high-granularity lead/liquid-argon (LAr) calorimeters, with an additional thin LAr presampler covering $|\eta| < 1.8$ to correct for energy loss in material upstream of the calorimeters. Hadronic calorimetry is provided by the steel/scintillator-tile calorimeter, segmented into three barrel structures within $|\eta| < 1.7$, and two copper/LAr hadronic endcap calorimeters. The solid angle coverage is completed with forward copper/LAr and tungsten/LAr calorimeter modules optimized for electromagnetic and hadronic energy measurements, respectively.

The muon spectrometer comprises separate trigger and high-precision tracking chambers measuring the deflection of muons in a magnetic field generated by the superconducting air-core toroidal magnets. The field integral of the toroids ranges between 2.0 and 6.0 T m across most of the detector. Three layers of precision chambers, each consisting of layers of monitored drift tubes, cover the region $|\eta| < 2.7$. These were complemented in the innermost layer of the endcap region by cathode-strip chambers in Run 2, which were replaced in Run 3 by layers of small-strip thin-gap chambers and Micromegas chambers, both providing precision tracking in the region $1.3 < |\eta| < 2.7$. The muon trigger system covers the range $|\eta| < 2.4$ with resistive-plate chambers in the barrel region, thin-gap chambers in the endcap regions, and, in Run 3, the aforementioned small-strip thin-gap chambers and Micromegas chambers in the innermost layer of the endcap.

The luminosity is measured mainly by the LUCID-2 detector, which records Cherenkov light produced in the quartz windows of photomultipliers located close to the beampipe.

Events are selected by the first-level trigger system implemented in custom hardware, followed by selections made by algorithms implemented in software in the high-level trigger [28]. The first-level trigger accepts events from the 40 MHz bunch crossings at a rate close to 100 kHz, which the high-level trigger reduces in order to record complete events to disk at an average rate of about 1.25 kHz and 3 kHz in Run 2 and Run 3, respectively.

Compared with its Run-2 configuration, the ATLAS detector benefits from several upgrades to maintain high performance at the higher pile-up levels in Run 3. The improvements include the new innermost layer of the muon spectrometer in the endcap region, which provides higher redundancy and a large reduction in fake muon triggers. The trigger system also benefits from new LAr calorimeter digital electronics with significantly increased granularity. These and other upgrades are described in more detail in Ref. [27].

A software suite [29] is used in data simulation, in the reconstruction and analysis of real and simulated data, in detector operations, and in the trigger and data acquisition systems of the experiment.

3 Data and simulation samples

This study uses data collected from proton–proton (pp) collisions by the ATLAS experiment during LHC Run 2 in 2015–2018 at $\sqrt{s} = 13$ TeV and LHC Run 3 in 2024 at $\sqrt{s} = 13.6$ TeV. After imposing data quality requirements to ensure that the ATLAS detector was operating properly [30], the integrated luminosities of the Run-2 and Run-3 data samples are 140.1 ± 1.2 fb^{-1} [31] and 109.4 ± 2.2 fb^{-1} [32], respectively.

Monte Carlo simulations are used to model SM multijet production. The generated events were passed through a Geant4 [33] simulation of the ATLAS detector and its response [34]. The effect of multiple interactions in the same and neighbouring bunch crossings (pile-up) was modelled by overlaying [35] each simulated hard-scattering event with a mix of inelastic pp scattering events generated by either Epos 2.0.1.4 [36] or Pythia 8.308 [37]. The Epos event generator used a set of tuned parameters called the Epos LHC tune [38], while Pythia used the A3 tune [39] and the NNPDF2.3lo [40] set of parton distribution functions (PDF). Separate MC samples are used to model the different pile-up distributions observed in the 2015–2016, 2017, 2018 and 2024 data, and the simulated events are reweighted to reproduce the observed distribution of the average number of collisions per bunch crossing in each data-taking period. All simulated events are reconstructed with the same software as the data and corrected so that the trigger, object reconstruction and object identification efficiencies, and the energy scales and resolutions, match the data.

Pythia 8.235 [41] was used to produce the nominal simulation sample (referred to as the Pythia sample), which is based on dijet production matrix elements (ME) with leading-order (LO) QCD accuracy matched to a parton shower (PS) with leading-logarithm accuracy. In the nominal settings, the renormalization and factorization scales are set to the geometric mean of the squared transverse masses of the two outgoing particles in the matrix element. The NNPDF2.3lo PDF set was used in the ME generation, the parton shower, and the simulation of multiparton interactions. The parton shower and multiparton interaction modelling uses parameter values from the A14 tune [42], and the fragmentation and hadronization is based on the Lund string model [43, 44]. To populate the inclusive jet p_{T} spectrum efficiently, biased phase-space sampling was used in producing the Pythia sample; to compensate for this, the weighting of the simulated events was modified.

Alternative simulations that vary the modelling of dijet events are used to evaluate systematic uncertainties in the q/g tagger's performance. Uncertainties in perturbative calculations in the nominal simulation are propagated by using alternative weights for events in the Pythia sample. The alternative weights cover variations of the scales at which the strong coupling constant is evaluated in the initial- and final-state showers, changes in the PDF choice, and variations in the non-singular part of the splitting functions [45].

The impact of next-to-leading-order (NLO) corrections in the ME is evaluated by using Powheg Box v2 [46, 47] to calculate the dijet production ME [48], which is then interfaced with Pythia 8.245. This sample is referred to as Powheg+Pythia. The NNPDF3.0nlo [49] PDF set was used in the ME calculation, while the NNPDF2.3lo set and the A14 tune were used to model the parton showers and multiparton interactions.

To evaluate uncertainties stemming from the choice of hadronization modelling, multijet events were produced with Sherpa 2.2.5 [50] (referred to as Sherpa samples). These samples use the CT14nnlo PDF set [51] and employ $2 \rightarrow 2$ matrix elements at LO QCD accuracy in a showering algorithm based on Catani–Seymour dipole factorization with p_{T} ordering [52]. One sample was produced with the Sherpa AHADIC model for hadronization [53] based on cluster fragmentation ideas and is referred to as the Sherpa Cluster sample, while another (referred to as the Sherpa String sample) was generated using the Lund string fragmentation model, which is also implemented in Pythia 6 [54].

Multiple sets of multijet events were generated with Herwig [55–57] in order to assess how varying the PS algorithm changes the result. For the 13 TeV simulation, events were produced with an angle-ordered shower evolution [58], the NNPDF2.3lo PDF set, and the Lund string fragmentation model of Pythia 6 [54], where the Lund string implementation is used without tuning and does not include colour-reconnection effects (this sample is referred to as the Herwig String sample). The 13.6 TeV simulation instead uses the NNPDF3.0NLO PDF set and the cluster-based hadronization model with two shower configurations: one using the angle-ordered evolution (referred to as the Herwig Angular sample) and the other using the dipole algorithm [59] (referred to as the Herwig Dipole sample).

The nominal and alternative MC samples are summarized in Table 1.

Table 1: Nominal (first row) and alternative MC dijet samples with their configurations. The table shows PDF sets, generator versions, QCD accuracy (Order), parton shower algorithms (PS alg.), hadronization models (Had.), and centre-of-mass energies used in a given sample.

Name	PDF set	Generator	Order	PS alg.	Had.	$\sqrt{s}$ [TeV]
Pythia	NNPDF2.3LO	PYTHIA 8.235	LO	p_{T}-ord.	String	13 / 13.6
Powheg+Pythia	NNPDF3.0NLO	POWHEG+PYTHIA 8	NLO	p_{T}-ord.	String	13 / 13.6
Sherpa Cluster	CT14NNLO	SHERPA 2.2.5	LO	p_{T}-ord.	Cluster	13 / 13.6
Sherpa String	CT14NNLO	SHERPA 2.2.5	LO	p_{T}-ord.	String	13 / 13.6
Herwig String	NNPDF2.3LO	HERWIG 7	LO	Angle-ord.	String	13
Herwig Angular	NNPDF3.0NLO	HERWIG 7	LO	Angle-ord.	Cluster	13.6
Herwig Dipole	NNPDF3.0NLO	HERWIG 7	LO	Dipole	Cluster	13.6

4 Object reconstruction and event selection

Jets are reconstructed from particle-flow objects (PFOs) [60] by the anti-k_t algorithm [61] with a radius parameter of $R = 0.4$ as implemented in FastJet [62]. The PFOs are a collection of reconstructed objects formed by the particle-flow algorithm [60], which systematically combines charged-particle tracks and calorimeter objects called topological clusters (topoclusters) [63]. Specifically, PFO momenta are obtained by replacing the energy deposited by charged particles in a region of the calorimeter with the momenta of tracks that are matched to that specific calorimeter region. When some energy remains in the calorimeter region or when no matching track is found, neutral PFOs are created from the corresponding topoclusters. An overall jet-energy calibration [64] accounts for residual detector effects as well as contributions from pile-up.

In addition to PFOs, TopoTowers are employed as auxiliary jet variables. Calorimeter towers [65] are static grid elements with a size of $\Delta\eta \times \Delta\phi = 0.1 \times 0.1$, constructed from calorimeter cells. TopoTowers are calorimeter towers for which the only contributing cells are those associated with an energy cluster. While PFOs are used throughout the jet reconstruction and calibration chain, TopoTowers are ghost-associated [66] to jets and serve as supplementary input to the q/g tagger, providing higher-granularity calorimeter information in the forward region where tracking detector coverage is limited or absent. For jets fully outside the tracking acceptance ($|\eta| > 2.9$), there are on average 21 TopoTowers per PFO. TopoTowers are included only for $|\eta| > 2.0$ and are particularly impactful for $|\eta| > 3.4$. In this region, significant ambient energy is present and the forward calorimeter geometry is not aligned with an $\eta \times \phi$ representation; TopoTowers can therefore split individual topoclusters covering a large part of the sub-detector.

In each event of the MC simulation, a second set of $R = 0.4$ jets (called 'truth' jets) is built with the anti-k_t algorithm directly from the generated stable final-state particles[2] (excluding muons, neutrinos, and

[2] Particles are considered stable if their decay length is greater than 1 cm.

particles from pile-up interactions) before they interact with the detector. Information about the parton that initiated the jet is retrieved [15] from the parton shower record by identifying the highest-energy parton ghost-associated [66] with the truth jet. Truth jets are geometrically matched to the reconstructed ones by requiring their angular separation to be $\Delta R < 0.3$. No additional discriminating variables are used to differentiate heavy-flavour quark jets from light-flavour quark jets [67, 68]. When either a b-quark or c-quark is the highest-energy parton, the jet receives a quark jet label. Heavy-flavour jets comprise less than 2% of the total dataset across all considered p_{T} bins. Reconstructed jets remain unlabelled if no truth parton with $p_{\mathrm{T}} > 1$ GeV is found among the partons ghost-associated with the truth jet, or if they arise from pile-up. Unlabelled jets comprise less than 1% of the dataset considered, and they are thus ignored [69].

Events used in the analysis were selected with a set of single-jet triggers [28, 70]. The trigger strategy employs two complementary categories: central-jet triggers with detector pseudorapidity acceptance $|\eta| < 3.2$ and forward-jet triggers with $|\eta| > 3.2$. The central-jet triggers utilize p_{T} thresholds ranging from 35 GeV to 525 GeV, while the forward-jet triggers employ thresholds from 35 GeV to 350 GeV. Additionally, a single-jet trigger with no p_{T} threshold is included within the whole $|\eta|$ detector acceptance to allow jet p_{T} coverage down to 20 GeV in both the central and forward regions. Single-jet triggers with low p_{T} thresholds are prescaled to reduce the high trigger rates and record only a fraction of the events for online processing and data storage at an acceptable level. Only the highest-p_{T}-threshold triggers (both central and forward) are unprescaled, so as to record each observed event containing high-p_{T} jets. A leading-jet trigger strategy [71] is employed, where the trigger is accepted only if the leading (i.e. highest-p_{T}) jet fell within a predefined p_{T} range, achieving a trigger efficiency of at least 99.5%. The p_{T} thresholds differ between central- and forward-jet triggers, so the leading jet is classified according to its $|\eta|$ to determine the appropriate p_{T} range for trigger selection. To obtain a smooth p_{T} spectrum at reconstruction level, events are weighted according to the trigger prescale factors.

The offline selection requires events to contain at least two jets with 20 GeV $< p_{\mathrm{T}} <$ 2 TeV and $|\eta| < 4.5$, ensuring complete containment within the calorimeter acceptance. The jet vertex tagger (JVT) [72] is used to remove pile-up jets with $p_{\mathrm{T}} < 60$ GeV and $|\eta| < 2.5$ that are identified as not associated with the event's primary vertex. Similarly, pile-up jets in the forward region are suppressed with a 'forward JVT' (fJVT) [73] algorithm, which exploits jet shapes and topological jet correlations in pile-up interactions and is applied to all jets with $p_{\mathrm{T}} < 60$ GeV and $|\eta| > 2.5$. Simulated events are corrected for differences between data and MC simulation seen in JVT and fJVT efficiencies [72, 73]. The two highest-p_{T} jets (j_1 and j_2) must have azimuthal separation $\Delta\phi(j_1, j_2) > 2.8$ and if a third jet exists in the event its p_{T} is required to be smaller than 0.05 times the sum of the p_{T} values of j_1 and j_2, to better select events with a dijet topology. The performance of the q/g tagger is evaluated in bins of jet p_{T} and η, with at least one jet required to satisfy the conditions on p_{T} and η to belong to a certain bin.

5 Tagger definition

The q/g tagger considered in this paper is based on the DeParT model [20, 21]. The tagger is trained on the two highest-p_{T} jets in events generated in the nominal Pythia simulation with Run-2 conditions. It is preferred that the tagger is not reliant on the p_{T} and η of the jet for the q/g classification, allowing physics analyses to use either the full jet spectrum or a subset of it. Due to the limited size of the simulated event samples, the dijet events do not cover the entire phase space spanning 20–2000 GeV in p_{T} and $|\eta| < 4.5$. To overcome this problem, an ensemble of three subsamples covering different p_{T} and η ranges is used for training, and each subsample is reweighted to produce a uniform two-dimensional distribution in $p_{\mathrm{T}} \times \eta$

space. This ensures a flat distribution of jet p_{T} and η in the two dimensions, and the flattening procedure for each subsample is performed separately for quark and gluon jets to avoid a tagger bias towards one of the jet types. Each subsample is normalized such that the sum of weights is equal to the number of events in that subsample, and the total number of jets in the training ensemble is 102 M. The number of jets in each subsample is shown along with the corresponding p_{T} and $|\eta|$ ranges in Table 2. A statistically independent validation sample containing 10.2 M jets is constructed in the same way as the training sample and is used for model evaluation during training. Overfitting is prevented by evaluating the loss on this sample after each training epoch. The validation loss is monitored throughout training and does not diverge from the trend observed for the training loss, confirming the absence of overfitting.

Table 2: The p_{T} and η ranges of the three subsamples used to train the tagger and their relative and absolute sizes.

Index	p_{T} range	η range	Total size	Relative size
1.	$20 < p_{\mathrm{T}} < 160$ GeV	$\lvert\eta\rvert < 4.5$	50 M	49%
2.	$160 < p_{\mathrm{T}} < 1300$ GeV	$\lvert\eta\rvert < 2.1$	50 M	49%
3.	$1300 < p_{\mathrm{T}} < 2000$ GeV	$\lvert\eta\rvert < 1.2$	2.1 M	2%

The DeParT network takes as input several variables constructed from the jet constituents, namely the PFOs and TopoTowers. Such variables can be separated into constituent variables, where the individual constituent momenta are taken separately, and constituent interaction variables, where pairs of constituent momenta are considered.

Table 3: Constituent variables used as input to DeParT.

Constituent Variables
$\log(p_{\mathrm{T}}/p_{\mathrm{T}}^{\mathrm{jet}})$
$\log(E/p_{\mathrm{T}}^{\mathrm{jet}})$
$\Delta\eta = \eta - \eta^{\mathrm{jet}}$
$\Delta\phi = \phi - \phi^{\mathrm{jet}}$
$\Delta R = \sqrt{(\Delta\eta)^2 + (\Delta\phi)^2}$
isCharged
isTopo

Constituent variables include the logarithms of the ratios of the constituent's p_{T} or energy E to the jet's p_{T}; the pseudorapidity difference $\Delta\eta$ between the constituent and the jet axis; the azimuthal angle $\Delta\phi$ between the constituent and the jet axis; and the angular separation ΔR between the constituent and the jet axis. The logarithms of the constituent's p_{T} and energy are not included, unlike in Refs. [20, 21], since it was found that they do not improve the tagger's performance. A binary variable called 'isCharged' is used to distinguish between charged and neutral constituents: its value is one for PFOs with an associated track and zero for neutral PFOs and TopoTowers. An overlap between PFOs and TopoTowers is resolved by using the 'isTopo' constituent variable, which allows the model to learn the relationship between PFOs and TopoTowers through the attention mechanism during training. The value of 'isTopo' is zero for PFOs and one for TopoTowers. The complete list of constituent variables is shown in Table 3.

The constituent interaction variables are calculated for each pair (a, b) of constituents in a given jet. The variable Δ^{ab} represents the angular separation between two jet constituents. The invariant mass of the two constituents, $m^{2,ab}$, is calculated from their four-momenta and scaled by the total jet p_{T}. The k_{T}^{ab}

Table 4: List of constituent interaction variables used as input to DeParT. Indices a and b indicate the two constituents for which the interaction variables are calculated.

Constituent Interaction Variables
$\log \Delta^{ab} = \log \sqrt{(\eta^a - \eta^b)^2 + (\phi^a - \phi^b)^2}$
$\log m^{2,ab} = \log \left[(p^a + p^b)^2 / (p_\mathrm{T}^\mathrm{jet})^2 \right]$
$\log k_\mathrm{T}^{ab} = \log \left[\min(p_\mathrm{T}^a / p_\mathrm{T}^\mathrm{jet}, p_\mathrm{T}^b / p_\mathrm{T}^\mathrm{jet}) \Delta^{ab} \right]$
$z^{ab} = \min(p_\mathrm{T}^a, p_\mathrm{T}^b) / (p_\mathrm{T}^a + p_\mathrm{T}^b)$

variable characterizes the transverse momentum scale of the splitting, defined as the product of the softer constituent's momentum fraction and the angular separation Δ^{ab} between the two constituents. Unlike in Refs. [20, 21], the constituents' p_T fractions rather than their absolute p_T are used in the k_T^{ab} variable; this reduces the overall p_T dependence of the tagger. The last variable, z^{ab}, quantifies the momentum sharing between constituents, representing the fraction of their combined transverse momentum carried by the softer constituent. The complete list of constituent interaction variables is shown in Table 4.

Before being fed into the tagger, the distributions of all the variables were normalized to have a mean of zero and a standard deviation of one, ensuring that features at different natural scales contribute equally during training.

Due to GPU memory constraints and high memory usage by the transformers, only the 60 highest-p_T constituents of each jet are considered. This constraint affects only about 5.7% of the jets in a testing dataset with the physical p_T and η spectrum and 8.6% in the training dataset,[3] and it was found not to have any impact on the tagger's performance.

The DeParT model is trained for 10 epochs with a batch size of 1024. This number of epochs proved sufficient given the large size (102 M jets) of the dataset, with the model typically reaching minimum validation loss before completing all epochs. Training for additional epochs did not improve performance on the validation dataset. The Adam optimizer [74] is employed with a learning rate increasing linearly from zero to 10^{-4} for the first 20 k training steps, followed by cosine decay to 1% of the maximum learning rate over the subsequent 10 epochs. The architectural hyperparameters of the DeParT model are the same as those used in Ref. [20], and the total number of trainable parameters is 2.6 million. The training dataset size of 102 M jets provides sufficient statistical power to effectively constrain the 2.6 million model parameters and avoid overfitting.

The tagger's performance evaluated on the nominal Pythia sample with the physical p_T and η spectrum is shown in Figure 1. The efficiency of the quark (gluon) jet tagging, denoted by ε_q (ε_g), is the ratio of the number of correctly (incorrectly) classified quark (gluon) jets to the total number of quark (gluon) jets in the used sample. The symbol ε_g^{-1}, the inverse of ε_g, stands for the rejection of gluon jets. The metric used for comparison is ε_g^{-1} at a fixed ε_q value of 0.5, i.e. the 50% working point (WP), as a function of p_T for two $|\eta|$ bins. The score threshold defining the 50% WP is determined from the Pythia sample in each p_T and $|\eta|$ bin separately. The performance of the DeParT model is compared with that of a fully connected (FC) neural network with residual connections [75], which takes as input the jet variables defined in Ref. [20]. The FC network serves as a baseline because of its competitive performance among

[3] The difference between these fractions in the two datasets is attributed to the reweighting procedure applied to the training dataset.

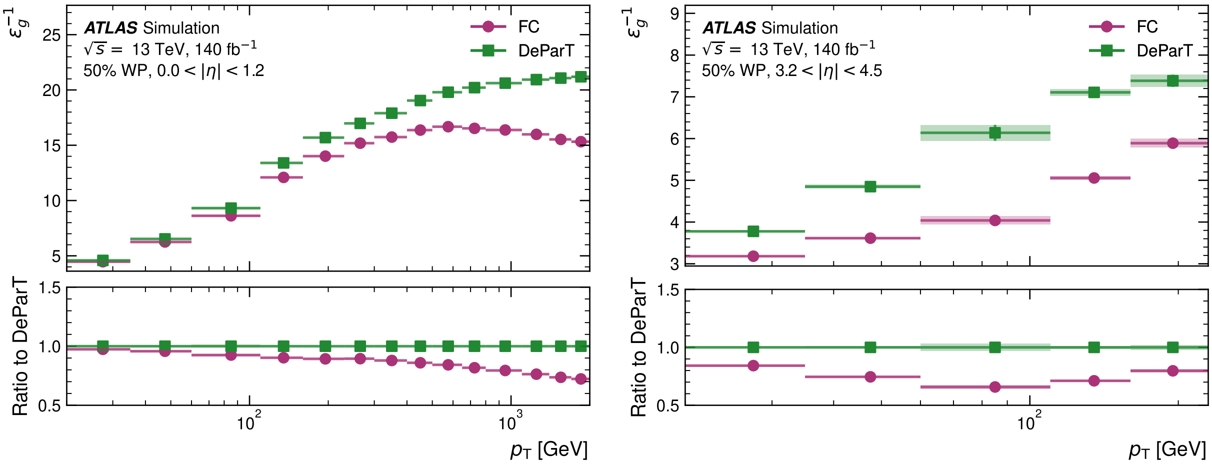

(a) (b)

Figure 1: The gluon jet rejection at 50% quark jet efficiency as a function of p_{T} for jets with (a) $|\eta| = 0.0$–1.2 and (b) $|\eta| = 3.2$–4.5 for the FC and DeParT models. The bottom panels show the FC-to-DeParT ratios. The error bars represent the statistical uncertainties.

previously developed taggers. The classification performance is seen to improve with increasing p_{T} for both models. This is expected because at higher jet p_{T} more jet constituents are available for feature extraction. DeParT performs better than the FC model in most p_{T} bins and $|\eta|$ regions. In the central region, shown in Figure 1(a), the additional complexity of the DeParT model is seen to gradually outperform the FC network with increasing jet p_{T}, taking advantage of the kinematic regime where the jets contain more constituents. The performance difference becomes more pronounced at higher p_{T} values in the central region. The TopoTowers incorporated in the DeParT architecture provide advantages in the forward region, with ε_g^{-1} exceeding the FC baseline value even at low p_{T}, as shown in Figure 1(b).

The DeParT score distributions for the jets selected from the Pythia sample and the measured data are presented in Figure 2, for different jet kinematic ranges. The pronounced peaks observed around 0.95 (0.15) for MC quark (gluon) jets in Figures 2(a) and 2(c) demonstrate the discrimination power of the tagger. The tagger scores for quark and gluon jets do not peak at the extreme values of 0 and 1, respectively, due to two contributing factors: the application of physical weights, in contrast to the flattening weights employed during the training phase, and the kinematic selection of jets within a specific p_{T} and $|\eta|$ range. The peak in tagger score closer to 0 is seen to be significantly smaller in data than in MC simulation, reaching only 60% of the peak height in the simulation. In the forward pseudorapidity region (Figures 2(b) and 2(d)), the distribution is dominated by a large peak near unity corresponding to quark jets. In contrast to the central region, the gluon jet component does not exhibit a prominent peak at low scores but instead shows a more uniform distribution across the tagger output range. Nevertheless, the separation between the quark and gluon score distributions remains sufficient to enable discrimination in this forward kinematic regime. Agreement between experimental data and MC simulation is much better in the forward region than in the central detector region. The observed differences between Run-2 and Run-3 datasets are not considered significant, with variations in Run-3 data attributable to lower statistical precision rather than systematic effects. The larger statistical uncertainties in the Run-3 data are due to the dataset being smaller than in Run 2 and the use of different trigger prescale factors.

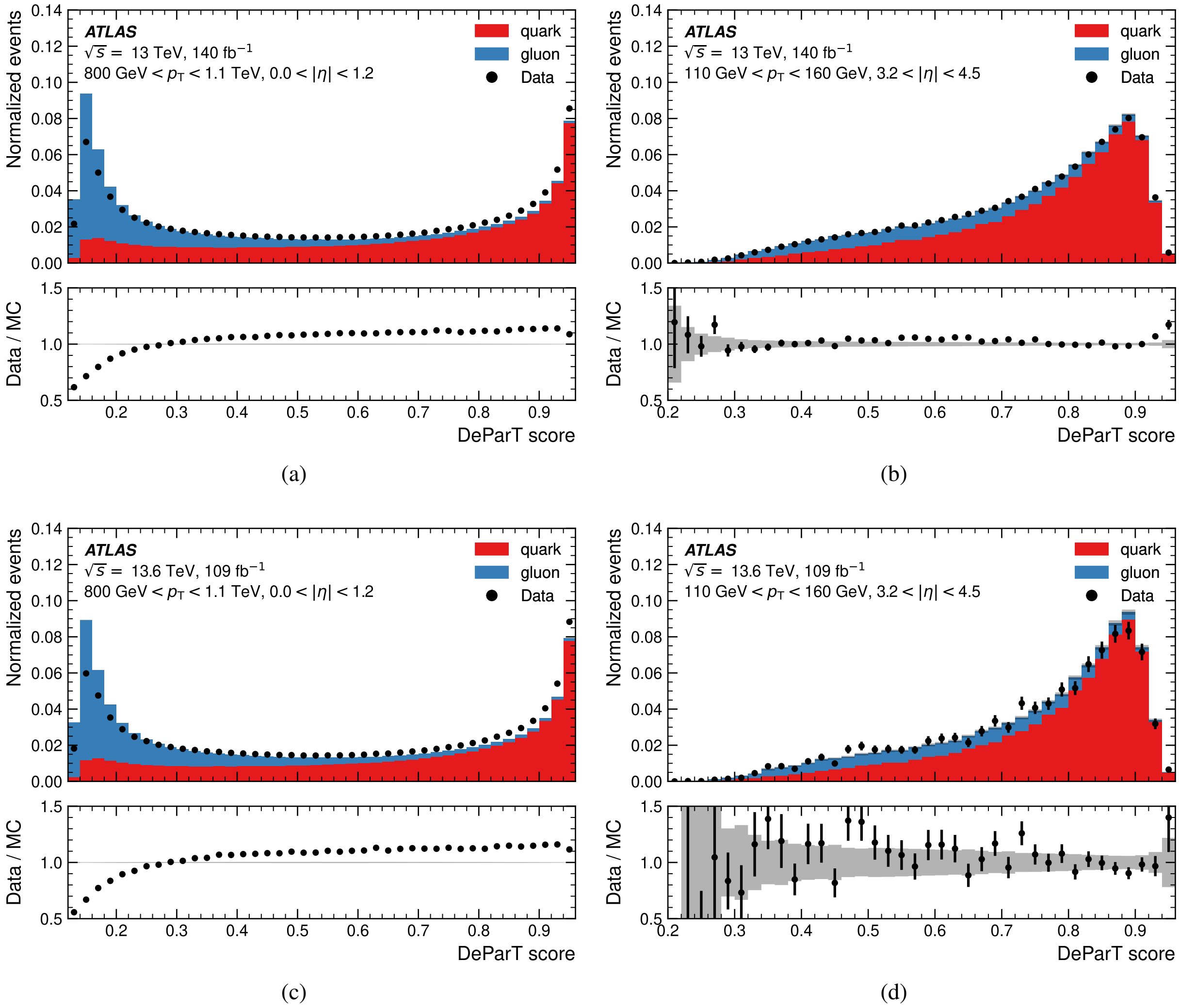

Figure 2: The DeParT score distributions for quark and gluon jets in MC events compared with (a) Run-2 and (c) Run-3 jets with $0.0 < |\eta| < 1.2$ and $800 < p_T < 1100$ GeV, and (b) Run-2 and (d) Run-3 jets with $3.2 < |\eta| < 4.5$ and $110 < p_T < 160$ GeV. The error bars represent the statistical uncertainties of data and the shaded bands represent the statistical uncertainties of MC events. The bottom panels show the data-to-MC ratios.

6 Extraction of quark and gluon distributions in data

Quark-only and gluon-only jet samples are necessary to measure the performance of a q/g tagger. In the context of the definition in Section 4, this can be accomplished in the MC simulation by using the underlying truth information associated with the jet, while for data this is of course not possible. Two extraction methods are used to obtain quark and gluon tagger score distributions in data. Both methods exploit the different q/g fractions in two samples, either quark- or gluon-enriched, and demix them into quark and gluon distributions.

Quark- and gluon-enriched samples are defined from the two highest-p_T jets in each event: the jet with the higher $|\eta|$ value is selected to populate the quark-enriched sample and the one with lower $|\eta|$ is assigned to a gluon-enriched sample. This classification strategy leverages the fact that in the high proton-momentum-fraction range, the PDF has a higher probability of including valence quarks. Consequently, the ensemble of jets which are more forward (higher $|\eta|$) have a higher probability of being quark jets, whereas the ensemble of jets which are more central (lower $|\eta|$) have a higher probability of being gluon jets [76]. The fraction of dijet events where the two highest-p_T jets consist of one quark jet and one gluon jet ranges approximately from 36% to 68% depending on the jet p_T and η. The quark-enriched (gluon-enriched) sample is referred to as the forward (central) sample in the following.

Jet fragmentation is expected to be η-independent at the particle level. Consequently, the distributions of the tagger score x for quark jets, $p_q(x)$, and gluon jets, $p_g(x)$, are assumed identical in the central and forward samples. This allows the central distribution $p_C(x)$ and the forward distribution $p_F(x)$ as

$$p_C(x) = f_C^q p_q(x) + (1 - f_C^q) p_g(x) , \tag{1}$$

$$p_F(x) = f_F^q p_q(x) + (1 - f_F^q) p_g(x) , \tag{2}$$

where f_C^q and f_F^q are the fractions of quark jets in the central and forward samples, respectively.

6.1 Central-to-forward sample reweighting

As mentioned in the previous section, the score distributions are expected to be identical at particle level, but detector-level measurements can depend on η because of changes in the type of detector technology or the amount of detector material traversed. These detector effects cause the $p_q(x)$ and $p_g(x)$ distributions to each have different shapes in the central and forward samples, resulting in non-closure of the extraction methods described below. To ensure that the shapes of the $p_q(x)$ and $p_g(x)$ distributions are independent of whether they are evaluated in the central or forward sample, a reweighting procedure is applied in bins of jet p_T and η as described in Ref. [19]. Various possibilities exist for implementing this reweighting: the central distributions can be adjusted to match the forward ones or vice versa, and the weights can be derived from either the quark or gluon distributions. As a nominal choice, weights are derived from MC simulations to match the central quark distribution to the forward quark distribution, with these MC-derived weights subsequently applied identically to both data and MC central distributions. The alternative reweightings are used to estimate the uncertainties associated with this choice. The values of the resulting weights range approximately from 0.5 to 2.7 for well-populated bins of the score distributions with a statistical uncertainty below 20%. The reweighting procedure is performed before applying either of the two demixing methods described below.

6.2 Matrix method

The first method used to extract quark and gluon distributions from data is the matrix method [16, 19], which assumes the fractions f_C^q and f_F^q from Pythia MC simulation and allows one to solve the system of Eqs. (1) and (2) for $p_q(x)$ and $p_g(x)$ in every p_T and η bin separately. The fractions f_C^q and f_F^q obtained from the nominal Pythia simulation are shown in Figure 3 for two $|\eta|$ regions. It is clear that this demixing method relies heavily on the assumed MC simulation and is therefore prone to systematic uncertainties.

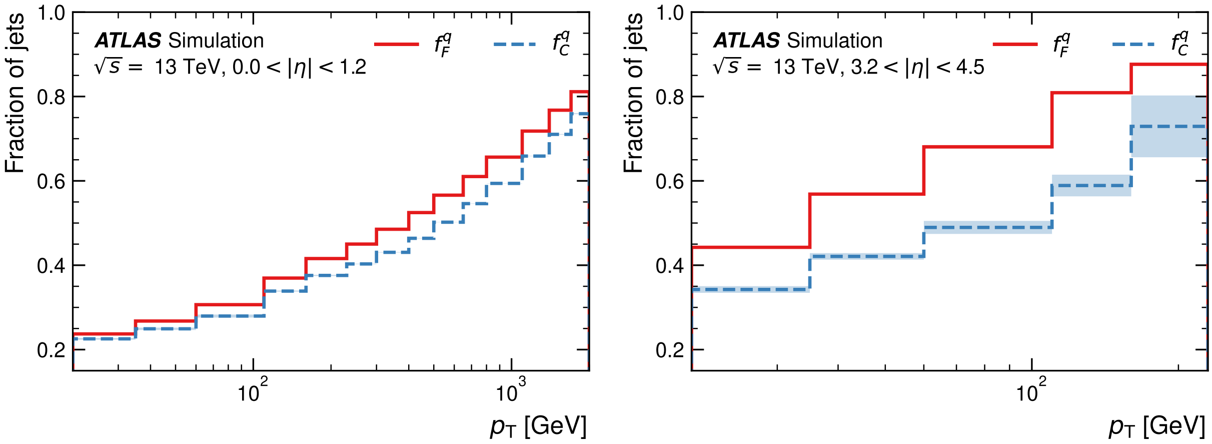

Figure 3: Fractions of quark jets in the forward (f_{F}^{q}) and central (f_{C}^{q}) samples as estimated from Pythia MC simulation for jets with (a) $0.0 < |\eta| < 1.2$ and (b) $3.2 < |\eta| < 4.5$. The error bands represent the statistical uncertainties.

6.3 Jet topics method

The second method is the jet topics method [23], which removes the reliance on MC simulations by computing quark and gluon distributions by maximally subtracting the gluon-enriched central distribution from the quark-enriched forward distribution, and vice versa, as

$$p_q(x) = \frac{p_{\mathrm{F}}(x) - \kappa(\mathrm{F}|\mathrm{C})p_{\mathrm{C}}(x)}{1 - \kappa(\mathrm{F}|\mathrm{C})}\,, \tag{3}$$

$$p_g(x) = \frac{p_{\mathrm{C}}(x) - \kappa(\mathrm{C}|\mathrm{F})p_{\mathrm{F}}(x)}{1 - \kappa(\mathrm{C}|\mathrm{F})}\,. \tag{4}$$

The so-called reducibility factors $\kappa(\mathrm{F}|\mathrm{C})$ and $\kappa(\mathrm{C}|\mathrm{F})$ are given by

$$\kappa(\mathrm{F}|\mathrm{C}) = \min_x \frac{p_{\mathrm{F}}(x)}{p_{\mathrm{C}}(x)}\,, \tag{5}$$

$$\kappa(\mathrm{C}|\mathrm{F}) = \min_x \frac{p_{\mathrm{C}}(x)}{p_{\mathrm{F}}(x)}\,. \tag{6}$$

To minimize the statistical uncertainty in calculating the factors, the $p_{\mathrm{F}}(x)$ and $p_{\mathrm{C}}(x)$ distributions are rebinned from an initial uniform binning scheme of 200 bins into a variable-width binning configuration of 20 bins, where the bin boundaries are optimized such that the summed distribution $p_{\mathrm{F}}(x) + p_{\mathrm{C}}(x)$ exhibits an approximately uniform population across all bins [24].

The version of the jet topics method summarized in Eqs. (3) to (6) requires the quark tagger score distributions to not be a mixture of the gluon ones and some other distributions and vice versa, an assumption referred to as 'mutual irreducibility'. This condition is not fully satisfied in this analysis and hence a correction is needed. In this modified version, the maximal subtraction yields a gluon-subtracted quark distribution $p_{q|g}(x)$ and a quark-subtracted gluon distribution $p_{g|q}(x)$ instead:

$$p_{q|g}(x) = \frac{p_{\mathrm{F}}(x) - \kappa(\mathrm{F}|\mathrm{C})p_{\mathrm{C}}(x)}{1 - \kappa(\mathrm{F}|\mathrm{C})} ,$$
$$p_{g|q}(x) = \frac{p_{\mathrm{C}}(x) - \kappa(\mathrm{C}|\mathrm{F})p_{\mathrm{F}}(x)}{1 - \kappa(\mathrm{C}|\mathrm{F})} .$$

The quark and the gluon distributions are then given by

$$p_q(x) = \frac{p_{q|g}(x)(1 - \kappa(q|g)) + (1 - \kappa(g|q))\kappa(q|g)p_{g|q}(x)}{1 - \kappa(g|q)\kappa(q|g)} ,$$
$$p_g(x) = \frac{p_{g|q}(x)(1 - \kappa(g|q)) + (1 - \kappa(q|g))\kappa(g|q)p_{q|g}(x)}{1 - \kappa(q|g)\kappa(g|q)} ,$$

where $\kappa(q|g)$ and $\kappa(g|q)$ are the reducibility factors for the quark and gluon distributions [23]. The mutual irreducibility condition is satisfied when $\kappa(q|g) = \kappa(g|q) = 0$, indicating no mixing of the distributions. For each jet p_{T} and η bin, this condition was evaluated by computing the reducibility factors from MC simulations, using formulas similar to Eqs. (5) and (6). In the majority of kinematic bins, the condition was violated with non-zero reducibility factors, necessitating MC-based corrections obtained by analytically computing $\kappa(q|g)$ and $\kappa(g|q)$. The impact of such corrections is visible in Figure 4, where the extracted quark and gluon score distributions for the matrix and jet topic methods are compared.

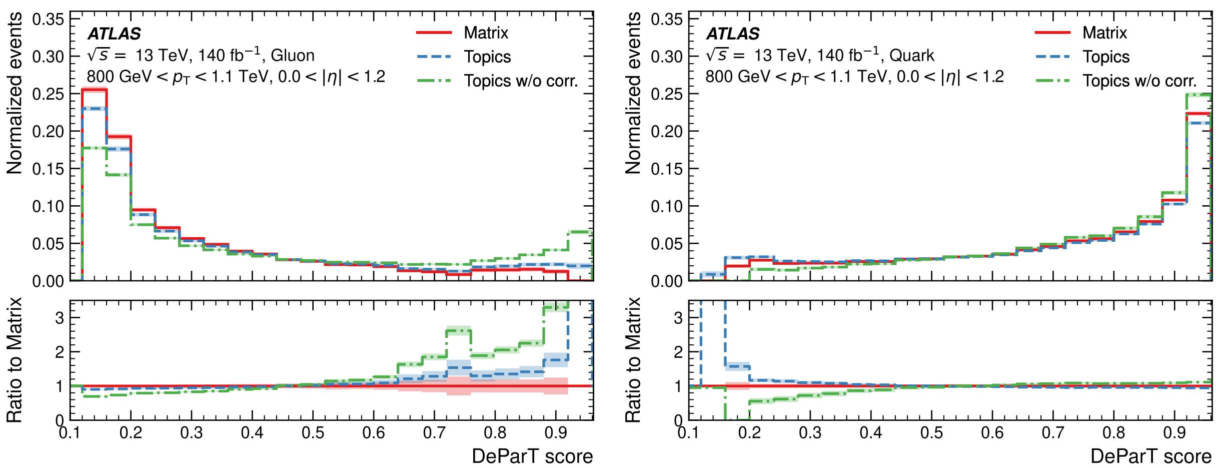

(a) (b)

Figure 4: The (a) gluon and (b) quark DeParT score distributions extracted from Run-2 data with the matrix method (solid red), jet topics without MC correction (dash dotted green), and jet topics with MC correction (dashed blue). The bottom panels show ratios of jet topics to matrix method results. The error bands represent statistical uncertainties.

7 Tagging efficiency measurement strategy

The extracted quark and gluon score distributions are used to measure the performance of the tagger. In the following, the score distributions $p_q(x)$ and $p_g(x)$ are normalized to unity. The quark efficiency is computed from the quark score distribution according to

$$\varepsilon_q(x_{\text{WP}}) = \int_{x_{\text{WP}}}^{1} p_q(x)\, dx,$$

where $p_q(x)$ represents the quark score distribution and x_{WP} denotes the score threshold defining the working point. The working point x_{WP} is determined by requiring a fixed quark efficiency value in the nominal Pythia sample within each jet p_{T} and η bin. Working points corresponding to fixed quark efficiencies of 50%, 60%, 70%, and 80% were investigated, with their respective scale factors demonstrating similar characteristics. The gluon efficiency is calculated from the gluon score distribution as

$$\varepsilon_g(x_{\text{WP}}) = \int_{x_{\text{WP}}}^{1} p_g(x)\, dx,$$

where $p_g(x)$ is the gluon score distribution.

Discrepancies between the tagging efficiencies measured in experimental data and those predicted by MC simulation are quantified through data-to-MC scale factors (SF) computed for each p_{T} and η bin at a specified working point x_{WP}. The quark efficiency scale factor, which corrects the number of quark jets tagged as quarks, is defined as the ratio of data to MC quark efficiencies:

$$\text{SF}_q = \frac{\varepsilon_q^{\text{data}}}{\varepsilon_q^{\text{MC}}}.$$

The gluon efficiency scale factor, defined analogously to correct the number of gluon jets tagged as gluons, is expressed as the ratio of data to MC $1 - \varepsilon_g$ values:

$$\text{SF}_g = \frac{1 - \varepsilon_g^{\text{data}}}{1 - \varepsilon_g^{\text{MC}}}.$$

This definition takes into account that gluon jets constitute a minority of the jet population at the working points considered and hence the gluon scale factor serves primarily as a measure of background efficiency. The measurements of the 50%-efficiency working-point scale factors are presented in Section 9.

8 Systematic uncertainties

The SF measurements are affected by multiple sources of systematic uncertainty, with contributions which are shared by the matrix and jet topics approaches and others which affect the two methods individually. Both methodologies are subject to experimental uncertainties arising from the pile-up reweighting, the calibration of the jet energy scale (JES) and jet energy resolution (JER) [64], and the JVT and fJVT SF uncertainties [72, 73]. Theory uncertainties in the MC simulation also affect both models, but their impact is smaller for the jet topic method because that approach depends on MC simulation only through corrections to data-driven estimates. Additionally, methodology-specific uncertainties are considered. These include uncertainties associated with the reweighting procedure and the residual MC non-closure, which affect both extraction methods, and an uncertainty originating from the determination of the reducibility factors, which only affects the jet topics method.

8.1 Experimental uncertainty

Experimental uncertainties come from three sources: the JES/JER calibration, the JVT/fJVT SFs, and the pile-up reweighting. The impact of other sources of systematic uncertainty, such as the tracks and PFO identification, was found to be negligible [77]. The JES uncertainty includes components related to the in situ calibration of jets and pile-up, and its extrapolation to higher transverse momentum. The JER uncertainty is estimated with the dijet balance and random cones measurement methods. A SF is obtained for each JES/JER variation, and its deviation from the nominal SF value is taken as the systematic uncertainty. The uncertainty from the reweighting of the MC pile-up distribution to match the distribution in data is evaluated by varying the visible inelastic cross section by its uncertainty.

The statistical uncertainty of the measurements is evaluated using a bootstrapping procedure, wherein each data or MC event is assigned a random weight drawn from a Poisson distribution with unit mean (applied in addition to the nominal weight assigned to a MC event), and the standard deviation of the resulting SFs across 100 independent replicas is taken as the statistical uncertainty estimate.

8.2 Theory uncertainty

The theory uncertainty arises from several sources. The uncertainty from the PS modelling is estimated by comparing SFs obtained with the same ME and hadronization model but different shower algorithms. In the case of Run-2 data, the envelope of the SFs obtained with the Pythia, Herwig String, and Sherpa String samples is taken as the PS uncertainty. Using the Herwig String sample, which employs an untuned Lund string fragmentation model without colour-reconnection effects, yields a conservative uncertainty estimate. The Run-3 PS uncertainty is estimated from the difference between the SFs obtained with the Herwig Angular and Herwig Dipole samples. This was made possible by the availability of new MC samples developed for Run-3 conditions. In recent measurements of the Lund subjet multiplicities [78], which are observables sensitive to the PS modelling and relevant to q/g tagging, discrepancies of more than 50% between various MC generators and data were seen. This is consistent with the present analysis finding the PS uncertainty to be the dominant theory uncertainty.

The impact of initial-state radiation uncertainties is evaluated by varying the Var3c set of parameters in the A14 tune of the PS [42, 79]. Variations of the renormalization (μ_{r}) and factorization (μ_{f}) scales for initial- and final-state radiation are used to estimate the uncertainty due to missing higher-order corrections in the PS modelling. Seven possibilities for ($\mu_{\mathrm{r}}, \mu_{\mathrm{f}}$), where their nominal values are multiplied by factors of $(0.5, 0.5)$, $(0.5, 1)$, $(1, 0.5)$, $(1, 1)$, $(2, 1)$, $(1, 2)$ and $(2, 2)$, are used to estimate an envelope of SF values for the Pythia sample. The width of this envelope is taken as the associated uncertainty.

Splitting-kernel variations [45] are also propagated to alternative SF measurements, and the uncertainty associated with the non-singular part of the splitting functions for the initial- and final-state radiation is taken as the envelope of those SF values.

The systematic uncertainty due to the hadronization modelling is estimated as the difference between the SFs obtained with the Sherpa String and Sherpa Cluster samples for both Run-2 and Run-3 data. An additional uncertainty covering differences in the ME calculation, and its matching to the PS algorithm, is estimated from the differences between the SFs obtained by using the Powheg+Pythia and nominal Pythia samples. The uncertainty due to the PDF is evaluated in accord with the LHAPDF recommendations [80] by using variations of the NNPDF2.3lo PDF set in the nominal Pythia sample.

8.3 Methodology uncertainty

Both the matrix and jet topics methods suffer from uncertainties associated with the central-to-forward reweighting process and with the residual MC non-closure. To estimate the systematic uncertainty from the reweighting process, the nominal reweighting choice described in Section 6 is varied by using either the quark or gluon jet distributions to derive the weights, and by applying the correction in either direction, matching $p_{\mathrm{C}}(x)$ to $p_{\mathrm{F}}(x)$ or matching $p_{\mathrm{F}}(x)$ to $p_{\mathrm{C}}(x)$. The SF envelope obtained from these four alternative reweighting configurations is taken as the systematic uncertainty.

The MC non-closure uncertainty is obtained from the difference between the truth-level particle distributions obtained directly from simulation and the distributions extracted via the matrix method or jet topics procedure when applied to the same MC samples. Additionally, the nominal SFs and efficiencies are shifted by the MC non-closure.

The jet topics method uncertainties arise from the calculation of the reducibility factors. As explained in Section 6, the calculation is based on finding the minimum of a distribution and suffers from significant statistical fluctuations. Two calculation methods, described in Ref. [24], are used to estimate the uncertainty: the quantiled log-likelihood method with a rebinning into 10 bins and a degree 2 polynomial fit to find the minimum, and the ROC fit method with a degree 2 polynomial. The envelope of the SFs obtained with the two methods is taken as the uncertainty associated with the reducibility factors computation.

9 Results

The measured DeParT tagger efficiencies, extracted via the jet topics method from Run-2 data, are compared with MC predictions from the nominal Pythia sample in Figure 5. The quark and gluon efficiencies are evaluated at a fixed working point corresponding to 50% quark efficiency in the MC simulation and their values and statistical uncertainties are smoothed. The smoothing employs Gaussian kernels as in Ref. [64], applied to 100 bootstrapped resamples of the efficiency distribution. For each resample, bin contents are drawn from Gaussian distributions with means and standard deviations equal to the nominal bin contents and their uncertainties. The smoothed value and its uncertainty are determined from the mean and standard deviation of the 100 smoothed distributions, respectively.

In the central pseudorapidity region ($0.0 < |\eta| < 1.2$), the ε_q measurements (Figure 5(a)) reveal a characteristic systematic shift of approximately 2–3% relative to MC predictions throughout the intermediate transverse momentum range of 200 GeV to 1 TeV. At p_{T} values below 200 GeV the measured ε_q agree with MC expectations within statistical uncertainties. In the forward pseudorapidity region with $3.2 < |\eta| < 4.5$, the measured ε_q values (Figure 5(b)) are approximately 5–6% lower than the MC predictions across the entire p_{T} spectrum. The $1 - \varepsilon_g$ data measurements in the central region (Figure 5(c)) are consistently lower than the MC predictions between 20 GeV and 200 GeV. Between 200 GeV and 800 GeV the measured $1 - \varepsilon_g$ agree with MC expectations within statistical uncertainties. Above 800 GeV, the measured $1 - \varepsilon_g$ are systematically lower than MC expectations, signalling potential deficiencies in the modelling of high-p_{T} gluon jet properties. The forward region $1 - \varepsilon_g$ measurements (Figure 5(d)) exhibit a systematic downward shift with respect to the MC predictions across the p_{T} spectrum.

The SFs measured using the jet topics method and the Run-2 data are presented for gluon and quark jets in their full kinematic phase space in Figures 6 and 7, respectively. Individual components of the total uncertainty are smoothed using a Gaussian kernel without bootstrapping as is done in Ref. [64], while

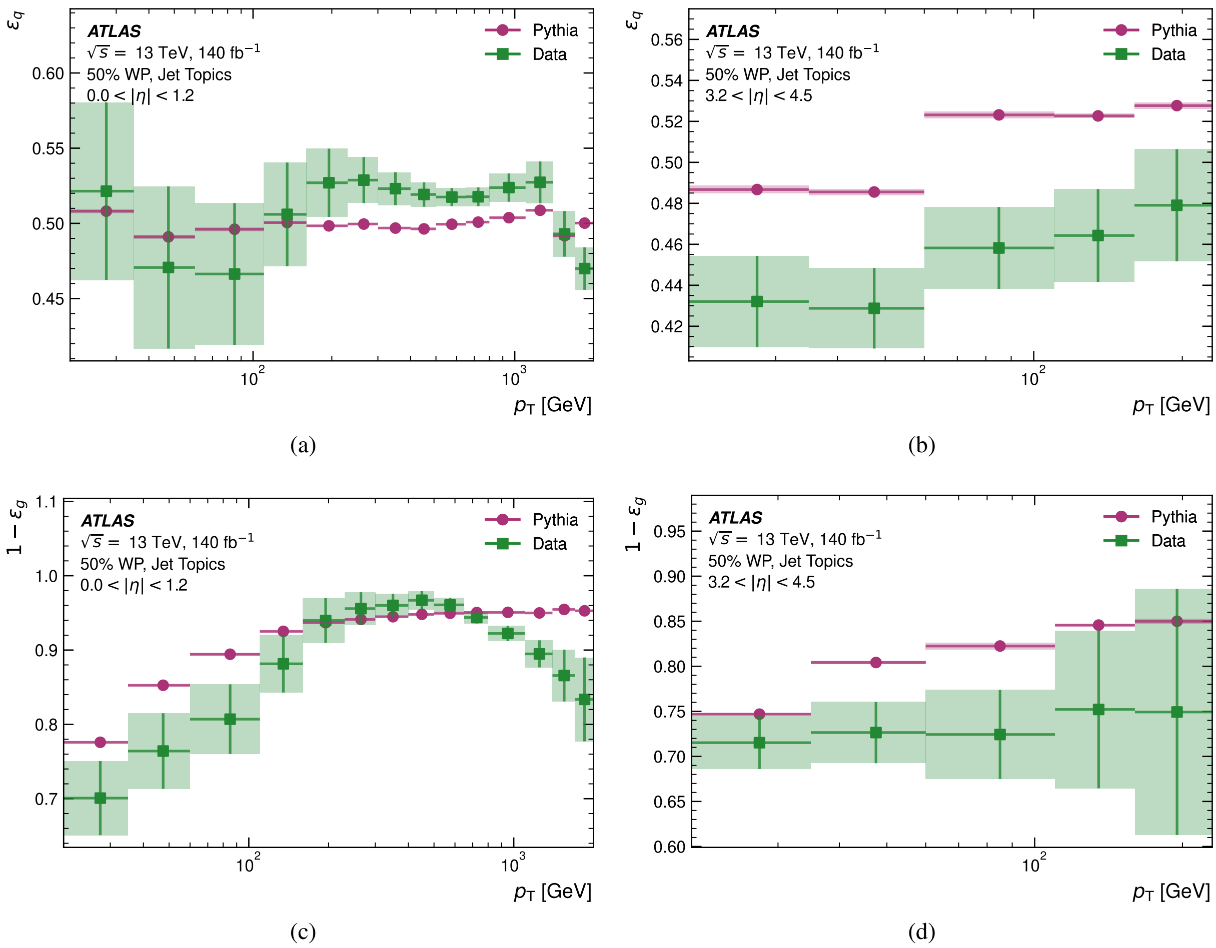

Figure 5: The MC efficiencies for truth-labelled (a) quark jets with $0.0 < |\eta| < 1.2$, (b) quark jets with $3.2 < |\eta| < 4.5$, (c) gluon jets with $0.0 < |\eta| < 1.2$, and (d) gluon jets with $3.2 < |\eta| < 4.5$, compared with the efficiencies measured for Run-2 data with the jet topics method. Gluon efficiencies are reported as $1 - \varepsilon_g$ to ease their comparison with the gluon SF measurements. The 50% WP corresponds to a score threshold defined by a fixed 0.5 quark efficiency in the Pythia sample in each p_T and $|\eta|$ bin. The deviations of the truth quark-jet efficiencies from 0.5 are due to the finite binning of the DeParT score used in the efficiency calculation. Only the statistical uncertainties are shown.

the nominal SF values are smoothed using a bootstrapped Gaussian kernel as described above for the efficiencies. The gluon SF values (Figure 6) are generally consistent with unity within the total uncertainty across the measured phase space. The nominal SF values range from 0.61 to 1.05. Similarly, the quark SFs (Figure 7) are also consistent with unity, with values ranging from 0.88 to 1.30 and the total relative uncertainty becoming larger for low p_T and reaching about 70%.

A breakdown of the uncertainties affecting the SFs measured using the jet topics method for Run-2 data is shown in Figure 8 for both the quark and gluon jets in the central and forward $|\eta|$ regions. Both the quark and gluon SFs in the $0.0 < |\eta| < 1.2$ region are dominated by the PS uncertainty between approximately 100 GeV and 500 GeV and by methodological uncertainties at p_T above 1 TeV. The low-p_T region is dominated by both experimental and methodological uncertainties for quark SFs and by experimental uncertainties for gluon SFs. In the $3.2 < |\eta| < 4.5$ region, the reweighting and experimental uncertainties dominate in the quark SF case, while the extraction and experimental uncertainties are the

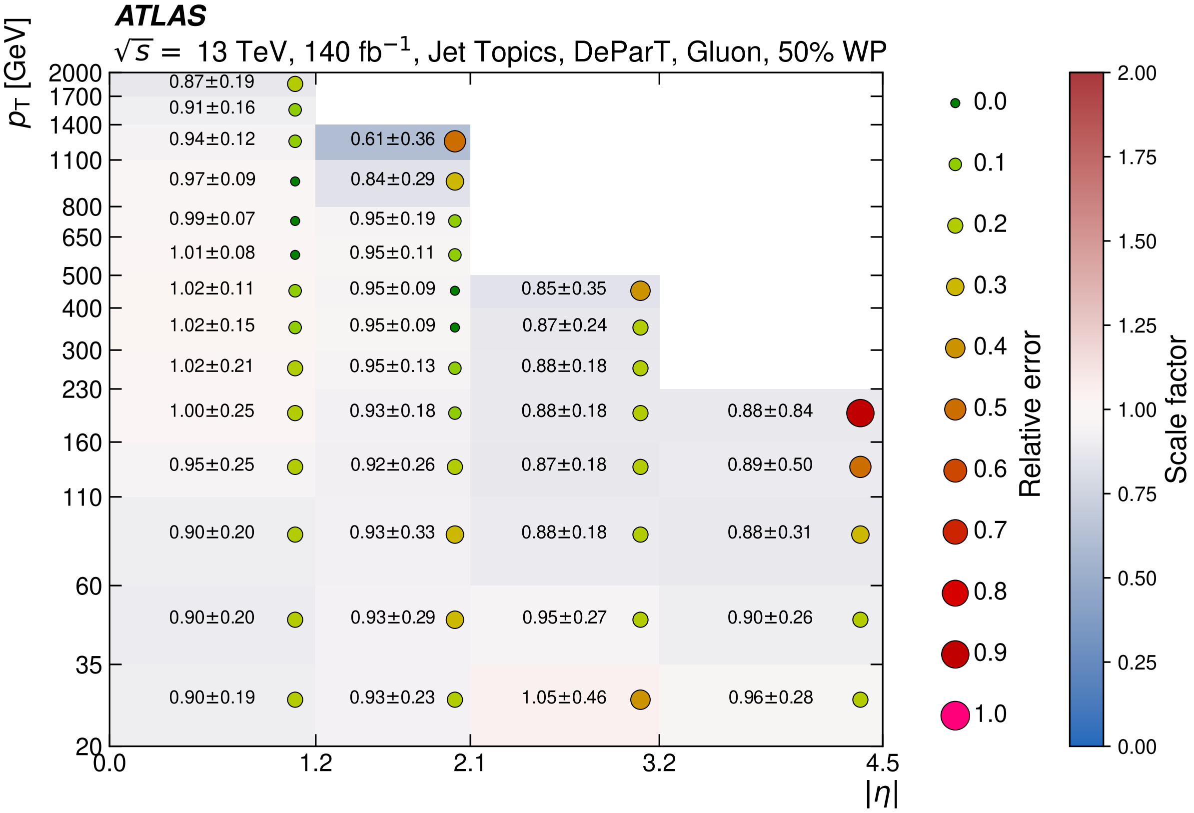

Figure 6: The gluon efficiency scale factors derived with the jet topics method in each p_T and $|\eta|$ bin for Run-2 jets. The size and the colour of the dots represents the relative total uncertainty of the scale factor. The 50% WP corresponds to a score threshold defined by a fixed 0.5 quark efficiency in the Pythia sample in each p_T and $|\eta|$ bin. The nominal scale factor's value and total uncertainty is shown in each bin.

leading contributions for the gluon SFs. The total relative uncertainty of gluon SFs ranges approximately from 10% to 25% in the $0.0 < |\eta| < 1.2$ region and 30% to 95% in the $3.2 < |\eta| < 4.5$ region. The quark SF uncertainties range approximately from 10% to 70% in the $0.0 < |\eta| < 1.2$ region and 35% to 50% in the $3.2 < |\eta| < 4.5$ region. The intermediate pseudorapidity region, $1.2 < |\eta| < 3.2$, exhibits similar trends in the total uncertainties, as demonstrated in Figures 6 and 7. Statistical uncertainties become significant at the highest p_T values, where the available sample is much smaller, and also at the lowest p_T values, due to the use of prescaled triggers. The MC non-closure uncertainty exhibits pronounced p_T dependence, becoming increasingly significant at lower p_T values. There the PDF properties render the quark and gluon fractions in the forward sample more similar to those in the central sample, thereby reducing the effective discrimination power of the pseudorapidity-based selection strategy and making the extraction procedure numerically unstable.

A comparison of the scale factors derived via the jet topics and matrix methods is presented in Figure 9, revealing distinct precision advantages that vary across kinematic regimes and jet flavours. The two extraction methodologies demonstrate consistency in their central SF values while exhibiting differences in their associated uncertainties. For quark jets in the central pseudorapidity region (Figure 9(a)), the jet topics method reduces the total uncertainties, delivering improvements of up to 15% in relative uncertainty in the intermediate p_T range of 300–1000 GeV, where theory uncertainties typically dominate. Although its

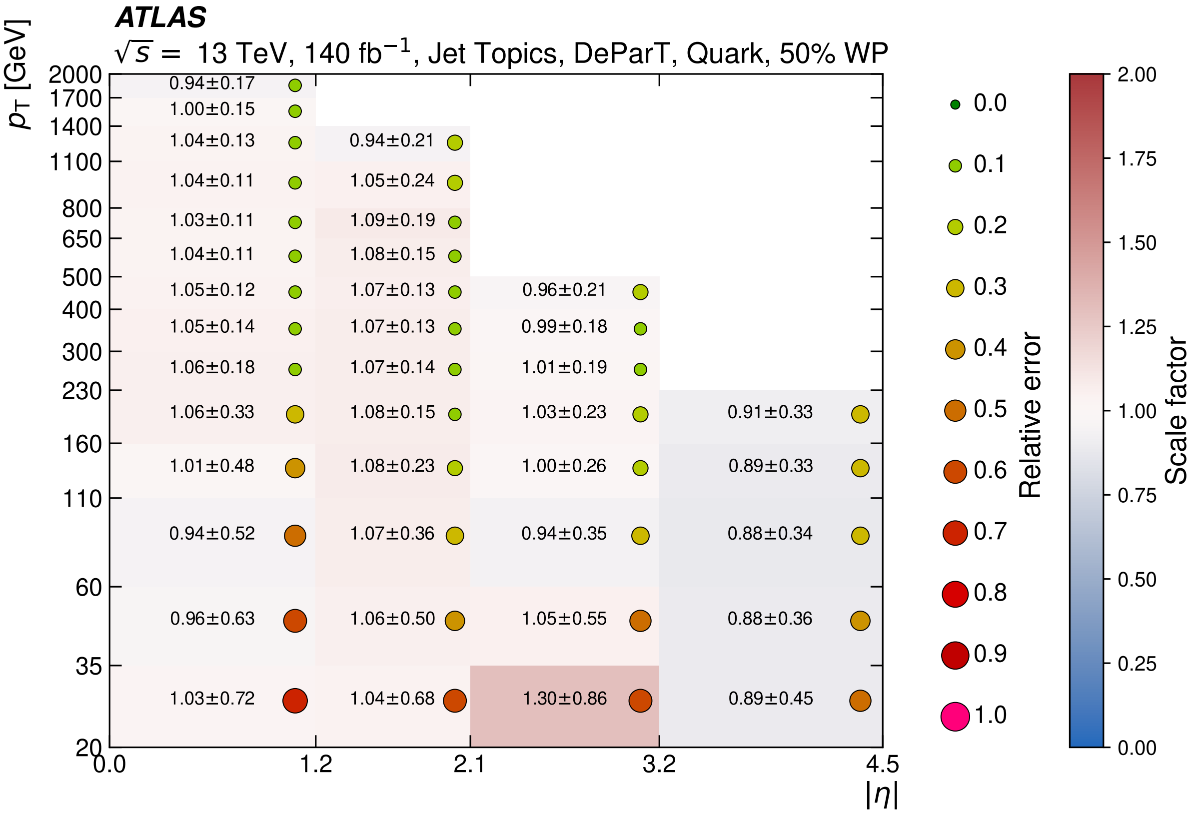

Figure 7: The quark efficiency scale factors derived with the jet topics method in each p_{T} and $|\eta|$ bin for Run-2 jets. The size and the colour of the dots represents the relative total uncertainty of the scale factor. The 50% WP corresponds to a score threshold defined by a fixed 0.5 quark efficiency in the Pythia sample in each p_{T} and $|\eta|$ bin. The nominal scale factor's value and total uncertainty is shown in each bin.

better precision persists into the forward region (Figure 9(b)), the jet topics method's advantage decreases markedly, likely due to both methods becoming statistically limited by smaller event yields. The gluon SF measurements reveal a more nuanced uncertainty landscape: in the central region (Figure 9(c)) the jet topics method demonstrates superior precision at low p_{T}, achieving up to 20% smaller uncertainties in the 20–110 GeV range. Above 110 GeV, the two methods yield comparable uncertainties. An improvement also emerges in the forward pseudorapidity region for gluon jets (Figure 9(d)), where the jet topics method consistently reduces the uncertainties, with improvements of up to 15%. The jet topics method achieves these improvements over the matrix method primarily by reducing the PS and ME uncertainties via less dependence on MC simulation, relying on it only for the MC correction described in Section 6.3.

The SFs derived with the jet topics method for Run-3 data are compared with those from Run 2 in Figure 10. The differences between the two runs' results arise from several factors: different integrated luminosities, different numbers of simulated events, different pile-up conditions, differences in trigger strategies, and the use of different MC generators for deriving the PS uncertainty. At low jet p_{T}, the number of simulated events available for Run-3 conditions is around 30% of that for Run-2 conditions, much lower than the ratio of the integrated luminosities of the two data-taking periods (around 70%). This statistical limitation directly impacts the systematic uncertainties, as the reweighting described in Section 6.1 uses weights derived from ratios of MC distributions, whereby statistical fluctuations lead to larger uncertainties in the

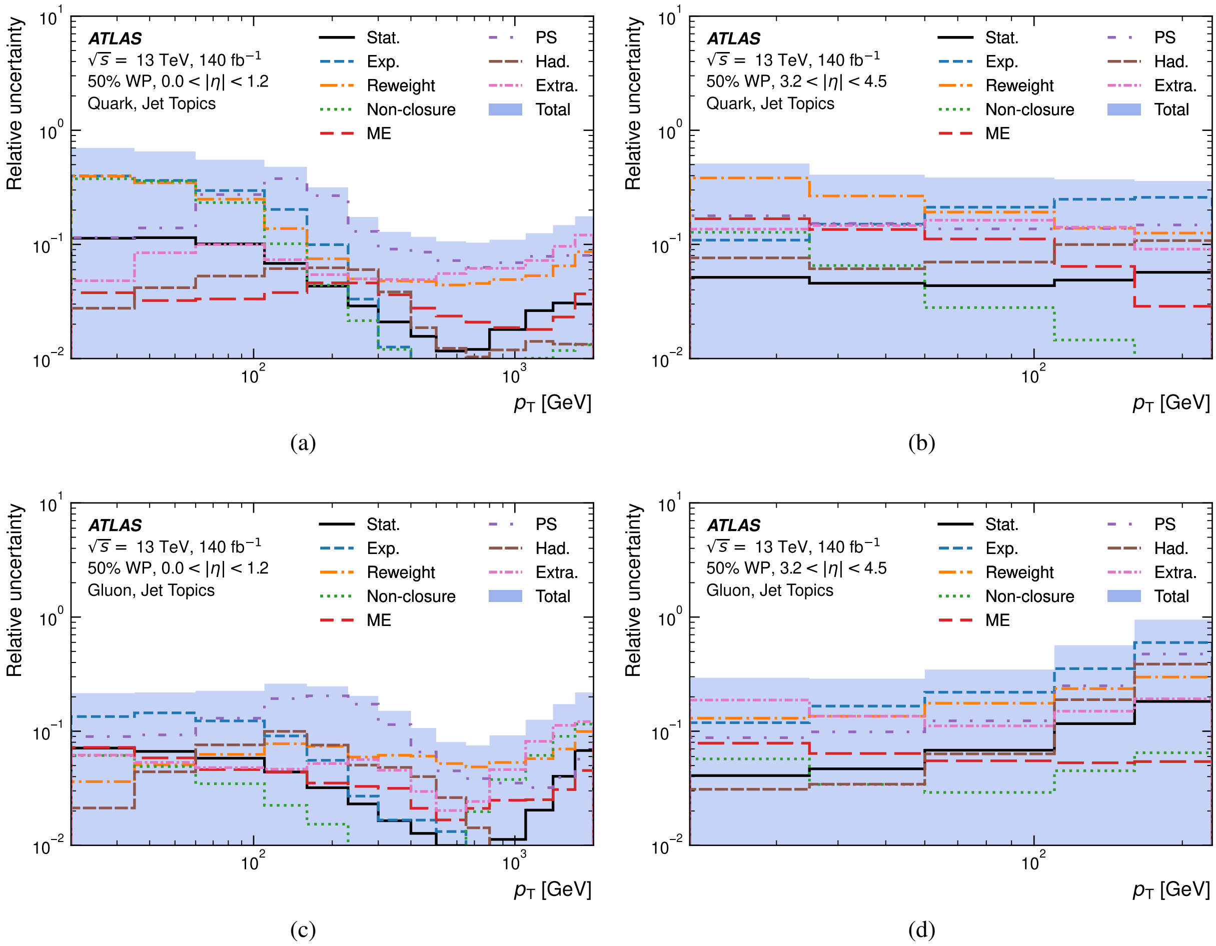

Figure 8: The scale factor uncertainties derived with the jet topics method for Run-2 (a) quark jets with $0.0 < |\eta| < 1.2$, (b) quark jets with $3.2 < |\eta| < 4.5$, (c) gluon jets with $0.0 < |\eta| < 1.2$, and (d) gluon jets with $3.2 < |\eta| < 4.5$. The 50% WP corresponds to a score threshold defined by a fixed 0.5 quark efficiency in the Pythia sample in each p_T and $|\eta|$ bin. The PDF uncertainty is not shown, as it is negligible in the considered phase space. The PS component stands for the quadrature sum of the following components: comparison of PS modelling by different MC generators, Var3c parameter variations, μ_r and μ_f scale variations, and splitting-kernel variations. The theory uncertainty due to hadronization modelling is denoted as 'Had.' and the systematic uncertainty arising from the calculation of the reducibility factors, the extraction uncertainty, is denoted as 'Extra.'. The total uncertainty is represented by the blue shaded band, with individual systematic components shown as coloured lines.

corrected distributions. The PS uncertainty in Run 2 is taken from the envelope of the SFs obtained with the Pythia, Herwig String, and Sherpa String samples, while in Run 3 the uncertainty is estimated from the difference between the SFs obtained with the Herwig Angular and Herwig Dipole samples. In Run 3 the total uncertainties reach over 100% for quark SFs at low p_T in the $0.0 < |\eta| < 1.2$ region and for gluon SFs at high p_T in the $3.2 < |\eta| < 4.5$ region. A detailed breakdown of the relative systematic uncertainties in the SFs measured using the jet topics method in Run-3 data is illustrated in Figure 11 for both the quark and gluon jets in the central and forward $|\eta|$ regions.

Since analyses interested in using the results reported above may use different MC samples, a MC-to-MC SF is obtained by using each of the alternative MC samples in the SF definition and treating the Pythia samples

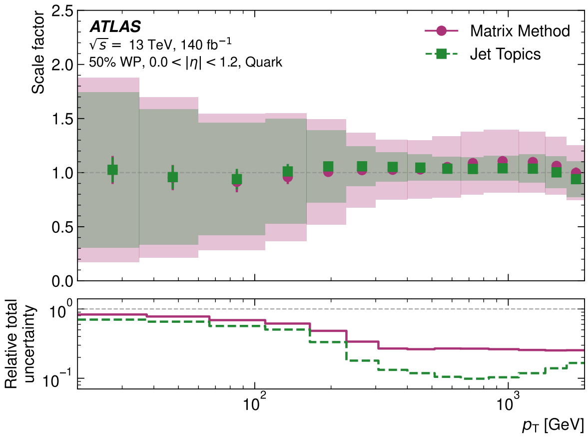

(a)

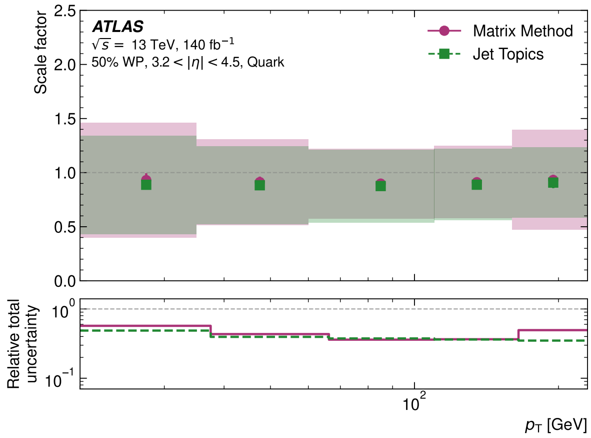

(b)

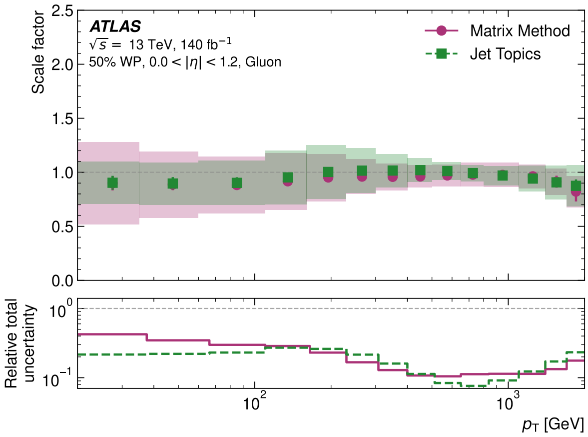

(c)

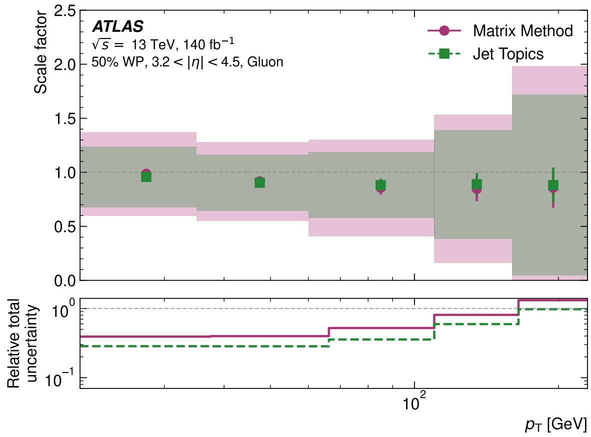

(d)

Figure 9: Comparison of SFs and total uncertainties derived with the jet topics method and matrix method for Run-2 (a) quark jets with $0.0 < |\eta| < 1.2$, (b) quark jets with $3.2 < |\eta| < 4.5$, (c) gluon jets with $0.0 < |\eta| < 1.2$, and (d) gluon jets with $3.2 < |\eta| < 4.5$. The 50% WP corresponds to a score threshold defined by a fixed 0.5 quark efficiency in the Pythia sample in each p_{T} and $|\eta|$ bin. The error bars represent the statistical uncertainties and the shaded bands represent the total uncertainties. The bottom panels show the relative total uncertainties for the jet topics and matrix methods.

as pseudo-data, to account for modelling differences between the Pythia and alternative MC samples. The MC-to-MC SFs are shown in Figure 12 for quark and gluon jets in the central and forward regions. In the central region, the quark MC-to-MC SF (Figure 12(a)) has a relatively large value above unity for the Herwig String sample, which is inconsistent with all the other samples. For the gluon MC-to-MC SF (Figure 12(c)), all the samples diverge from unity for small p_{T} values, in both the forward and central regions, with the Sherpa Cluster sample being the furthest from unity.

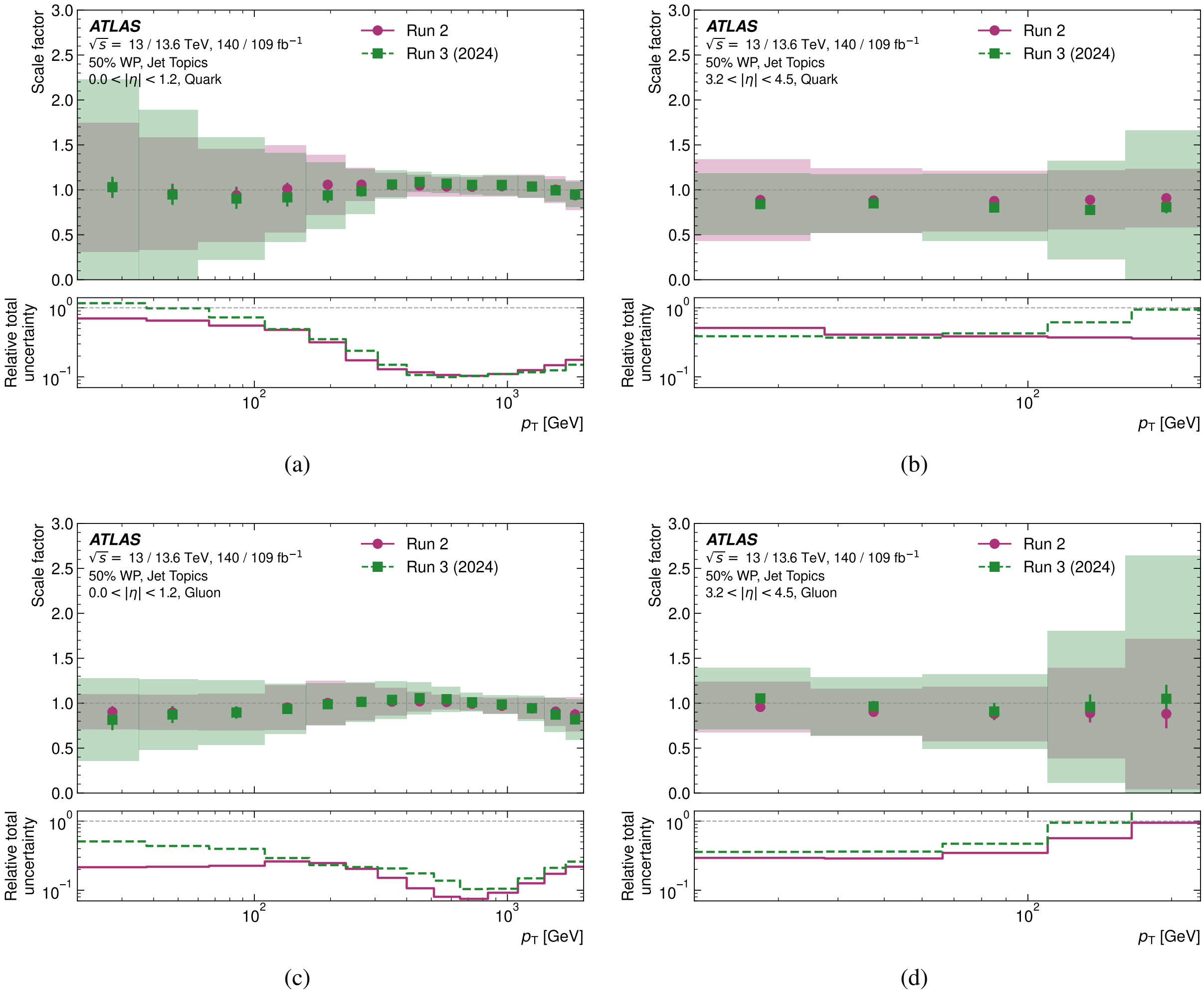

Figure 10: Comparison of SFs and total uncertainties derived with the jet topics method with Run-2 and Run-3 data for (a) quark jets with $0.0 < |\eta| < 1.2$, (b) quark jets with $3.2 < |\eta| < 4.5$, (c) gluon jets with $0.0 < |\eta| < 1.2$, and (d) gluon jets with $3.2 < |\eta| < 4.5$. The 50% WP corresponds to a score threshold defined by a fixed 0.5 quark efficiency in the Pythia sample in each p_T and $|\eta|$ bin. The error bars represent the statistical uncertainties and the shaded bands represent the total uncertainties. The bottom panels show the relative total uncertainties for Run 2 and Run 3.

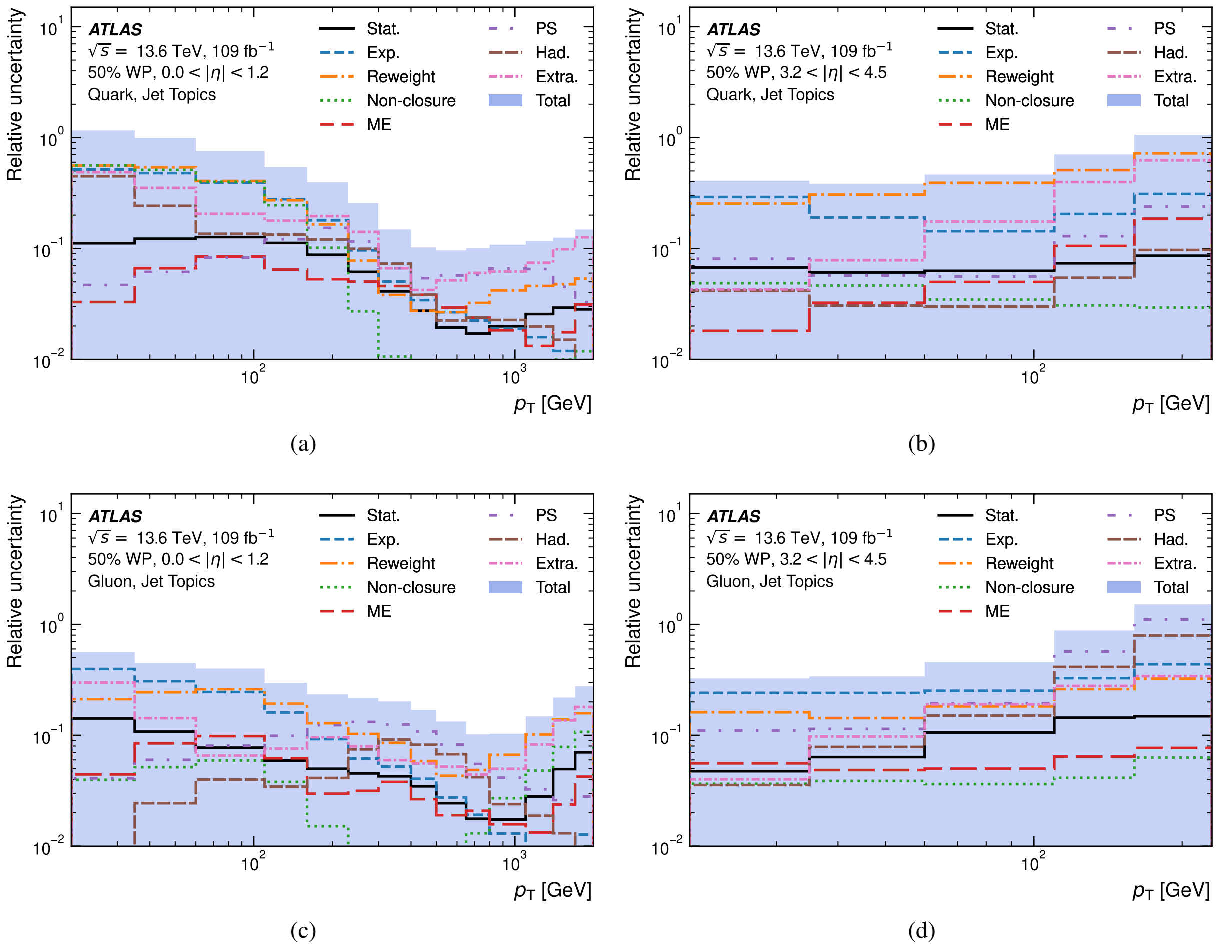

Figure 11: The scale factor uncertainties derived with the jet topics method for Run-3 (a) quark jets with $0.0 < |\eta| < 1.2$, (b) quark jets with $3.2 < |\eta| < 4.5$, (c) gluon jets with $0.0 < |\eta| < 1.2$, and (d) gluon jets with $3.2 < |\eta| < 4.5$. The 50% WP corresponds to a score threshold defined by a fixed 0.5 quark efficiency in the Pythia sample in each p_T and $|\eta|$ bin. The PDF uncertainty is not shown, as it is negligible in the considered phase space. The PS component stands for the quadrature sum of the following components: comparison of PS modelling by different MC generators, Var3c parameter variations, μ_r and μ_f scale variations, and splitting-kernel variations. The theory uncertainty due to hadronization modelling is denoted as 'Had.' and the systematic uncertainty arising from the calculation of the reducibility factors, the extraction uncertainty, is denoted as 'Extra.'. The total uncertainty is represented by the blue shaded band, with individual systematic components shown as coloured lines.

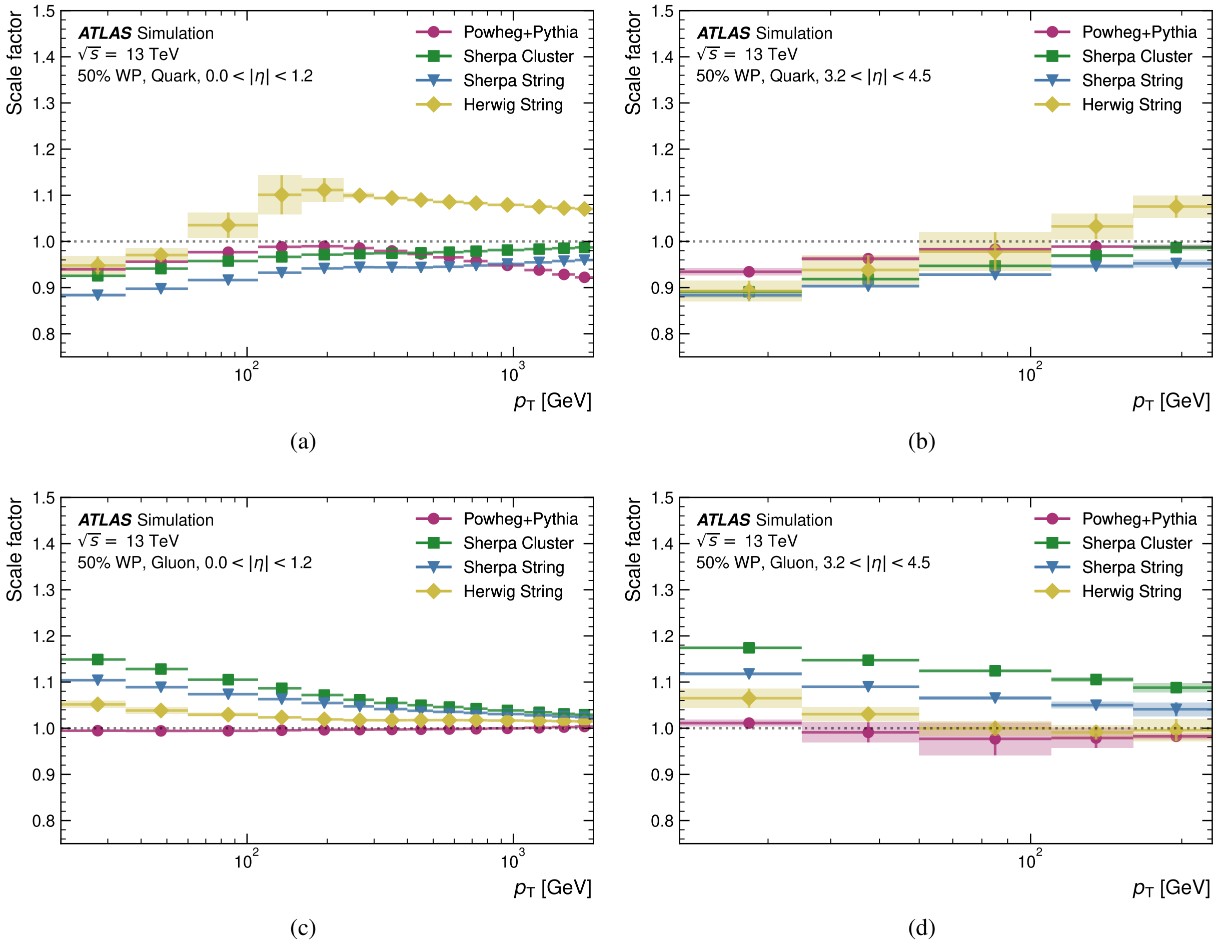

Figure 12: The MC-to-MC scale factors for (a) quark jets with $0.0 < |\eta| < 1.2$, (b) quark jets with $3.2 < |\eta| < 4.5$, (c) gluon jets with $0.0 < |\eta| < 1.2$, and (d) gluon jets with $3.2 < |\eta| < 4.5$. The 50% WP corresponds to a score threshold defined by a fixed 0.5 quark efficiency in the Pythia sample in each p_{T} and $|\eta|$ bin. The statistical uncertainties are shown as error bars.

10 Conclusions

This paper presents DeParT, a novel ATLAS q/g tagger leveraging modern deep-learning techniques and directly processing variables derived from jet constituents. Compared to previous similar ATLAS taggers, the DeParT q/g tagger covers an extended phase space where jets have transverse momentum $p_{\mathrm{T}} > 20$ GeV and pseudorapidity $|\eta| < 4.5$.

The tagger's performance was evaluated by selecting dijet events from pp collisions at $\sqrt{s} = 13$ TeV and 13.6 TeV recorded by the ATLAS detector during Runs 2 and 3 of the LHC. Two methods were employed to extract quark and gluon jet tagger score distributions from data: a novel method called jet topics, and the matrix method used in the previous ATLAS studies. The two methods yield compatible results, and consistency is observed between the Run-2 and Run-3 data-taking periods.

The efficiencies of the DeParT q/g tagger measured in data, for a tagger working point corresponding to a 50% quark tagging efficiency in the nominal simulation, were found to range from 0.43 to 0.53 for the quark-initiated jet sample, and from 0.04 to 0.3 for the gluon-initiated one. These efficiency measurements were compared with the values predicted by Monte Carlo simulations, thereby deriving factors which account for the observed jet-tagging efficiency differences between data and simulation. The correction factors on the tagging efficiency for quark-initiated jets and on one minus the tagging efficiency for gluon-initiated jets were found to range from 0.88 to 1.30 and 0.61 to 1.05, with uncertainties of 10%–70% and 10%–95%, respectively. Tagging efficiency correction factors were also evaluated to account for differences in jet fragmentation modelling, with values ranging from 0.9 to 1.2.

The DeParT q/g tagger represents a significant advancement in the ATLAS q/g tagging capabilities, providing a robust tool for future analyses involving quark- and gluon-initiated jets. The jet topics method demonstrated its potential as a reliable technique for extracting quark and gluon jet samples from data, offering a promising alternative to traditional methods such as the matrix method. Systematic uncertainties associated with the jet topics method are smaller than those of the matrix method in an important part of the phase space. This reduction in systematic uncertainty, particularly pronounced in regions where traditional methods face limitations, establish the jet topics approach as a powerful complementary technique that enhances the robustness of q/g tagging measurements across the full ATLAS detector acceptance.

Acknowledgements

We thank CERN for the very successful operation of the LHC and its injectors, as well as the support staff at CERN and at our institutions worldwide without whom ATLAS could not be operated efficiently.

The crucial computing support from all WLCG partners is acknowledged gratefully, in particular from CERN, the ATLAS Tier-1 facilities at TRIUMF/SFU (Canada), NDGF (Denmark, Norway, Sweden), CC-IN2P3 (France), KIT/GridKA (Germany), INFN-CNAF (Italy), NL-T1 (Netherlands), PIC (Spain), RAL (UK) and BNL (USA), the Tier-2 facilities worldwide and large non-WLCG resource providers. Major contributors of computing resources are listed in Ref. [81].

We gratefully acknowledge the support of ANPCyT, Argentina; YerPhI, Armenia; ARC, Australia; BMWFW and FWF, Austria; ANAS, Azerbaijan; CNPq and FAPESP, Brazil; NSERC, NRC and CFI, Canada; CERN; ANID, Chile; CAS, MOST and NSFC, China; Minciencias, Colombia; MEYS CR, Czech Republic; DNRF and DNSRC, Denmark; IN2P3-CNRS and CEA-DRF/IRFU, France; SRNSFG, Georgia; BMFTR, HGF and MPG, Germany; GSRI, Greece; RGC and Hong Kong SAR, China; ICHEP and Academy of Sciences and Humanities, Israel; INFN, Italy; MEXT and JSPS, Japan; CNRST, Morocco; NWO, Netherlands; RCN, Norway; MNiSW, Poland; FCT, Portugal; MNE/IFA, Romania; MSTDI, Serbia; MSSR, Slovakia; ARIS and MVZI, Slovenia; DSI/NRF, South Africa; MICIU/AEI, Spain; SRC and Wallenberg Foundation, Sweden; SERI, SNSF and Cantons of Bern and Geneva, Switzerland; NSTC, Taipei; TENMAK, Türkiye; STFC/UKRI, United Kingdom; DOE and NSF, United States of America.

Individual groups and members have received support from BCKDF, CANARIE, CRC and DRAC, Canada; CERN-CZ, FORTE and PRIMUS, Czech Republic; COST, ERC, ERDF, Horizon 2020 and Marie Skłodowska-Curie Actions, European Union; Investissements d'Avenir Labex, Investissements d'Avenir Idex and ANR, France; DFG and AvH Foundation, Germany; Herakleitos, Thales and Aristeia programmes co-financed by EU-ESF and the Greek NSRF, Greece; BSF-NSF and MINERVA, Israel; NCN and NAWA, Poland; La Caixa Banking Foundation, CERCA Programme Generalitat de Catalunya and PROMETEO and GenT Programmes Generalitat Valenciana, Spain; Göran Gustafssons Stiftelse, Sweden; The Royal Society and Leverhulme Trust, United Kingdom.

In addition, individual members wish to acknowledge support from Chile: Agencia Nacional de Investigación y Desarrollo (FONDECYT 1230812, FONDECYT 1240864, Fondecyt 3240661, Fondecyt Regular 1240721); China: Chinese Ministry of Science and Technology (MOST-2023YFA1605700, MOST-2023YFA1609300), National Natural Science Foundation of China (NSFC - 12175119, NSFC 12275265); Czech Republic: Czech Science Foundation (GACR - 24-11373S), Ministry of Education Youth and Sports (ERC-CZ-LL2327, FORTE CZ.02.01.01/00/22_008/0004632), PRIMUS Research Programme (PRIMUS/21/SCI/017); EU: H2020 European Research Council (ERC - 101002463); European Union: European Research Council (BARD No. 101116429, ERC - 948254, ERC 101089007), European Regional Development Fund (SMASH COFUND 101081355, SLO ERDF), European Union, Future Artificial Intelligence Research (FAIR-NextGenerationEU PE00000013); France: Agence Nationale de la Recherche (ANR-21-CE31-0022, ANR-22-EDIR-0002, ANR-24-CE31-0504-01); Germany: Deutsche Forschungsgemeinschaft (DFG - 469666862, DFG - CR 312/5-2); China: Research Grants Council (GRF); Italy: Ministero dell'Università e della Ricerca (NextGenEU 153D23001490006 M4C2.1.1, NextGenEU I53D23000820006 M4C2.1.1, NextGenEU I53D23001490006 M4C2.1.1, SOE2024_0000023); Japan: Japan Society for the Promotion of Science (JSPS KAKENHI JP22H01227, JSPS KAKENHI JP22H04944, JSPS KAKENHI JP22KK0227, JSPS KAKENHI JP24K23939, JSPS KAKENHI JP24KK0251, JSPS KAKENHI JP25H00650, JSPS KAKENHI JP25H01291, JSPS KAKENHI JP25K01023); Norway: Research Council of Norway (RCN-314472); Poland: Ministry of Science and Higher Education (IDUB AGH, POB8, D4 no 9722), Polish National Science Centre (NCN 2021/42/E/ST2/00350, NCN OPUS 2023/51/B/ST2/02507, NCN UMO-2019/34/E/ST2/00393, UMO-2022/47/O/ST2/00148, UMO-2023/49/B/ST2/04085, UMO-2023/51/B/ST2/00920, UMO-2024/53/N/ST2/00869); Portugal: Foundation for Science and Technology (FCT); Spain: Generalitat Valenciana (ASFAE/2022/008), Ministry of Science and Innovation (RYC2019-028510-I, RYC2020-030254-I, RYC2021-031273-I, RYC2022-038164-I), Ministerio de Ciencia, Innovación y Universidades/Agencia Estatal de Investigación (PID2022-142604OB-C22); Sweden: Carl Trygger Foundation (Carl Trygger Foundation CTS 22:2312), Swedish Research Council (Swedish Research Council 2023-04654, VR 2021-03651, VR 2022-03845, VR 2022-04683, VR 2023-03403, VR 2024-05451), Knut and Alice Wallenberg Foundation (KAW 2018.0458, KAW 2022.0358, KAW 2023.0366); Switzerland: Swiss National Science Foundation (SNSF - PCEFP2_194658); United Kingdom: The Binks Trust, Royal Society (NIF-R1-231091); United States of America: U.S. Department of Energy (ECA DE-AC02-76SF00515), John Templeton Foundation (John Templeton Foundation 63206), Neubauer Family Foundation.

References

[1] L. Evans and P. Bryant, *LHC Machine*, JINST **3** (2008) S08001.

[2] A. Banfi, G. P. Salam and G. Zanderighi, *Infrared-safe definition of jet flavour*, Eur. Phys. J. C **47** (2006) 113, arXiv: hep-ph/0601139.

[3] F. Caola et al., *Flavored jets with exact anti-k_T kinematics and tests of infrared and collinear safety*, Phys. Rev. D **108** (2023) 094010, arXiv: 2306.07314 [hep-ph].

[4] S. Bright-Thonney and B. Nachman, *Investigating the Topology Dependence of Quark and Gluon Jets*, JHEP **03** (2019) 098, arXiv: 1810.05653 [hep-ph].

[5] ATLAS Collaboration, *Properties of jet fragmentation using charged particles measured with the ATLAS detector in pp collisions at $\sqrt{s} = 13$ TeV*, Phys. Rev. D **100** (2019) 052011, arXiv: 1906.09254 [hep-ex].

[6] ATLAS Collaboration, *Search for dijet resonances in events with an isolated charged lepton using $\sqrt{s} = 13$ TeV proton–proton collision data collected by the ATLAS detector*, JHEP **06** (2020) 151, arXiv: 2002.11325 [hep-ex].

[7] CMS Collaboration, *Search for high mass dijet resonances with a new background prediction method in proton–proton collisions at $\sqrt{s} = 13$ TeV*, JHEP **05** (2020) 033, arXiv: 1911.03947 [hep-ex].

[8] CMS Collaboration, *Search for new physics in multijet events with at least one photon and large missing transverse momentum in proton–proton collisions at* 13 *TeV*, JHEP **10** (2023) 046, arXiv: 2307.16216 [hep-ex].

[9] ATLAS Collaboration, *Search for R-parity-violating supersymmetric particles in multi-jet final states produced in $p - p$ collisions at $\sqrt{s} = 13$ TeV using the ATLAS detector at the LHC*, Phys. Lett. B **785** (2018) 136, arXiv: 1804.03568 [hep-ex].

[10] ATLAS Collaboration, *Search for new resonances in mass distributions of jet pairs using 139 fb^{-1} of pp collisions at $\sqrt{s} = 13$ TeV with the ATLAS detector*, JHEP **03** (2020) 145, arXiv: 1910.08447 [hep-ex].

[11] CMS Collaboration, *Search for top squarks in final states with two top quarks and several light-flavor jets in proton–proton collisions at $\sqrt{s} = 13$ TeV*, Phys. Rev. D **104** (2021) 032006, arXiv: 2102.06976 [hep-ex].

[12] ATLAS Collaboration, *Characterising the Higgs boson with ATLAS data from the LHC Run-2*, Phys. Rept. **1116** (2025) 4, arXiv: 2404.05498 [hep-ex].

[13] CMS Collaboration, *Combination and interpretation of differential Higgs boson production cross sections in proton–proton collisions at $\sqrt{s} = 13$ TeV*, (2025), arXiv: 2504.13081 [hep-ex].

[14] ATLAS Collaboration, *New techniques for jet calibration with the ATLAS detector*, Eur. Phys. J. C **83** (2023) 761, arXiv: 2303.17312 [hep-ex].

[15] ATLAS Collaboration, *Light-quark and gluon jet discrimination in pp collisions at $\sqrt{s} = 7$ TeV with the ATLAS detector*, Eur. Phys. J. C **74** (2014) 3023, arXiv: 1405.6583 [hep-ex].

[16] ATLAS Collaboration, *Quark versus Gluon Jet Tagging Using Charged-Particle Constituent Multiplicity with the ATLAS Detector*, ATL-PHYS-PUB-2017-009, 2017, URL: https://cds.cern.ch/record/2263679.

[17] A. J. Larkoski, G. P. Salam and J. Thaler, *Energy Correlation Functions for Jet Substructure*, JHEP **06** (2013) 108, arXiv: 1305.0007 [hep-ph].

[18] ATLAS Collaboration, *Quark versus Gluon Jet Tagging Using Jet Images with the ATLAS Detector*, ATL-PHYS-PUB-2017-017, 2017, URL: https://cds.cern.ch/record/2275641.

[19] ATLAS Collaboration, *Performance and calibration of quark/gluon-jet taggers using* $140\,fb^{-1}$ *of* pp *collisions at* $\sqrt{s} = 13$ *TeV with the ATLAS detector*, Chin. Phys. C **48** (2024) 023001, arXiv: 2308.00716 [hep-ex].

[20] ATLAS Collaboration, *Constituent-Based Quark Gluon Tagging using Transformers with the ATLAS detector*, ATL-PHYS-PUB-2023-032, 2023, URL: https://cds.cern.ch/record/2878932.

[21] H. Qu, C. Li and S. Qian, *Particle Transformer for Jet Tagging*, Proceedings of Machine Learning Research **162** (2022) 18281, arXiv: 2202.03772 [hep-ph].

[22] A. Vaswani et al., *Attention Is All You Need*, 2023, arXiv: 1706.03762 [cs.CL].

[23] E. M. Metodiev and J. Thaler, *jet topics: Disentangling Quarks and Gluons at Colliders*, Phys. Rev. Lett. **120** (2018) 241602, arXiv: 1802.00008 [hep-ph].

[24] P. T. Komiske, S. Kryhin and J. Thaler, *Disentangling quarks and gluons in CMS open data*, Phys. Rev. D **106** (2022) 094021, arXiv: 2205.04459 [hep-ph].

[25] M. LeBlanc, B. Nachman and C. Sauer, *Going off topics to demix quark and gluon jets in* α_S *extractions*, JHEP **02** (2023) 150, arXiv: 2206.10642 [hep-ph].

[26] ATLAS Collaboration, *The ATLAS Experiment at the CERN Large Hadron Collider*, JINST **3** (2008) S08003.

[27] ATLAS Collaboration, *The ATLAS experiment at the CERN Large Hadron Collider: a description of the detector configuration for Run 3*, JINST **19** (2024) P05063, arXiv: 2305.16623 [physics.ins-det].

[28] ATLAS Collaboration, *The ATLAS trigger system for LHC Run 3 and trigger performance in 2022*, JINST **19** (2024) P06029, arXiv: 2401.06630 [hep-ex].

[29] ATLAS Collaboration, *Software and computing for Run 3 of the ATLAS experiment at the LHC*, Eur. Phys. J. C **85** (2025) 234, arXiv: 2404.06335 [hep-ex].

[30] ATLAS Collaboration, *ATLAS data quality operations and performance for 2015–2018 data-taking*, JINST **15** (2020) P04003, arXiv: 1911.04632 [physics.ins-det].

[31] ATLAS Collaboration, *Luminosity determination in* pp *collisions at* $\sqrt{s} = 13$ *TeV using the ATLAS detector at the LHC*, Eur. Phys. J. C **83** (2023) 982, arXiv: 2212.09379 [hep-ex].

[32] ATLAS Collaboration, *Preliminary luminosity calibration of the ATLAS* 13.6 *TeV data recorded in 2024 and combination with the 2022 and 2023 measurements*, ATL-DAPR-PUB-2025-001, 2025, URL: https://cds.cern.ch/record/2948582.

[33] S. Agostinelli et al., *Geant4 – a simulation toolkit*, Nucl. Instrum. Meth. A **506** (2003) 250.

[34] ATLAS Collaboration, *The ATLAS Simulation Infrastructure*, Eur. Phys. J. C **70** (2010) 823, arXiv: 1005.4568 [physics.ins-det].

[35] ATLAS Collaboration, *Emulating the impact of additional proton–proton interactions in the ATLAS simulation by presampling sets of inelastic Monte Carlo events*, Comput. Softw. Big Sci. **6** (2022) 3, arXiv: 2102.09495 [hep-ex].

[36] K. Werner, F.-M. Liu and T. Pierog, *Parton ladder splitting and the rapidity dependence of transverse momentum spectra in deuteron–gold collisions at the BNL Relativistic Heavy Ion Collider*, Phys. Rev. C **74** (2006) 044902, arXiv: hep-ph/0506232 [hep-ph].

[37] C. Bierlich et al., *A comprehensive guide to the physics and usage of PYTHIA 8.3*, SciPost Phys. Codebases (2022) 8, arXiv: 2203.11601 [hep-ph].

[38] T. Pierog, I. Karpenko, J. M. Katzy, E. Yatsenko and K. Werner, *EPOS LHC: Test of collective hadronization with data measured at the CERN Large Hadron Collider*, Phys. Rev. C **92** (2015) 034906, arXiv: 1306.0121 [hep-ph].

[39] ATLAS Collaboration, *The Pythia 8 A3 tune description of ATLAS minimum bias and inelastic measurements incorporating the Donnachie–Landshoff diffractive model*, ATL-PHYS-PUB-2016-017, 2016, URL: https://cds.cern.ch/record/2206965.

[40] NNPDF Collaboration, R. D. Ball et al., *Parton distributions with LHC data*, Nucl. Phys. B **867** (2013) 244, arXiv: 1207.1303 [hep-ph].

[41] T. Sjöstrand et al., *An introduction to PYTHIA 8.2*, Comput. Phys. Commun. **191** (2015) 159, arXiv: 1410.3012 [hep-ph].

[42] ATLAS Collaboration, *ATLAS Pythia 8 tunes to* 7 *TeV data*, ATL-PHYS-PUB-2014-021, 2014, URL: https://cds.cern.ch/record/1966419.

[43] B. Andersson, G. Gustafson, G. Ingelman and T. Sjöstrand, *Parton fragmentation and string dynamics*, Phys. Rept. **97** (1983) 31.

[44] T. Sjöstrand, *Jet fragmentation of multiparton configurations in a string framework*, Nucl. Phys. B **248** (1984) 469.

[45] S. Mrenna and P. Skands, *Automated parton-shower variations in PYTHIA 8*, Phys. Rev. D **94** (2016) 074005, arXiv: 1605.08352 [hep-ph].

[46] P. Nason, *A new method for combining NLO QCD with shower Monte Carlo algorithms*, JHEP **11** (2004) 040, arXiv: hep-ph/0409146.

[47] S. Frixione, P. Nason and C. Oleari, *Matching NLO QCD computations with parton shower simulations: the POWHEG method*, JHEP **11** (2007) 070, arXiv: 0709.2092 [hep-ph].

[48] S. Alioli, K. Hamilton, P. Nason, C. Oleari and E. Re, *Jet pair production in POWHEG*, JHEP **04** (2011) 081, arXiv: 1012.3380 [hep-ph].

[49] NNPDF Collaboration, R. D. Ball et al., *Parton distributions for the LHC run II*, JHEP **04** (2015) 040, arXiv: 1410.8849 [hep-ph].

[50] E. Bothmann et al., *Event generation with Sherpa 2.2*, SciPost Phys. **7** (2019) 034, arXiv: 1905.09127 [hep-ph].

[51] S. Dulat et al., *New parton distribution functions from a global analysis of quantum chromodynamics*, Phys. Rev. D **93** (2016) 033006, arXiv: 1506.07443 [hep-ph].

[52] S. Schumann and F. Krauss,
A parton shower algorithm based on Catani–Seymour dipole factorisation, JHEP **03** (2008) 038,
arXiv: 0709.1027 [hep-ph].

[53] J.-C. Winter, F. Krauss and G. Soff, *A modified cluster-hadronisation model*,
Eur. Phys. J. C **36** (2004) 381, arXiv: hep-ph/0311085.

[54] T. Sjöstrand, S. Mrenna and P. Skands, *PYTHIA 6.4 physics and manual*, JHEP **05** (2006) 026,
arXiv: hep-ph/0603175.

[55] M. Bähr et al., *Herwig++ physics and manual*, Eur. Phys. J. C **58** (2008) 639,
arXiv: 0803.0883 [hep-ph].

[56] J. Bellm et al., *Herwig 7.0/Herwig++ 3.0 release note*, Eur. Phys. J. C **76** (2016) 196,
arXiv: 1512.01178 [hep-ph].

[57] J. Bellm et al., *Herwig 7.1 Release Note*, (2017), arXiv: 1705.06919 [hep-ph].

[58] B. R. Webber, *A QCD Model for Jet Fragmentation Including Soft Gluon Interference*,
Nucl. Phys. B **238** (1984) 492.

[59] Plätzer, Simon and Gieseke, Stefan, *Coherent Parton Showers with Local Recoils*,
JHEP **01** (2011) 024, arXiv: 0909.5593 [hep-ph].

[60] ATLAS Collaboration,
Jet reconstruction and performance using particle flow with the ATLAS Detector,
Eur. Phys. J. C **77** (2017) 466, arXiv: 1703.10485 [hep-ex].

[61] M. Cacciari, G. P. Salam and G. Soyez, *The anti-k_t jet clustering algorithm*, JHEP **04** (2008) 063,
arXiv: 0802.1189 [hep-ph].

[62] M. Cacciari, G. P. Salam and G. Soyez, *FastJet user manual*, Eur. Phys. J. C **72** (2012) 1896,
arXiv: 1111.6097 [hep-ph].

[63] ATLAS Collaboration,
Topological cell clustering in the ATLAS calorimeters and its performance in LHC Run 1,
Eur. Phys. J. C **77** (2017) 490, arXiv: 1603.02934 [hep-ex].

[64] ATLAS Collaboration, *Jet energy scale and resolution measured in proton–proton collisions at $\sqrt{s} = 13$ TeV with the ATLAS detector*, Eur. Phys. J. C **81** (2021) 689,
arXiv: 2007.02645 [hep-ex].

[65] ATLAS Collaboration,
Jet energy measurement with the ATLAS detector in proton–proton collisions at $\sqrt{s} = 7$ TeV,
Eur. Phys. J. C **73** (2013) 2304, arXiv: 1112.6426 [hep-ex].

[66] M. Cacciari and G. P. Salam, *Pileup subtraction using jet areas*, Phys. Lett. B **659** (2008) 119,
arXiv: 0707.1378 [hep-ph].

[67] CDF Collaboration,
Measurement of b-jet shapes in inclusive jet production in $p\bar{p}$ collisions at $\sqrt{s} = 1.96$ TeV,
Phys. Rev. D **78** (2008) 072005, arXiv: 0806.1699 [hep-ex].

[68] ATLAS Collaboration,
Measurement of jet shapes in top-quark pair events at $\sqrt{s} = 7$ TeV using the ATLAS detector,
Eur. Phys. J. C **73** (2013) 2676, arXiv: 1307.5749 [hep-ex].

[69] ATLAS Collaboration, *Measurement of the flavour composition of dijet events in pp collisions at $\sqrt{s} = 7$ TeV with the ATLAS detector*, Eur. Phys. J. C **73** (2013) 2301, arXiv: 1210.0441 [hep-ex].

[70] ATLAS Collaboration, *Operation of the ATLAS trigger system in Run 2*, JINST **15** (2020) P10004, arXiv: 2007.12539 [physics.ins-det].

[71] V. Lendermann et al., *Combining Triggers in HEP data analysis*, Nucl. Instrum. Meth. A **604** (2009) 707, arXiv: 0901.4118 [hep-ex].

[72] ATLAS Collaboration, *Performance of pile-up mitigation techniques for jets in pp collisions at $\sqrt{s} = 8$ TeV using the ATLAS detector*, Eur. Phys. J. C **76** (2016) 581, arXiv: 1510.03823 [hep-ex].

[73] ATLAS Collaboration, *Identification and rejection of pile-up jets at high pseudorapidity with the ATLAS detector*, Eur. Phys. J. C **77** (2017) 580, arXiv: 1705.02211 [hep-ex], Erratum: Eur. Phys. J. C **77** (2017) 712.

[74] D. P. Kingma and J. Ba, *Adam: A Method for Stochastic Optimization*, 2017, arXiv: 1412.6980 [cs.LG].

[75] R. K. Srivastava, K. Greff and J. Schmidhuber, *Highway Networks*, 2015, arXiv: 1505.00387 [cs.LG].

[76] ATLAS Collaboration, *Measurement of jet charge in dijet events from $\sqrt{s} = 8$ TeV pp collisions with the ATLAS detector*, Phys. Rev. D **93** (2016) 052003, arXiv: 1509.05190 [hep-ex].

[77] ATLAS Collaboration, *Accuracy versus precision in boosted top tagging with the ATLAS detector*, JINST **19** (2024) P08018, arXiv: 2407.20127 [hep-ex].

[78] ATLAS Collaboration, *Measurements of Lund subjet multiplicities in 13 TeV proton–proton collisions with the ATLAS detector*, Phys. Lett. B **859** (2024) 139090, arXiv: 2402.13052 [hep-ex].

[79] ATLAS Collaboration, *Studies on top-quark Monte Carlo modelling with Sherpa and MG5_aMC@NLO*, ATL-PHYS-PUB-2017-007, 2017, URL: https://cds.cern.ch/record/2261938.

[80] A. Buckley et al., *LHAPDF6: parton density access in the LHC precision era*, Eur. Phys. J. C **75** (2015) 132, arXiv: 1412.7420 [hep-ph].

[81] ATLAS Collaboration, *ATLAS Computing Acknowledgements*, ATL-SOFT-PUB-2025-001, 2025, URL: https://cds.cern.ch/record/2922210.

The ATLAS Collaboration

G. Aad[103], E. Aakvaag[17], B. Abbott[122], S. Abdelhameed[118a], K. Abeling[55], N.J. Abicht[49], S.H. Abidi[30], M. Aboelela[45], A. Aboulhorma[36e], H. Abramowicz[156], B.S. Acharya[69a,69b,m], A. Ackermann[63a], C. Adam Bourdarios[4], L. Adamczyk[86a], S.V. Addepalli[148], M.J. Addison[102], J. Adelman[117], A. Adiguzel[22c], T. Adye[136], A.A. Affolder[138], Y. Afik[40], M.N. Agaras[13], A. Aggarwal[101], C. Agheorghiesei[28c], F. Ahmadov[39,ad], S. Ahuja[96], S. Ahuja[168], X. Ai[142b], G. Aielli[76a,76b], A. Aikot[168], M. Ait Tamlihat[36e], B. Aitbenchikh[36a], T.P.A. Åkesson[99], D. Akiyama[173], N.N. Akolkar[25], S. Aktas[171], G.L. Alberghi[24b], J. Albert[170], U. Alberti[20], P. Albicocco[53], G.L. Albouy[60], S. Alderweireldt[52], Z.L. Alegria[123], M. Aleksa[37], I.N. Aleksandrov[39], C. Alexa[28b], T. Alexopoulos[10], F. Alfonsi[24b], M. Algren[56], M. Alhroob[172], B. Ali[134], H.M.J. Ali[92,v], S. Ali[32], S.W. Alibocus[93], M. Aliev[34c], G. Alimonti[71a], W. Alkakhi[55], C. Allaire[66], B.M.M. Allbrooke[151], D.R. Allen[123], J.S. Allen[102], J.F. Allen[52], C.S. Alley[1], A. Aloisio[72a,72b], F. Alonso[91], C. Alpigiani[141], Z.M.K. Alsolami[92], A. Alvarez Fernandez[101], M. Alves Cardoso[56], M.G. Alviggi[72a,72b], M. Aly[102], Y. Amaral Coutinho[82b], A. Ambler[105], C. Amelung[37], M. Amerl[102], T. Amezza[129], B. Amini[54], K. Amirie[160], A. Amirkhanov[39], S.P. Amor Dos Santos[132a], D. Amperiadou[157], S. An[83], C. Anastopoulos[144], T. Andeen[11], J.K. Anders[93], A.C. Anderson[59], A. Andreazza[71a,71b], S. Angelidakis[9], A. Angerami[42], A.V. Anisenkov[39], A. Annovi[74a], C. Antel[37], E. Antipov[150], M. Antonelli[53], F. Anulli[75a], M. Aoki[83], T. Aoki[158], M.A. Aparo[13], L. Aperio Bella[48], M. Apicella[31], C. Appelt[156], A. Apyan[27], M. Arampatzi[10], S.J. Arbiol Val[87], C. Arcangeletti[53], A.T.H. Arce[51], J-F. Arguin[109], S. Argyropoulos[157], J.-H. Arling[48], O. Arnaez[4], H. Arnold[150], G. Artoni[75a,75b], H. Asada[112], S. Asatryan[178], N.A. Asbah[37], R.A. Ashby Pickering[172], A.M. Aslam[96], K. Assamagan[30], R. Astalos[29a], K.S.V. Astrand[99], S. Atashi[164], R.J. Atkin[34a], H. Atmani[36f], P.A. Atmasiddha[130], K. Augsten[134], A.D. Auriol[41], V.A. Austrup[102], A.S. Avad[95], G. Avolio[37], K. Axiotis[56], A. Azzam[13], D. Babal[29b], H. Bachacou[137], K. Bachas[157,p], A. Bachiu[35], E. Bachmann[50], M.J. Backes[63a], A. Badea[40], T.M. Baer[107], M. Bahmani[19], D. Bahner[54], K. Bai[125], L. Baines[95], O.K. Baker[177], D. Bakshi Gupta[8], L.E. Balabram Filho[82b], V. Balakrishnan[122], R. Balasubramanian[4], E.M. Baldin[38], P. Balek[86a], E. Ballabene[24b,24a], F. Balli[137], L.M. Baltes[63a], W.K. Balunas[128], J. Balz[101], I. Bamwidhi[118b], E. Banas[87], M. Bandieramonte[131], A. Bandyopadhyay[25], S. Bansal[25], L. Barak[156], M. Barakat[48], E.L. Barberio[106], D. Barberis[18b], M. Barbero[103], M.Z. Barel[116], T. Barillari[111], M-S. Barisits[37], T. Barklow[148], P. Baron[135], D.A. Baron Moreno[102], A. Baroncelli[62], A.J. Barr[128], J.D. Barr[97], F. Barreiro[100], J. Barreiro Guimarães da Costa[14], M.G. Barros Teixeira[132a], S. Barsov[38], F. Bartels[63a], R. Bartoldus[148], A.E. Barton[92], P. Bartos[29a], M. Baselga[49], S. Bashiri[87], A. Bassalat[66,b], M.J. Basso[161a], S. Bataju[45], R. Bate[169], R.L. Bates[59], S. Batlamous[100], M. Battaglia[138], D. Battulga[19], M. Bauce[75a,75b], L. Bauckhage[48], P. Bauer[25], L.T. Bayer[48], L.T. Bazzano Hurrell[31], J.B. Beacham[111], T. Beau[129], J.Y. Beaucamp[91], P.H. Beauchemin[163], P. Bechtle[25], H.P. Beck[20,o], K. Becker[172], A.J. Beddall[81], V.A. Bednyakov[39], C.P. Bee[150], L.J. Beemster[16], M. Begalli[82d], M. Begel[30], J.K. Behr[48], J.F. Beirer[37], F. Beisiegel[25], M. Belfkir[118b], G. Bella[156], L. Bellagamba[24b], A. Bellerive[35], C.D. Bellgraph[68], P. Bellos[21], K. Beloborodov[38], I. Benaoumeur[21], D. Benchekroun[36a], F. Bendebba[36a], Y. Benhammou[156], K.C. Benkendorfer[61], L. Beresford[48], M. Beretta[53], E. Bergeaas Kuutmann[166], N. Berger[4], B. Bergmann[134], J. Beringer[18a], G. Bernardi[5], C. Bernius[148], F.U. Bernlochner[25],

A. Berrocal Guardia[13], T. Berry[96], P. Berta[135], A. Berti[132a], R. Bertrand[103], S. Bethke[111],
A. Betti[75a,75b], A.J. Bevan[95], L. Bezio[56], N.K. Bhalla[54], S. Bharthuar[111], S. Bhatta[150],
P. Bhattarai[148], Z.M. Bhatti[119], K.D. Bhide[54], V.S. Bhopatkar[123], R.M. Bianchi[131],
G. Bianco[24b,24a], O. Biebel[110], M. Biglietti[77a], P. Bijl[54], C.S. Billingsley[45], Y. Bimgdi[36f],
M. Bindi[55], A. Bingham[176], A. Bingul[22b], C. Bini[75a,75b], G.A. Bird[33], M. Birman[174],
M. Biros[135], S. Biryukov[151], T. Bisanz[49], E. Bisceglie[24b,24a], J.P. Biswal[136], D. Biswas[146],
I. Bloch[48], A. Blue[59], U. Blumenschein[95], V.S. Bobrovnikov[39], L. Boccardo[57b,57a],
M. Boehler[54], B. Boehm[171], D. Bogavac[13], A.G. Bogdanchikov[38], L.S. Boggia[129],
V. Boisvert[96], P. Bokan[166], T. Bold[86a], M. Bomben[5], M. Bona[95], M. Boonekamp[137],
A.G. Borbély[59], I.S. Bordulev[38], G. Borissov[92], D. Bortoletto[128], D. Boscherini[24b],
M. Bosman[13], K. Bouaouda[36a], L. Boudet[4], J. Boudreau[131], E.V. Bouhova-Thacker[92],
D. Boumediene[41], R. Bouquet[57b,57a], A. Boveia[121], J. Boyd[37], D. Boye[30], I.R. Boyko[39],
L. Bozianu[56], J. Bracinik[21], N. Brahimi[4], G. Brandt[176], O. Brandt[33], B. Brau[104],
R. Brener[174], L. Brenner[116], R. Brenner[166], S. Bressler[174], G. Brianti[116], D. Britton[59],
D. Britzger[111], I. Brock[25], R. Brock[108], H. Bronson[130], G. Brooijmans[42], A.J. Brooks[68],
E.M. Brooks[161b], E. Brost[30], L.M. Brown[170,161a], L.E. Bruce[61], T.L. Bruckler[128],
P.A. Bruckman de Renstrom[87], B. Brüers[48], A. Bruni[24b], G. Bruni[24b], D. Brunner[47a,47b],
M. Bruschi[24b], N. Bruscino[75a,75b], T. Buanes[17], Q. Buat[141], D. Buchin[111], A.G. Buckley[59],
M. Buhring[50], O. Bulekov[81], B.A. Bullard[148], S. Burdin[93], C.D. Burgard[49], A.M. Burger[90],
B. Burghgrave[8], O. Burlayenko[54], J. Burleson[167], J.C. Burzynski[147], V. Büscher[101],
P.J. Bussey[59], O. But[25], J.M. Butler[26], C.M. Buttar[59], J.M. Butterworth[97], P. Butti[37],
W. Buttinger[136], C.J. Buxo Vazquez[108], A.R. Buzykaev[39], S. Cabrera Urbán[168],
L. Cadamuro[66], H. Cai[37], Y. Cai[24b,113c,24a], Y. Cai[113a], V.M.M. Cairo[37], O. Cakir[3a],
N. Calace[37], P. Calafiura[18a], G. Calderini[129], P. Calfayan[35], L. Calic[99], G. Callea[59],
L.P. Caloba[82b], D. Calvet[41], S. Calvet[41], R. Camacho Toro[129], S. Camarda[37],
D. Camarero Munoz[27], P. Camarri[76a,76b], C. Camincher[37], M. Campanelli[97], A. Camplani[43],
V. Canale[72a,72b], A.C. Canbay[3a], E. Canonero[96], J. Cantero[168], Y. Cao[167], F. Capocasa[27],
M. Capua[44b,44a], A. Carbone[71a,71b], R. Cardarelli[76a], J.C.J. Cardenas[8], M.P. Cardiff[27],
G. Carducci[44b,44a], T. Carli[37], G. Carlino[72a], J.I. Carlotto[13], B.T. Carlson[131,q],
E.M. Carlson[170], L. Carminati[71a,71b], A. Carnelli[4], M. Carnesale[37], S. Caron[115],
E. Carquin[139g], I.B. Carr[106], S. Carrá[73a,73b], G. Carratta[24b,24a], C. Carrion Martinez[168],
A.M. Carroll[125], M.P. Casado[13,h], P. Casolaro[72a,72b], M. Caspar[48], W.R. Castiglioni[40],
F.L. Castillo[4], L. Castillo Garcia[13], V. Castillo Gimenez[168], N.F. Castro[132a,132e],
A. Catinaccio[37], J.R. Catmore[127], T. Cavaliere[4], V. Cavaliere[30], L.J. Caviedes Betancourt[23b],
E. Celebi[81], S. Cella[156], V. Cepaitis[56], K. Cerny[124], A.S. Cerqueira[82a], A. Cerri[74a,am],
L. Cerrito[76a,76b], F. Cerutti[18a], B. Cervato[71a,71b], A. Cervelli[24b], G. Cesarini[53], S.A. Cetin[81],
P.M. Chabrillat[129], R. Chakkappai[66], S. Chakraborty[172], A. Chambers[61], J. Chan[18a],
W.Y. Chan[158], J.D. Chapman[33], E. Chapon[137], B. Chargeishvili[154b], D.G. Charlton[21],
C. Chauhan[133], Y. Che[113a], S. Chekanov[6], G.A. Chelkov[39,a], B. Chen[170], H. Chen[30],
J. Chen[143a], J. Chen[147], M. Chen[128], S. Chen[88], S.J. Chen[113a], X. Chen[143a], X. Chen[15,ah],
Z. Chen[62], C.L. Cheng[175], H.C. Cheng[64a], S. Cheong[148], A. Cheplakov[39],
E. Cherepanova[116], E. Cheu[7], K. Cheung[65], L. Chevalier[137], G. Chiarelli[74a],
G. Chiodini[70a], A.S. Chisholm[21], A. Chitan[28b], M. Chitishvili[168], M.V. Chizhov[39,r],
K. Choi[11], Y. Chou[141], E.Y.S. Chow[115], K.L. Chu[174], M.C. Chu[64a], Z. Chubinidze[53],
J. Chudoba[133], J.J. Chwastowski[87], D. Cieri[111], K.M. Ciesla[86a], V. Cindro[94], A. Ciocio[18a],
F. Cirotto[72a,72b], Z.H. Citron[174], M. Citterio[71a], D.A. Ciubotaru[28b], A. Clark[56], P.J. Clark[52],
N. Clarke Hall[97], C. Clarry[160], S.E. Clawson[48], C. Clement[47a,47b], L. Clissa[24b,24a],

Y. Coadou[103], M. Cobal[69a,69c], A. Coccaro[57b], R.F. Coelho Barrue[132a], R. Coelho Lopes De Sa[104], S. Coelli[71a], M.M. Cohen[130], L.S. Colangeli[160], B. Cole[42], P. Collado Soto[100], J. Collot[60], R. Coluccia[70a,70b], P. Conde Muiño[132a,132g], M.P. Connell[34c], S.H. Connell[34c], E.I. Conroy[128], M. Contreras Cossio[11], F. Conventi[72a,aj], A.M. Cooper-Sarkar[128], L. Corazzina[75a,75b], F.A. Corchia[24b,24a], A. Cordeiro Oudot Choi[141], L.D. Corpe[41], M. Corradi[75a,75b], F. Corriveau[105,ab], A. Cortes-Gonzalez[158], M.J. Costa[168], F. Costanza[4], D. Costanzo[144], J. Couthures[4], G. Cowan[96], K. Cranmer[175], L. Cremer[49], D. Cremonini[24b,24a], S. Crépé-Renaudin[60], F. Crescioli[129], T. Cresta[73a,73b], M. Cristinziani[146], M. Cristoforetti[78a,78b], E. Critelli[97], G. Crosetti[44b,44a], A. Cueto[100], H. Cui[97], Z. Cui[7], B.M. Cunnett[151], W.R. Cunningham[59], F. Curcio[168], J.R. Curran[52], M.J. Da Cunha Sargedas De Sousa[57b,57a], J.V. Da Fonseca Pinto[82b], C. Da Via[102], W. Dabrowski[86a], T. Dado[37], S. Dahbi[153], T. Dai[107], D. Dal Santo[20], C. Dallapiccola[104], M. Dam[43], G. D'amen[30], V. D'Amico[110], J.R. Dandoy[35], M. D'Andrea[57b,57a], D. Dannheim[37], G. D'anniballe[74a,74b], M. Danninger[147], V. Dao[150], G. Darbo[57b], S.J. Das[30], F. Dattola[48], S. D'Auria[71a,71b], A. D'Avanzo[72a,72b], T. Davidek[135], J. Davidson[172], I. Dawson[95], K. De[8], C. De Almeida Rossi[160], R. De Asmundis[72a], N. De Biase[48], S. De Castro[24b,24a], N. De Groot[115], P. de Jong[116], H. De la Torre[117], A. De Maria[113a], A. De Salvo[75a], U. De Sanctis[76a,76b], F. De Santis[70a,70b], A. De Santo[151], J.B. De Vivie De Regie[60], J. Debevc[94], D.V. Dedovich[39], J. Degens[93], A.M. Deiana[45], J. Del Peso[100], L. Delagrange[129], F. Deliot[137], C.M. Delitzsch[49], M. Della Pietra[72a,72b], D. Della Volpe[56], A. Dell'Acqua[37], L. Dell'Asta[71a,71b], M. Delmastro[4], C.C. Delogu[57b,57a], P.A. Delsart[60], S. Demers[177], M. Demichev[39], S.P. Denisov[38], H. Denizli[22a,l], M.G. Depala[93], L. D'Eramo[41], D. Derendarz[87], F. Derue[129], P. Dervan[93,*], A.M. Desai[1], K. Desch[25], F.A. Di Bello[74a,74b], A. Di Ciaccio[76a,76b], L. Di Ciaccio[4], C. Di Donato[72a,72b], A. Di Girolamo[37], G. Di Gregorio[66], A. Di Luca[78a,78b], B. Di Micco[77a,77b], R. Di Nardo[77a,77b], K.F. Di Petrillo[40], M. Diamantopoulou[35], F.A. Dias[116], M.A. Diaz[139a,139b], A.R. Didenko[39], M. Didenko[168], S.D. Diefenbacher[18a], E.B. Diehl[107], S. Díez Cornell[48], C. Diez Pardos[146], C. Dimitriadi[149], A. Dimitrievska[21], A. Dimri[150], Y. Ding[62], J. Dingfelder[25], T. Dingley[128], I-M. Dinu[28b], S.J. Dittmeier[63b], F. Dittus[37], M. Divisek[135], B. Dixit[93], F. Djama[103], T. Djobava[154b], C. Doglioni[102,99], A. Dohnalova[29a], Z. Dolezal[135], K. Domijan[86a], K.M. Dona[40], M. Donadelli[82d], B. Dong[108], J. Donini[41], A. D'Onofrio[72a,72b], M. D'Onofrio[93], J. Dopke[136], A. Doria[72a], N. Dos Santos Fernandes[132a], I.A. Dos Santos Luz[82e], P. Dougan[45], M.T. Dova[91], A.T. Doyle[59], M.P. Drescher[55], E. Dreyer[174], I. Drivas-koulouris[10], M. Drnevich[119], D. Du[62], T.A. du Pree[116], Z. Duan[113a], M. Dubau[4], F. Dubinin[39], M. Dubovsky[29a], E. Duchovni[174], G. Duckeck[110], P.K. Duckett[97], O.A. Ducu[28b], D. Duda[52], A. Dudarev[37], M.M. Dudek[87], E.R. Duden[27], M. D'uffizi[102], L. Duflot[66], M. Dührssen[37], I. Duminica[28g], A.E. Dumitriu[28b], M. Dunford[63a], A. Duperrin[103], H. Duran Yildiz[3a], A. Durglishvili[154b], G.I. Dyckes[18a], M. Dyndal[86a], B.S. Dziedzic[37], Z.O. Earnshaw[151], G.H. Eberwein[128], B. Eckerova[29a], S. Eggebrecht[55], E. Egidio Purcino De Souza[82e], G. Eigen[17], K. Einsweiler[18a], T. Ekelof[166], P.A. Ekman[99], S. El Farkh[36b], Y. El Ghazali[62], H. El Jarrari[105], A. El Moussaouy[36a], I. Elbaz[156], D. Elitez[37], M. Ellert[166], F. Ellinghaus[176], T.A. Elliot[96], J. Elmsheuser[30], M. Elsawy[118a], M. Elsing[37], D. Emeliyanov[136], Y. Enari[83], S. Epari[109], D. Ernani Martins Neto[87], F. Ernst[37], M. Escalier[66], C. Escobar[168], R. Estevam De Paula[82c], E. Etzion[156], G. Evans[132a,132b], H. Evans[68], L.S. Evans[48], A. Ezhilov[38], S. Ezzarqtouni[36a], F. Fabbri[24b,24a], L. Fabbri[24b,24a], G. Facini[97], V. Fadeyev[138], R.M. Fakhrutdinov[38], D. Fakoudis[101], S. Falciano[75a], L.F. Falda Ulhoa Coelho[27], F. Fallavollita[111], G. Falsetti[44b,44a], J. Faltova[135], C. Fan[167], K.Y. Fan [64b], Y. Fan [14], Y. Fang [14,113c], M. Fanti [71a,71b], M. Faraj [69a,69c], Z. Farazpay [98], A. Farbin [8], A. Farilla [77a], K. Farman [153], J.N. Farr [177], M.S. Farrington [61], S.M. Farrington [136,52], F. Fassi [36e], D. Fassouliotis [9], L. Fayard [66], P. Federic [135], P. Federicova [133], O.L. Fedin [38,a], M. Feickert [175], L. Feligioni [103], D.E. Fellers [18a], C. Feng [142a], Y. Feng[14], Z. Feng [66], B. Fernandez Barbadillo [92], P. Fernandez Martinez [67], M.J.V. Fernoux [103], J. Ferrando [92], A. Ferrari [166], P. Ferrari [116,115], R. Ferrari [73a], D. Ferrere [56], C. Ferretti [107], M.P. Fewell [1], D. Fiacco [75a,75b], F. Fiedler [101], P. Fiedler [134], S. Filimonov [39], M.S. Filip [28b,s], A. Filipčič [94], E.K. Filmer [161a], F. Filthaut [115], M.C.N. Fiolhais [132a,132c,c], L. Fiorini [168], W.C. Fisher [108], T. Fitschen [102], P.M. Fitzhugh[137], I. Fleck [146], P. Fleischmann [107], T. Flick [176], M. Flores [34d,ag], L.R. Flores Castillo [64a], M. Foll [127], F.M. Follega [78a,78b], N. Fomin [33], J.H. Foo [160], A. Formica [137], A.C. Forti [102], E. Fortin [150], A.W. Fortman [18a], L. Foster [18a], L. Fountas [9], H. Fox [92], P. Francavilla [74a,74b], S. Francescato [61], S. Franchellucci [56], M. Franchini [24b,24a], S. Franchino [63a], D. Francis[37], L. Franco [48], L. Franconi [48], M. Franklin [61], G. Frattari [27], Y.Y. Frid [156], J. Friend [59], N. Fritzsche [37], A. Froch [56], D. Froidevaux [37], J.A. Frost [136], Y. Fu [108], S. Fuenzalida Garrido [139g], M. Fujimoto [150], K.Y. Fung [64a], E. Furtado De Simas Filho [82e], M. Furukawa [158], M. Fuste Costa[48], J. Fuster [168], A. Gaa [55], A. Gabrielli [24b,24a], A. Gabrielli [160], P. Gadow [37], G. Gagliardi [57b,57a], L.G. Gagnon [18a], S. Gaid [84b], S. Galantzan [156], J. Gallagher [1], E.J. Gallas [128], A.L. Gallen [166], B.J. Gallop [136], K.K. Gan [121], Y. Gao [52], Z. Gao [113a], A. Garabaglu [141], F.M. Garay Walls [139a,139b], C. García [168], A. Garcia Alonso [116], A.G. Garcia Caffaro [177], J.E. García Navarro [168], M.A. Garcia Ruiz [23b], M. Garcia-Sciveres [18a], G.L. Gardner [130], R.W. Gardner [40], N. Garelli [163], R.B. Garg [148], J.M. Gargan [33], C.A. Garner[160], C.M. Garvey [34a], V.K. Gassmann[163], G. Gaudio [73a], V. Gautam[13], J. Gavranovic [94], I.L. Gavrilenko [132a], A. Gavrilyuk [38], C. Gay [169], G. Gaycken [125], A. Gekow[121], C. Gemme [57b], M.H. Genest [60], A.D. Gentry [114], S. George [96], T. Geralis [46], A.A. Gerwin [122], P. Gessinger-Befurt [37], M. Ghani [172], K. Ghorbanian [95], A. Ghosal [146], A. Ghosh [164], A. Ghosh [7], B. Giacobbe [24b], S. Giagu [75a,75b], A. Giannini [62], S.M. Gibson [96], D.T. Gil [86b], A.K. Gilbert [86a], B.J. Gilbert [42], D. Gillberg [35], G. Gilles [116], D.M. Gingrich [2,ai], M.P. Giordani [69a,69c], P.F. Giraud [137], G. Giugliarelli [69a,69c], D. Giugni [71a], F. Giuli [76a,76b], I. Gkialas [9,i], L.K. Gladilin [38], C. Glasman [100], M. Glazewska [20], R.M. Gleason [164], G. Glemža [48], M. Glisic[125], I. Gnesi [44b], Y. Go [30], M. Goblirsch-Kolb [37], B. Gocke [49], D. Godin[109], B. Gokturk [22a], S. Goldfarb [106], T. Golling [56], M.G.D. Gololo [34c], A. Golub [141], D. Golubkov [38], J.P. Gombas [108], A. Gomes [132a,132b], G. Gomes Da Silva [146], A.J. Gomez Delegido [37], R. Gonçalo [132a], A. Gongadze [154c], F. Gonnella [21], J.L. Gonski [148], R.Y. González Andana [52], S. González de la Hoz [168], M.V. Gonzalez Rodrigues [48], R. Gonzalez Suarez [166], S. Gonzalez-Sevilla [56], L. Goossens [37], B. Gorini [37], E. Gorini [70a,70b], A. Gorišek [94], T.C. Gosart [130], A.T. Goshaw [51], M.I. Gostkin [39], S. Goswami [123], C.A. Gottardo [37], S.A. Gotz [110], M. Gouighri [36b], A.G. Goussiou [141], N. Govender [34c], R.P. Grabarczyk [128], I. Grabowska-Bold [86a], K. Graham [35], E. Gramstad [127], S. Grancagnolo [70a,70b], C.M. Grant[1], P.M. Gravila [28f], F.G. Gravili [70a,70b], H.M. Gray [18a], M. Greco [111], M.J. Green [1], C. Grefe [25], A.S. Grefsrud [17], I.M. Gregor [48], K.T. Greif [164], P. Grenier [148], S.G. Grewe[111], K. Grimm [32], S. Grinstein [13,x], E. Gross [174], J. Grosse-Knetter [55], L.H. Grossman [18b], L. Guan [107], G. Guerrieri [37], R. Guevara [127], R. Gugel [101], J.A.M. Guhit [107], A. Guida [19], E. Guilloton [172], S. Guindon [37], F. Guo [14,113c], J. Guo [143a], L. Guo [48], L. Guo [113b,u], Y. Guo [107], Y. Guo [42], A. Gupta [49], R. Gupta [131], S. Gupta [27], S. Gurbuz [25], S.S. Gurdasani [48], G. Gustavino [75a,75b], P. Gutierrez [122], L.F. Gutierrez Zagazeta [130], M. Gutsche [50], C. Gutschow [97], C. Gwenlan [128], C.B. Gwilliam [93], E.S. Haaland [127], A. Haas [119], M. Habedank [59], C. Haber [18a], H.K. Hadavand[8], A. Haddad[41], A. Hadef[50], A.I. Hagan[92], J.J. Hahn[146], M. Haleem[171], J. Haley[123], G.D. Hallewell[103], J.A. Hallford[48], K. Hamano[170], H. Hamdaoui[166], M. Hamer[25], S.E.D. Hammoud[66], E.J. Hampshire[96], L. Han[113a], L. Han[62], S. Han[14], K. Hanagaki[83], M. Hance[138], D.A. Hangal[42], H. Hanif[147], M.D. Hank[130], J.B. Hansen[43], P.H. Hansen[43], T. Harenberg[176], S. Harkusha[178], M.L. Harris[104], Y.T. Harris[25], J. Harrison[13], P.F. Harrison[172], M.L.E. Hart[97], N.M. Hartman[111], N.M. Hartmann[110], R.Z. Hasan[96,136], Y. Hasegawa[145], D. Hashimoto[112], F. Haslbeck[37], S. Hassan[17], R. Hauser[108], M. Haviernik[135], C.M. Hawkes[21], R.J. Hawkings[37], Y. Hayashi[158], D. Hayden[108], R.L. Hayes[116], C.P. Hays[128], J.M. Hays[95], H.S. Hayward[93], M. He[14,113c], Y. He[48], Y. He[97], N.B. Heatley[95], V. Hedberg[99], J. Heilman[35], S. Heim[48], T. Heim[18a], J.J. Heinrich[125], L. Heinrich[111], J. Hejbal[133], M. Helbig[50], A. Held[175], S. Hellesund[17], C.M. Helling[169], H. Herde[99], Y. Hernández Jiménez[150], L.M. Herrmann[25], G. Herten[54], R. Hertenberger[110], L. Hervas[37], M.E. Hesping[101], N.P. Hessey[161a], J. Hessler[111], M. Hidaoui[36b], N. Hidic[135], E. Hill[160], T.S. Hillersoy[17], S.J. Hillier[21], J.R. Hinds[108], F. Hinterkeuser[25], M. Hirose[126], S. Hirose[162], D. Hirschbuehl[176], T.G. Hitchings[102], B. Hiti[94], J. Hobbs[150], R. Hobincu[28e], N. Hod[174], A.M. Hodges[167], M.C. Hodgkinson[144], B.H. Hodkinson[128], A. Hoecker[37], D.D. Hofer[107], J. Hofer[168], J. Hofner[101], M. Holzbock[37], L.B.A.H. Hommels[33], V. Homsak[128], J.J. Hong[68], T.M. Hong[131], B.H. Hooberman[167], W.H. Hopkins[6], M.C. Hoppesch[167], Y. Horii[112], M.E. Horstmann[111], S. Hou[153], M.R. Housenga[167], J. Howarth[59], J. Hoya[6], M. Hrabovsky[124], T. Hryn'ova[4], P.J. Hsu[65], S.-C. Hsu[141], T. Hsu[66], M. Hu[18a], Q. Hu[62], S. Huang[33], X. Huang[14,113c], Y. Huang[135], Y. Huang[113b], Y. Huang[14], Z. Huang[66], Z. Hubacek[134], F. Huegging[25], T.B. Huffman[128], M. Hufnagel Maranha De Faria[82a], C.A. Hugli[48], M. Huhtinen[37], S.K. Huiberts[127], R. Hulsken[105], C.E. Hultquist[18a], D.L. Humphreys[104], N. Huseynov[12], J. Huston[108], B. Huth[37], J. Huth[61], L. Huth[48], R. Hyneman[7], G. Iacobucci[56], G. Iakovidis[30], L. Iconomidou-Fayard[66], J.P. Iddon[37], P. Iengo[72a,72b], Y. Iiyama[158], T. Iizawa[158], Y. Ikegami[83], D. Iliadis[157], N. Ilic[160], H. Imam[36a], G. Inacio Goncalves[82d], S.A. Infante Cabanas[139c], T. Ingebretsen Carlson[47a,47b], J.M. Inglis[95], G. Introzzi[73a,73b], M. Iodice[77a], V. Ippolito[75a,75b], R.K. Irwin[93], M. Ishino[158], W. Islam[175], C. Issever[19], S. Istin[22a,ao], K. Itabashi[126], H. Ito[173], R. Iuppa[78a,78b], A. Ivina[174], S. Izumiyama[112], V. Izzo[72a], P. Jacka[134], P. Jackson[1], P.R. Jacobson[51], P. Jain[48], K. Jakobs[54], T. Jakoubek[174], J. Jamieson[59], W. Jang[158], S. Jankovych[116], M. Javurkova[104], P. Jawahar[102], L. Jeanty[125], J. Jejelava[154a,ae], P. Jenni[54,f], C.E. Jessiman[35], H. Jia[169], J. Jia[150], X. Jia[111,113c], Z. Jia[113a], C. Jiang[52], Q. Jiang[64b], S. Jiggins[48], M. Jimenez Ortega[168], J. Jimenez Pena[13], S. Jin[113a], A. Jinaru[28b], O. Jinnouchi[140], P. Johansson[144], K.A. Johns[7], J.W. Johnson[138], F.A. Jolly[48], D.M. Jones[151], E. Jones[48], K.S. Jones[8], P. Jones[33], R.W.L. Jones[92], T.J. Jones[93], H.L. Joos[55], R. Joshi[121], J. Jovicevic[16], X. Ju[18a], J.J. Junggeburth[37], T. Junkermann[63a], A. Juste Rozas[13,x], M.K. Juzek[87], S. Kabana[139f], A. Kaczmarska[87], S.A. Kadir[148], M. Kado[111], H. Kagan[121], M. Kagan[148], A. Kahn[130], C. Kahra[101], T. Kaji[158], E. Kajomovitz[155], N. Kakati[174], N. Kakoty[13], S. Kandel[8], N. Kanellos[10], N.J. Kang[138], D. Kar[34j], E. Karentzos[25], K. Karki[8], O. Karkout[116], S.N. Karpov[39], Z.M. Karpova[39], V. Kartvelishvili[92,154b], A.N. Karyukhin[38], E. Kasimi[157], J. Katzy[48], S. Kaur[35], K. Kawade[145], M.P. Kawale[122], C. Kawamoto[88], E.F. Kay[37], S. Kazakos[108], K. Kazakova[103], V.F. Kazanin[38], J.M. Keaveney[34a], R. Keeler[170], G.V. Kehris[61], J.S. Keller[35], J.M. Kelly[170], J.J. Kempster[151], O. Kepka[133], J. Kerr[161b], B.P. Kerridge[136], B.P. Kerševan[94], L. Keszeghova[29a], R.A. Khan[131], A. Khanov[123], A.G. Kharlamov[38], T. Kharlamova[38], M. Kholodenko[132a], T.J. Khoo[19], G. Khoriauli[171],

Y. Khoulaki [36a], Y.A.R. Khwaira [129], D. Kim [6], D.W. Kim [18b], Y.K. Kim [40], N. Kimura [97], M.K. Kingston [55], C. Kirfel [25], F. Kirfel [25], J. Kirk [136], A.E. Kiryunin [111], S. Kita [162], O. Kivernyk [25], M. Klassen [163], C. Klein [35], L. Klein [171], M.H. Klein [45], S.B. Klein [56], U. Klein [93], A. Klimentov [30], P. Kluit [116], S. Kluth [111], E. Kneringer [79], T.M. Knight [160], A. Knue [49], M. Kobel [50], D. Kobylianskii [174], S.F. Koch [37], M. Kocian [148], P. Kodyš [135], D.M. Koeck [125], T. Koffas [35], O. Kolay [50], I. Koletsou [4], T. Komarek [87], K. Köneke [55], A.X.Y. Kong [1], T. Kono [120], N. Konstantinidis [97], P. Kontaxakis [56], B. Konya [99], R. Kopeliansky [42], S. Koperny [86a], R. Koppenhofer [54], K. Korcyl [87], K. Kordas [157,d], A. Korn [97], S. Korn [55], I. Korolkov [13], N. Korotkova [38], B. Kortman [116], O. Kortner [111], S. Kortner [111], W.H. Kostecka [117], M. Kostov [29a], V.V. Kostyukhin [146], A. Kotsokechagia [37], A. Kotwal [51], A. Koulouris [37], A. Kourkoumeli-Charalampidi [73a,73b], E. Kourlitis [111], O. Kovanda [125], R. Kowalewski [170], W. Kozanecki [125], A.S. Kozhin [38], V.A. Kramarenko [38], G. Kramberger [94], P. Kramer [25], A. Krasznahorkay [104], A.C. Kraus [117], J.W. Kraus [176], J.A. Kremer [48], N.B. Krengel [146], T. Kresse [50], L. Kretschmann [176], J. Kretzschmar [93], P. Krieger [160], K. Krizka [21], K. Kroeninger [49], H. Kroha [111], J. Kroll [133], J. Kroll [130], K.S. Krowpman [108], U. Kruchonak [39], H. Krüger [25], N. Krumnack[80], M.C. Kruse [51], O. Kuchinskaia [39], S. Kuday [3a], S. Kuehn [37], R. Kuesters [54], T. Kuhl [48], V. Kukhtin [39], Y. Kulchitsky [39], S. Kuleshov [139d,139b], J. Kull [1], E.V. Kumar [110], M. Kumar [34j], N. Kumari [48], P. Kumari [161b], A. Kupco [133], A. Kupich [38], O. Kuprash [54], H. Kurashige [85], L.L. Kurchaninov [161a], O. Kurdysh [4], A. Kurova [38], M. Kuze [140], A.K. Kvam [104], J. Kvita [124], N.G. Kyriacou [141], M. Laassiri [30], C. Lacasta [168], H. Lacker [19], D. Lacour [129], E. Ladygin [39], A. Lafarge [41], B. Laforge [129], T. Lagouri [177], F.Z. Lahbabi [36a], S. Lai [55], W.S. Lai [97], I.K. Lakomiec [55], J.E. Lambert [170], S. Lammers [68], W. Lampl [7], C. Lampoudis [157], G. Lamprinoudis [171], A.N. Lancaster [117], U. Landgraf [54], M.P.J. Landon [95], V.S. Lang [54], A.J. Lankford [164], F. Lanni [37], C.S. Lantz[167], K. Lantzsch [25], A. Lanza [73a], M. Lanzac Berrocal [168], T. Lari [71a], D. Larsen [17], L. Larson [11], F. Lasagni Manghi [24b], M. Lassnig [37], S.D. Lawlor [144], R. Lazaridou[164], M. Lazzaroni [71a,71b], E.T.T. Le [164], H.D.M. Le [108], E.M. Le Boulicaut [177], L.T. Le Pottier [18a], B. Leban [24b,24a], F. Ledroit-Guillon [60], T.F. Lee [161b], L.L. Leeuw [34h], M. Lefebvre [170], C. Leggett [18a], G. Lehmann Miotto [37], M. Leigh [56], W.A. Leight [104], W. Leinonen [115], A. Leisos [157,t], M.A.L. Leite [82c], C.E. Leitgeb [19], R. Leitner [135], K.J.C. Leney [45], T. Lenz [25], S. Leone [74a], C. Leonidopoulos [52], A. Leopold [149], J.H. Lepage Bourbonnais [35], R. Les [108], C.G. Lester [33], M. Levchenko [38], J. Levêque [4], L.J. Levinson [174], G. Levrini [24b,24a], M.P. Lewicki [87], C. Lewis [141], D.J. Lewis [4], L. Lewitt [144], A. Li [30], B. Li [142a], C. Li[107], C-Q. Li [111], H. Li [142a], H. Li [102], H. Li [15], H. Li[62], H. Li [142a], J. Li [143a], L. Li [143a], R. Li [177], S. Li [143b,143a], T. Li [5], Y. Li[14], Z. Li [14,113c], Z. Li [62], S. Liang [14,113c], Z. Liang [14], M. Liberatore [137], B. Liberti [76a], G.B. Libotte [82d], K. Lie [64c], J. Lieber Marin [82e], H. Lien [68], H. Lin [107], S.F. Lin [150], L. Linden [110], R.E. Lindley [7], J.H. Lindon [37], J. Ling [61], E. Lipeles [130], A. Lipniacka [17], A. Lister [169], J.D. Little [68], B. Liu [14], B.X. Liu [113b], D. Liu [155], D. Liu [138], E.H.L. Liu [21], J.K.K. Liu [119], K. Liu [143b], K. Liu [143b], M. Liu [62], M.Y. Liu [62], P. Liu [142a], Q. Liu [148], S. Liu [150], X. Liu [142a], Y. Liu [113b,113c], Y. Liu [167], Y.L. Liu [142a], Y.W. Liu [62], Z. Liu [66,j], S.L. Lloyd [95], E.M. Lobodzinska [48], P. Loch [7], E. Lodhi [160], K. Lohwasser [144], E. Loiacono [48], J.D. Lomas [21], I. Longarini [164], R. Longo [167], A. Lopez Solis [13], N.A. Lopez-canelas [7], N. Lorenzo Martinez [4], A.M. Lory [110], M. Losada [118a], G. Löschcke Centeno [4], X. Lou [14,113c], P.A. Love [92], M. Lu [66], S. Lu [130], Y.J. Lu [153], H.J. Lubatti [141], C. Luci [75a,75b], F.L. Lucio Alves [113a], F. Luehring [68], B.S. Lunday [130], O. Lundberg [149], J. Lunde [37], N.A. Luongo [6], M.S. Lutz [170], A.B. Lux [26], D. Lynn [30], R. Lysak [133], V. Lysenko [134], E. Lytken [99], V. Lyubushkin [39], T. Lyubushkina [39], M.M. Lyukova [150], H. Ma [30], K. Ma [62], L.L. Ma [142a], W. Ma [62], Y. Ma [123], J.C. MacDonald [101], P.C. Machado De Abreu Farias [82e], D. Macina [37], R. Madar [41], T. Madula [97], J. Maeda [85], T. Maeno [30], P.T. Mafa [34f], H. Maguire [144], M. Maheshwari [33], V. Maiboroda [66], A. Maio [132a,132b,132d], K. Maj [86a], O. Majersky [48], S. Majewski [125], R. Makhmanazarov [38], N. Makovec [66], V. Maksimovic [16], B. Malaescu [129], J. Malamant[127], Pa. Malecki [87], V.P. Maleev [38], F. Malek [60,n], M. Mali [94], D. Malito [96], A. Maloizel [5], A. Malvezzi Lopes [82d], S. Malyukov[39], J. Mamuzic [94], G. Mancini [53], M.N. Mancini [27], G. Manco [73a,73b], S.S. Mandarry [151], I. Mandić [94], L. Manhaes de Andrade Filho [82a], I.M. Maniatis [174], J. Manjarres Ramos [90], D.C. Mankad [174], A. Mann [110], T. Manoussos [37], M.N. Mantinan [40], S. Manzoni [37], L. Mao [143a], X. Mapekula [34c], A. Marantis [157], R.R. Marcelo Gregorio [1], G. Marchiori [5], C. Marcon [71a], E. Maricic [16], M. Marinescu [48], S. Marium [48], M. Marjanovic [122], A. Markhoos [54], M. Markovitch [66], M.K. Maroun [104], M.C. Marr [147], G.T. Marsden[102], E.J. Marshall [92], Z. Marshall [18a], S. Marti-Garcia [168], J. Martin [97], T.A. Martin [136], V.J. Martin [52], B. Martin dit Latour [17], L. Martinelli [75a,75b], P. Martinez Agullo [168], V.I. Martinez Outschoorn [104], P. Martinez Suarez [37], S. Martin-Haugh [136], G. Martinovicova [135], V.S. Martoiu [28b], A.C. Martyniuk [97], A. Marzin [37], D. Mascione [78a,78b], L. Masetti [101], J. Masik [102], A.L. Maslennikov [39], S.L. Mason [42], P. Massarotti [72a,72b], P. Mastrandrea [74a,74b], A. Mastroberardino [44b,44a], T. Masubuchi [126], T.T. Mathew [125], J. Matousek [135], D.M. Mattern [49], K. Mauer [48], J. Maurer [28b], T. Maurin [59], A.J. Maury [66], B. Maček [94], C. Mavungu Tsava [103], D.A. Maximov [38], A.E. May [102], E. Mayer [41], R. Mazini [34j], S.M. Mazza [138], E. Mazzeo [37], J.P. Mc Gowan [170], S.P. Mc Kee [107], C.A. Mc Lean [6], C.C. McCracken [169], E.F. McDonald [106], L.F. Mcelhinney [92], J.A. Mcfayden [151], R.P. McGovern [130], R.P. Mckenzie [34j], D.J. Mclaughlin [97], S.J. McMahon [136], C.M. Mcpartland [93], R.A. McPherson [170,ab], S. Mehlhase [110], A. Mehta [93], D. Melini [168], B.R. Mellado Garcia [34j], A.H. Melo [55], F. Meloni [48], A.M. Mendes Jacques Da Costa [102], L. Meng [92], S. Menke [111], M. Mentink [37], E. Meoni [44b,44a], G. Mercado [117], S. Merianos [157], C. Merlassino [69a,69c], C. Meroni [71a,71b], J. Metcalfe [6], A.S. Mete [6], E. Meuser [101], C. Meyer [68], J-P. Meyer [137], Y. Miao[113a], R.P. Middleton [136], M. Mihovilovic [66], L. Mijović [52], G. Mikenberg [174], M. Mikestikova [133], M. Mikuž [94], H. Mildner [101], A. Milic [37], D.W. Miller [40], E.H. Miller [148], A. Milov [174], D.A. Milstead[47a,47b], T. Min[113a], A.A. Minaenko [38], I.A. Minashvili [154b], A.I. Mincer [119], B. Mindur [86a], M. Mineev [39], Y. Mino [88], L.M. Mir [13], M. Miralles Lopez [59], M. Mironova [18a], M. Missio [41], A. Mitra [172], V.A. Mitsou [168], Y. Mitsumori [112], P.S. Miyagawa [95], T. Mkrtchyan [37], M. Mlinarevic [97], T. Mlinarevic [97], M. Mlynarikova [135], L. Mlynarska [86a], C. Mo [143a], S. Mobius [20], M.H. Mohamed Farook [114], S. Mohapatra [42], M.F. Mohd Soberi [52], S. Mohiuddin [123], G. Mokgatitswane [34j], L. Moleri [174], U. Molinatti [128], L.G. Mollier [20], B. Mondal [133], S. Mondal [135], K. Mönig [48], E. Monnier [103], L. Monsonis Romero[168], A. Montella [47a,47b], M. Montella [121], F. Montereali [77a,77b], F. Monticelli [91], S. Monzani [69a,69c], A. Morancho Tarda [43], N. Morange [66], M. Moreno Llácer [168], C. Moreno Martinez [56], J.M. Moreno Perez[23b], P. Morettini [57b], S. Morgenstern [63a], M. Morii [61], M. Morinaga [158], F. Morodei [75a,75b], P. Moschovakos [37], B. Moser [54], M. Mosidze [154b], T. Moskalets [45], P. Moskvitina [115], J. Moss [32], T. Motta Quirino [82d], A. Moussa [36d], Y. Moyal [174,k], H. Moyano Gomez [13], E.J.W. Moyse [104], T.G. Mroz [87], S. Muanza [103], M. Mucha [25], J. Mueller [131], R. Müller [37], G.A. Mullier [166], A.J. Mullin[33], J.J. Mullin[51], A.C. Mullins[45], A.E. Mulski [61], D.P. Mungo [160], D. Munoz Perez [168], F.J. Munoz Sanchez [102], W.J. Murray [172,136], E. Musajan [62], M. Muškinja [94], C. Mwewa [48], A.G. Myagkov [38,a], A.J. Myers [8], G. Myers [107], M. Myska [134], B.P. Nachman [148], K. Nagai [128], K. Nagano [83], R. Nagasaka[158], J.L. Nagle [30,al], E. Nagy [103], A.M. Nairz [37], Y. Nakahama [83], K. Nakamura [83],

K. Nakkalil [5], A. Nandi [63b], H. Nanjo [126], E.A. Narayanan [45], Y. Narukawa [158], I. Naryshkin [38], L. Nasella [71a,71b], S. Nasri [118b], C. Nass [25], G. Navarro [23a], A. Nayaz [19], P.Y. Nechaeva [38], S. Nechaeva [24b,24a], F. Nechansky [133], L. Nedic [128], A. Negri [73a,73b], M. Negrini [24b], C. Nellist [116], C. Nelson [105], K. Nelson [107], S. Nemecek [133], M. Nessi [37,g], M.S. Neubauer [167], J. Newell [93], P.R. Newman [21], Y.W.Y. Ng [167], B. Ngair [118a], H.D.N. Nguyen [109], J.D. Nichols [122], R. Nicolaidou [137], J. Nielsen [138], M. Niemeyer [55], J. Niermann [37], N. Nikiforou [37], V. Nikolaenko [38,a], I. Nikolic-Audit [129], P. Nilsson [30], G. Ninio [156], A. Nisati [75a], R. Nisius [111], N. Nitika [174], E.K. Nkadimeng [34b], T. Nobe [158], D. Noll [148], T. Nommensen [152], M.B. Norfolk [144], B.J. Norman [35], L.C. Nosler [18a], M. Noury [36a], J. Novak [94], T. Novak [94], P. Novotny [174], R. Novotny [134], L. Nozka [124], K. Ntekas [37], D. Ntounis [148], N.M.J. Nunes De Moura Junior [82b], J. Ocariz [129], I. Ochoa [132a], A. Odella Rodriguez [13], S. Oerdek [48,y], J.T. Offermann [40], A. Ogrodnik [87], A. Oh [102], C.C. Ohm [149], H. Oide [83], M.L. Ojeda [37], Y. Okumura [158], L.F. Oleiro Seabra [132a], I. Oleksiyuk [56], G. Oliveira Correa [13], D. Oliveira Damazio [30], J.L. Oliver [1], R. Omar [68], A.P. O'Neill [20], A. Onofre [132a,132e,e], P.U.E. Onyisi [11], M.J. Oreglia [40], D. Orestano [77a,77b], R. Orlandini [77a,77b], R.S. Orr [160], L.M. Osojnak [42], Y. Osumi [112], G. Otero y Garzon [31], H. Otono [89], M. Ouchrif [36d], F. Ould-Saada [127], T. Ovsiannikova [141], M. Owen [59], R.E. Owen [136], V.E. Ozcan [22a], F. Ozturk [87], N. Ozturk [8], S. Ozturk [81], H.A. Pacey [128], K. Pachal [161a], A. Pacheco Pages [13], C. Padilla Aranda [13], G. Padovano [75a,75b], S. Pagan Griso [18a], L. Pagani [76a,76b], J. Pampel [25], J. Pan [177], D.K. Panchal [11], C.E. Pandini [60], J.G. Panduro Vazquez [136], H.D. Pandya [1], H. Pang [137], P. Pani [48], G. Panizzo [69a,69c], L. Panwar [129,w], L. Paolozzi [56], S. Parajuli [167], A. Paramonov [6], C. Paraskevopoulos [53], D. Paredes Hernandez [64b], S.R. Paredes Saenz [52], A. Pareti [73a,73b], K.R. Park [42], T.H. Park [111], F. Parodi [57b,57a], J.A. Parsons [42], U. Parzefall [54], B. Pascual Dias [41], L. Pascual Dominguez [100], E. Pasqualucci [75a], S. Passaggio [57b], F. Pastore [96], P. Patel [87], U.M. Patel [51], J.R. Pater [102], T. Pauly [37], F. Pauwels [135], C.I. Pazos [163], M. Pedersen [127], R. Pedro [132a], S.V. Peleganchuk [38], O. Penc [133], S. Peng [15], G.D. Penn [177], K.E. Penski [110], M. Penzin [38], B.S. Peralva [82d], A.P. Pereira Peixoto [141], L. Pereira Sanchez [148], D.V. Perepelitsa [30,al], G. Perera [104], E. Perez Codina [37], M. Perganti [10], H. Pernegger [37], S. Perrella [75a,75b], K. Peters [48], R.F.Y. Peters [102], B.A. Petersen [37], T.C. Petersen [43], E. Petit [103], V. Petousis [134], A.R. Petri [71a,71b], T. Petru [135], M. Pettee [18a], A. Petukhov [81], K. Petukhova [37], R. Pezoa [139g], L. Pezzotti [24b,24a], G. Pezzullo [177], L. Pfaffenbichler [37], A.J. Pfleger [79], T.M. Pham [175], T. Pham [106], P.W. Phillips [136], G. Piacquadio [150], E. Pianori [18a], F. Piazza [125], R. Piegaia [31], D. Pietreanu [28b], A.D. Pilkington [102], M. Pinamonti [69a,69c], J.L. Pinfold [2], G. Pinheiro Matos [42], B.C. Pinheiro Pereira [132a], J. Pinol Bel [13], A.E. Pinto Pinoargote [129], L. Pintucci [69a,69c], A. Pirttikoski [56], D.A. Pizzi [35], L. Pizzimento [64b], A. Plebani [33], M.-A. Pleier [30], V. Pleskot [135], E. Plotnikova [39], G. Poddar [95], R. Poettgen [99], L. Poggioli [129], S. Polacek [135], G. Polesello [73a], A. Poley [147], A. Polini [24b], C.S. Pollard [172], Z.B. Pollock [121], E. Pompa Pacchi [122], N.I. Pond [97], D. Ponomarenko [68], L. Pontecorvo [37], S. Popa [28a], G.A. Popeneciu [28d], A. Poreba [63a], D.M. Portillo Quintero [161a], S. Pospisil [134], M.A. Postill [144], P. Postolache [28c], K. Potamianos [172], P.A. Potepa [86a], I.N. Potrap [39], C.J. Potter [33], H. Potti [152], J. Poveda [168], M.E. Pozo Astigarraga [37], R. Pozzi [37], A. Prades Ibanez [76a,76b], S.R. Pradhan [144], J. Pretel [170], D. Price [102], M. Primavera [70a], L. Primomo [69a,69c], M.A. Principe Martin [100], R. Privara [124], T. Procter [86b], M.L. Proffitt [141], N. Proklova [130], K. Prokofiev [64c], G. Proto [111], J. Proudfoot [6], M. Przybycien [86a], W.W. Przygoda [86b], A. Psallidas [46], J.E. Puddefoot [144], D. Pudzha [53], P. Puhl [58], H.I. Purnell [1], D. Pyatiizbyantseva [115], J. Qian [107], R. Qian [108], D. Qichen [128], Y. Qin [13], T. Qiu [52], A. Quadt [55], M. Queitsch-Maitland [102], G. Quetant [56], R.P. Quinn [169], G. Rabanal Bolanos [61], D. Rafanoharana [111], F. Raffaeli [76a,76b], J.L. Rainbolt [40],

S. Rajagopalan[30], E. Ramakoti[39], L. Rambelli[57b,57a], I.A. Ramirez-Berend[35], K. Ran[107,113c], D.S. Rankin[130], N.P. Rapheeha[34j], H. Rasheed[28b], A. Rastogi[18a], S. Rave[101], S. Ravera[57b,57a], B. Ravina[37], I. Ravinovich[174], M. Raymond[37], A.L. Read[127], N.P. Readioff[144], D.M. Rebuzzi[73a,73b], A.S. Reed[59], K. Reeves[27], D. Reikher[37], A. Rej[49], C. Rembser[37], H. Ren[62], M. Renda[28b], F. Renner[48], A.G. Rennie[59], M. Repik[56], A.L. Rescia[57b,57a], S. Resconi[71a], M. Ressegotti[57b,57a], S. Rettie[116], W.F. Rettie[35], M.M. Revering[33], O.L. Rezanova[39], P. Reznicek[135], H. Riani[36d], N. Ribaric[51], B. Ricci[69a,69c], E. Ricci[78a,78b], R. Richter[111], S. Richter[47a,47b], E. Richter-Was[86b], M. Ridel[129], S. Ridouani[36d], P. Rieck[119], P. Riedler[37], E.M. Riefel[47a,47b], J.O. Rieger[116], M. Rimoldi[34c], L. Rinaldi[24b,24a], P. Rincke[166,55], G. Ripellino[166], I. Riu[13], J.C. Rivera Vergara[170], F. Rizatdinova[123], E. Rizvi[95], B.R. Roberts[40], S.S. Roberts[138], D. Robinson[33], A. Robson[59], A. Rocchi[76a,76b], C. Roda[74a,74b], F.A. Rodriguez[117], S. Rodriguez Bosca[37], Y. Rodriguez Garcia[23a], A.M. Rodríguez Vera[117], S. Roe[37], J.T. Roemer[37], O. Røhne[127], R.A. Rojas[37], C.P.A. Roland[129], A. Romaniouk[79], E. Romano[73a,73b], M. Romano[24b], N. Rompotis[93], L. Roos[129], S. Rosati[75a], B.J. Rosser[40], E. Rossi[128], E. Rossi[72a,72b], L.P. Rossi[61], L. Rossini[54], R. Rosten[121], M. Rotaru[28b], D. Rousseau[66], D. Rousso[48], S. Roy-Garand[160], A. Rozanov[103], Z.M.A. Rozario[59], Y. Rozen[155], A. Rubio Jimenez[168], V.H. Ruelas Rivera[19], T.A. Ruggeri[1], A. Ruggiero[128], A. Ruiz-Martinez[168], A. Rummler[37], G.B. Rupnik Boero[37], Z. Rurikova[54], N.A. Rusakovich[39], S. Ruscelli[49], H.L. Russell[170], G. Russo[138], J.P. Rutherfoord[7], S. Rutherford Colmenares[119], M. Rybar[135], P. Rybczynski[86a], A. Ryzhov[45], F. Safai Tehrani[75a], S. Saha[1], B. Sahoo[174], A. Saibel[168], B.T. Saifuddin[122], M. Saimpert[137], G.T. Saito[82c], M. Saito[158], T. Saito[158], A. Sala[71a,71b], A. Salnikov[148], J. Salt[168], A. Salvador Salas[156], F. Salvatore[151], A. Salzburger[37], D. Sammel[54], E. Sampson[92], D. Sampsonidis[157,d], D. Sampsonidou[125], M.A.A. Samy[59], J. Sánchez[168], V. Sanchez Sebastian[168], H. Sandaker[127], C.O. Sander[48], J.A. Sandesara[175], M. Sandhoff[176], C. Sandoval[23b], L. Sanfilippo[63a], D.P.C. Sankey[136], T. Sano[88], A. Sansoni[53], M. Santana Queiroz[18b], L. Santi[37], C. Santoni[41], H. Santos[132a,132b], L. Santos Pereira Trigo[48], E. Sanzani[24b,24a], K.A. Saoucha[84b], J.G. Saraiva[132a,132d], J. Sardain[7], O. Sasaki[83], K. Sato[162], C. Sauer[37], E. Sauvan[4], P. Savard[160,ai], R. Sawada[158], C. Sawyer[136], L. Sawyer[98], A.M. Sayed[27], C. Sbarra[24b], A. Sbrizzi[24b,24a], T. Scanlon[97], J. Schaarschmidt[141], U. Schäfer[101], A.C. Schaffer[66,45], D. Schaile[110], R.D. Schamberger[150], C. Scharf[19], M.M. Schefer[20], V.A. Schegelsky[38], D. Scheirich[135], M. Schernau[139f], C. Scheulen[56], C. Schiavi[57b,57a], M. Schioppa[44b,44a], S. Schlenker[37], J. Schmeing[176], E. Schmidt[111], M.A. Schmidt[176], K. Schmieden[25], C. Schmitt[101], N. Schmitt[101], S. Schmitt[48], N.A. Schneider[110], L. Schoeffel[137], A. Schoening[63b], P.G. Scholer[35], E. Schopf[146], M. Schott[25], S. Schramm[56], T. Schroer[56], H-C. Schultz-Coulon[63a], M. Schumacher[54], B.A. Schumm[138], Ph. Schune[137], H.R. Schwartz[7], A. Schwartzman[148], T.A. Schwarz[107], Ph. Schwemling[137], R. Schwienhorst[108], F.G. Sciacca[20], A. Sciandra[30], G. Sciolla[27], S.A. Scoville[131], F. Scuri[74a], C.D. Sebastiani[37], K. Sedlaczek[117], S.C. Seidel[114], B.D. Seidlitz[42], C. Seitz[48], J.M. Seixas[82b], G. Sekhniaidze[72a], L. Selem[129], N. Semprini-Cesari[24b,24a], A. Semushin[178], D. Sengupta[56], V. Senthilkumar[116], L. Serin[66], M. Sessa[72a,72b], H. Severini[122], F. Sforza[57b,57a], A. Sfyrla[56], Q. Sha[14], H. Shaddix[117], A.H. Shah[33], R. Shaheen[149], J.D. Shahinian[130], M. Shamim[37], L.Y. Shan[14], M. Shapiro[18a], A. Sharma[37], A.S. Sharma[169], P. Sharma[30], P.B. Shatalov[38], K. Shaw[151], S.M. Shaw[102], Q. Shen[14], D.J. Sheppard[147], P. Sherwood[97], L. Shi[97], X. Shi[14], S. Shimizu[83], I.P.J. Shipsey[128,*], S. Shirabe[89], M. Shiyakova[39,z], M.J. Shochet[40], D.R. Shope[127], B. Shrestha[122], S. Shrestha[121,an], I. Shreyber[39], M.J. Shroff[105], P. Sicho[133], A.M. Sickles[167], E. Sideras Haddad[34j,165], A.C. Sidley[116], A. Sidoti[24b], F. Siegert[50], Dj. Sijacki[16], F. Sili[62], J.M. Silva[52], I. Silva Ferreira[82b], M.V. Silva Oliveira[30], S.B. Silverstein[47a], S. Simion[66], R. Simoniello[37], E.L. Simpson[102], H. Simpson[151], L.R. Simpson[6], S. Simsek[81], S. Sindhu[55], S.N. Singh[27], S. Singh[30], S. Sinha[48], S. Sinha[102], M. Sioli[24b,24a], K. Sioulas[9], I. Siral[37], E. Sitnikova[48], J. Sjölin[47a,47b], A. Skaf[55], E. Skorda[21], P. Skubic[122], M. Slawinska[87], I. Slazyk[17], I. Sliusar[127], V. Smakhtin[174], B.H. Smart[136], S.Yu. Smirnov[139b], Y. Smirnov[34c], L.N. Smirnova[38,a], O. Smirnova[99], A.C. Smith[42], J.L. Smith[102], M.B. Smith[35], R. Smith[148], H. Smitmanns[101], M. Smizanska[92], K. Smolek[134], P. Smolyanskiy[134], A.A. Snesarev[39], H.L. Snoek[116], R.M. Snyder[51], S. Snyder[30], R. Sobie[170,ab], A. Soffer[156], C.A. Solans Sanchez[37], E.Yu. Soldatov[39], U. Soldevila[168], A.A. Solodkov[34j], S. Solomon[27], A. Soloshenko[39], K. Solovieva[54], O.V. Solovyanov[41], P. Sommer[50], A. Sonay[13], A. Sopczak[134], A.L. Sopio[52], F. Sopkova[29b], J.D. Sorenson[114], I.R. Sotarriva Alvarez[140], V. Sothilingam[63a], O.J. Soto Sandoval[139c,139b], S. Sottocornola[68], R. Soualah[84a], Z. Soumaimi[36e], D. South[48], N. Soybelman[174], S. Spagnolo[70a,70b], A.S. Spellman[125], D. Sperlich[54], B. Spisso[72a,72b], L. Splendori[103], M. Spousta[135], E.J. Staats[35], R. Stamen[63a], E. Stanecka[87], W. Stanek-Maslouska[48], M.V. Stange[50], B. Stanislaus[18a], M.M. Stanitzki[48], E.A. Starchenko[38], G.H. Stark[138], J. Stark[90], P. Staroba[133], P. Starovoitov[84b], R. Staszewski[87], C. Stauch[110], G. Stavropoulos[46], A. Stefl[37], A. Stein[101], P. Steinberg[30], B. Stelzer[147,161a], H.J. Stelzer[131], O. Stelzer[161a], H. Stenzel[58], T.J. Stevenson[151], G.A. Stewart[48], G. Stoicea[28b], M. Stolarski[132a], S. Stonjek[111], A. Straessner[50], J. Strandberg[149], S. Strandberg[47a,47b], M. Stratmann[176], M. Strauss[122], T. Strebler[103], P. Strizenec[29b], R. Ströhmer[171], D.M. Strom[125], R. Stroynowski[45], A. Strubig[47a,47b], S.A. Stucci[30], B. Stugu[17], J. Stupak[122], N.A. Styles[48], D. Su[148], S. Su[62], X. Su[62], D. Suchy[29a], A.D. Sudhakar Ponnu[55], L. Sudit[174], Y. Sue[83], K. Sugizaki[130], V.V. Sulin[38], D.M.S. Sultan[128], L. Sultanaliyeva[25], S. Sultansoy[3b], S. Sun[175], W. Sun[14], S. Sundar Raman[169], N. Sur[99], N. Suri Jr[177], M.R. Sutton[151], M. Svatos[133], P.N. Swallow[33], M. Swiatlowski[161a], A. Swoboda[37], I. Sykora[29a], M. Sykora[135], T. Sykora[135], D. Ta[101], K. Tackmann[48,y], A. Taffard[164], R. Tafirout[161a], Y. Takubo[83], M. Talby[103], A.A. Talyshev[38], N.M. Tamir[156], A. Tanaka[158], J. Tanaka[158], R. Tanaka[66], M. Tanasini[150], Z. Tao[169], S. Tapia Araya[139g], S. Tapprogge[101], A. Tarek Abouelfadl Mohamed[37], S. Tarem[155], K. Tariq[14], G. Tarna[37], G.F. Tartarelli[71a], M.J. Tartarin[90], P. Tas[135], M. Tasevsky[133], E. Tassi[44b,44a], A.C. Tate[167], Y. Tayalati[36e,aa], G.N. Taylor[106], W. Taylor[161b], R.J. Taylor Vara[168], A.S. Tegetmeier[90], P. Teixeira-Dias[96], J.J. Teoh[160], K. Terashi[158], J. Terron[100], S. Terzo[13], M. Testa[53], R.J. Teuscher[160,ab], A. Thaler[79], O. Theiner[56], T. Theveneaux-Pelzer[103], J.P. Thomas[21], E.A. Thompson[18a], P.D. Thompson[21], E. Thomson[130], R.E. Thornberry[45], C. Tian[62], Y. Tian[56], V. Tikhomirov[81], Yu.A. Tikhonov[39], S. Timoshenko[38], D. Timoshyn[135], E.X.L. Ting[1], P. Tipton[177], A. Tishelman-Charny[30], K. Todome[140], S. Todorova-Nova[135], L. Toffolin[69a,69c], M. Togawa[83], J. Tojo[89], S. Tokár[29a], O. Toldaiev[68], G. Tolkachev[103], M. Tomoto[83], L. Tompkins[148], E. Torrence[125], H. Torres[90], D.I. Torres Arza[139g], E. Torró Pastor[168], M. Toscani[31], C. Tosciri[40], M. Tost[11], D.R. Tovey[144], T. Trefzger[171], P.M. Tricarico[13], A. Tricoli[30], I.M. Trigger[161a], S. Trincaz-Duvoid[129], D.A. Trischuk[170], A. Tropina[39], D. Truncali[76a,76b], L. Truong[34c], M. Trzebinski[87], A. Trzupek[87], F. Tsai[150], M. Tsai[107], A. Tsiamis[157], P.V. Tsiareshka[39], S. Tsigaridas[161a], A. Tsirigotis[157,t], V. Tsiskaridze[154a], E.G. Tskhadadze[154a], Y. Tsujikawa[88], I.I. Tsukerman[38], V. Tsulaia[18a], K. Tsuri[120], D. Tsybychev[150], Y. Tu[64b], A. Tudorache[28b], V. Tudorache[28b], S.B. Tuncay[128], S. Turchikhin[57b,57a], I. Turk Cakir[3a],

R. Turra [71a], T. Turtuvshin [39,ac], P.M. Tuts [42], Y. Uematsu [83], F. Ukegawa [162], P.A. Ulloa Poblete [139c,139b], G. Unal [37], A. Undrus [30], J. Urban [29b], P. Urrejola [139e], G. Usai [8], R. Ushioda [159], M. Usman [109], F. Ustuner [52], Z. Uysal [81], V. Vacek [134], B. Vachon [105], T. Vafeiadis [37], A. Vaitkus [97], C. Valderanis [110], E. Valdes Santurio [47a,47b], M. Valente [37], S. Valentinetti [24b,24a], A. Valero [168], E. Valiente Moreno [168], A. Vallier [90], J.A. Valls Ferrer [168], D.R. Van Arneman [116], R. Van Den Broucke [129], A. Van Der Graaf [49], H.Z. Van Der Schyf [34j], P. Van Gemmeren [6], M. Van Rijnbach [37], S. Van Stroud [97], I. Van Vulpen [116], P. Vana [135], M. Vanadia [76a,76b], U.M. Vande Voorde [149], W. Vandelli [37], E.R. Vandewall [148], D. Vannicola [156], L. Vannoli [53], R. Vari [75a], M. Varma [177], E.W. Varnes [7], C. Varni [79], D. Varouchas [66], L. Varriale [168], K.E. Varvell [152], M.E. Vasile [28b], L. Vaslin[83], M.D. Vassilev [148], A. Vasyukov [39], L.M. Vaughan [123], R. Vavricka[135], T. Vazquez Schroeder [13], J. Veatch [32], V. Vecchio [102], M.J. Veen [104], I. Veliscek [30], I. Velkovska [94], L.M. Veloce [160], F. Veloso [132a,132c], A.G. Veltman [52], S. Veneziano [75a], A. Ventura [70a,70b], A. Verbytskyi [111], M. Verducci [74a,74b], C. Vergis [95], M. Verissimo De Araujo [82b], W. Verkerke [116], J.C. Vermeulen [116], C. Vernieri [148], M. Vessella [164], M.C. Vetterli [147,ai], A. Vgenopoulos [101], N. Viaux Maira [139g,af], T. Vickey [144], O.E. Vickey Boeriu [144], G.H.A. Viehhauser [128], L. Vigani [63b], M. Vigl [111], M. Villa [24b,24a], M. Villaplana Perez [168], E.M. Villhauer[40], E. Vilucchi [53], M. Vincent [168], M.G. Vincter [35], A. Visibile [116], A. Visive [116], C. Vittori [37], I. Vivarelli [24b,24a], M.I. Vivas Albornoz [48], E. Voevodina [111], F. Vogel [110], J.C. Voigt [50], P. Vokac [134], Yu. Volkotrub [86b], L. Vomberg [25], E. Von Toerne [25], B. Vormwald [37], K. Vorobev [51], M. Vos [168], K. Voss [146], M. Vozak [37], L. Vozdecky [122], N. Vranjes [16], M. Vranjes Milosavljevic [16], M. Vreeswijk [116], N.K. Vu [143b,143a], R. Vuillermet [37], O. Vujinovic [101], I. Vukotic [40], I.K. Vyas [35], J.F. Wack [33], A. Wada [112], S. Wada [162], C. Wagner[148], J.M. Wagner [18a], W. Wagner [176], S. Wahdan [176], H. Wahlberg [91], C.H. Waits [122], J. Walder [136], R. Walker [110], K. Walkingshaw Pass [59], W. Walkowiak [146], A. Wall [130], E.J. Wallin [99], T. Wamorkar [148], K. Wandall-Christensen [168], A. Wang [62], A.Z. Wang [138], C. Wang [48], C. Wang [11], H. Wang [18a], J. Wang [64c], P. Wang [102], P. Wang [97], R. Wang [61], R. Wang [107], R. Wang [6], S.M. Wang [153], S. Wang [14], T. Wang [115], T. Wang [62], W.T. Wang [128], X. Wang [167], X. Wang [143a], X. Wang [48], Y. Wang [150], Y. Wang [114], Z. Wang [107], Z. Wang [143b], Z. Wang [107], C. Wanotayaroj [83], A. Warburton [105], A.L. Warnerbring [146], S. Waterhouse [96], A.T. Watson [21], H. Watson [52], M.F. Watson [21], E. Watton [37], G. Watts [141], B.M. Waugh [97], J.M. Webb [54], C. Weber [30], M.S. Weber [20], C. Wei [62], Y. Wei [54], A.R. Weidberg [128], E.J. Weik [119], J. Weingarten [49], C. Weiser [54], C.J. Wells [48], T. Wenaus [30], T. Wengler [37], N.S. Wenke[111], N. Wermes [25], M. Wessels [63a], A.M. Wharton [92], A.S. White [37], A. White [8], M.J. White [1], D. Whiteson [164], L. Wickremasinghe [126], W. Wiedenmann [175], M. Wielers [136], R. Wierda [149], C. Wiglesworth [43], H.G. Wilkens [37], J.J.H. Wilkinson [33], S. Williams [33], S. Willocq [104], D.J. Wilson [102], P.J. Windischhofer [40], F.I. Winkel [31], F. Winklmeier [125], B.T. Winter [54], M. Wittgen[148], M. Wobisch [98], T. Wojtkowski[60], Z. Wolffs [116], J. Wollrath[37], M.W. Wolter [87], H. Wolters [132a,132c], M.C. Wong[138], E.L. Woodward [42], S.D. Worm [48], B.K. Wosiek [87], K.W. Woźniak [87], S. Wozniewski [55], K. Wraight [59], C. Wu [160], C. Wu [21], J. Wu [158], M. Wu [113b], M. Wu [115], S.L. Wu [175], S. Wu [14], X. Wu [62], Y.Q. Wu [160], Y. Wu [62], Z. Wu [4], Z. Wu [113a], J. Wuerzinger [111], T.R. Wyatt [102], B.M. Wynne [52], S. Xella [43], L. Xia [113a], M. Xie [62], A. Xiong [125], D. Xu [14], H. Xu [62], L. Xu [62], R. Xu [130], T. Xu [107], W. Xu[113a], Y. Xu [141], Z. Xu [52], R. Xue [131], B. Yabsley [152], S. Yacoob [11], Y. Yamaguchi [83], E. Yamashita [158], H. Yamauchi [162], T. Yamazaki [18a], Y. Yamazaki [85], S. Yan [59], Z. Yan [104], H.J. Yang [143a], H.T. Yang [62], S. Yang [62], X. Yang [37], X. Yang [14], Y. Yang [158], Y. Yang[62], W-M. Yao [18a], C.L. Yardley [151], J. Ye [14], S. Ye [30], X. Ye [62], Y. Yeh [97], I. Yeletskikh [39], B. Yeo [18b], M.R. Yexley [97], T.P. Yildirim [128], K. Yorita [173], C.J.S. Young [37], C. Young [148], I.N.L. Young [59], N.D. Young[125], Y. Yu [62], J. Yuan [14,113c], M. Yuan [107], R. Yuan [143b], L. Yue [97], M. Zaazoua [62], B. Zabinski [87], I. Zahir [36a], A. Zaio[57b,57a], Z.K. Zak [87], T. Zakareishvili [168], S. Zambito [56], J.A. Zamora Saa [139d], J. Zang [158], R. Zanzottera [71a,71b], O. Zaplatilek [134], C. Zeitnitz [176], H. Zeng [14], D.T. Zenger Jr [27], O. Zenin [38], T. Ženiš [29a], S. Zenz [95], D. Zerwas [66], B. Zhang [172], D.F. Zhang [144], G. Zhang [14,ak], J. Zhang [142a], J. Zhang [6], L. Zhang [62], L. Zhang [113a], P. Zhang [14,113c], R. Zhang [113a], S. Zhang [90], Y. Zhang [141], Y. Zhang [97], Y. Zhang [62], Y. Zhang [113a], Z. Zhang [18a], Z. Zhang [142a], Z. Zhang [66], H. Zhao [141], T. Zhao [142a], Y. Zhao [35], Z. Zhao [62], Z. Zhao [62], A. Zhemchugov [39], J. Zheng [113a], K. Zheng [167], L. Zheng [142a], X. Zheng [62], Z. Zheng [148], D. Zhong [167], B. Zhou [107], B. Zhou [143b,143a], H. Zhou [7], N. Zhou [143a], Y. Zhou [15], Y. Zhou [113a], Y. Zhou[7], J. Zhu [107], X. Zhu[143b], Y. Zhu [143a], X. Zhuang [14], K. Zhukov [68], N.I. Zimine [39], J. Zinsser [63b], M. Ziolkowski [146], L. Živković [16], A. Zoccoli [24b,24a], K. Zoch [61], A. Zografos [37], T.G. Zorbas [144], O. Zormpa [46], L. Zwalinski [37].

[1]Department of Physics, University of Adelaide, Adelaide; Australia.
[2]Department of Physics, University of Alberta, Edmonton AB; Canada.
[3](a)Department of Physics, Ankara University, Ankara;(b)Division of Physics, TOBB University of Economics and Technology, Ankara; Türkiye.
[4]LAPP, Université Savoie Mont Blanc, CNRS/IN2P3, Annecy; France.
[5]APC, Université Paris Cité, CNRS/IN2P3, Paris; France.
[6]High Energy Physics Division, Argonne National Laboratory, Argonne IL; United States of America.
[7]Department of Physics, University of Arizona, Tucson AZ; United States of America.
[8]Department of Physics, University of Texas at Arlington, Arlington TX; United States of America.
[9]Physics Department, National and Kapodistrian University of Athens, Athens; Greece.
[10]Physics Department, National Technical University of Athens, Zografou; Greece.
[11]Department of Physics, University of Texas at Austin, Austin TX; United States of America.
[12]Institute of Physics, Azerbaijan Academy of Sciences, Baku; Azerbaijan.
[13]Institut de Física d'Altes Energies (IFAE), Barcelona Institute of Science and Technology, Barcelona; Spain.
[14]Institute of High Energy Physics, Chinese Academy of Sciences, Beijing; China.
[15]Physics Department, Tsinghua University, Beijing; China.
[16]Institute of Physics, University of Belgrade, Belgrade; Serbia.
[17]Department for Physics and Technology, University of Bergen, Bergen; Norway.
[18](a)Physics Division, Lawrence Berkeley National Laboratory, Berkeley CA;(b)University of California, Berkeley CA; United States of America.
[19]Institut für Physik, Humboldt Universität zu Berlin, Berlin; Germany.
[20]Albert Einstein Center for Fundamental Physics and Laboratory for High Energy Physics, University of Bern, Bern; Switzerland.
[21]School of Physics and Astronomy, University of Birmingham, Birmingham; United Kingdom.
[22](a)Department of Physics, Bogazici University, Istanbul;(b)Department of Physics Engineering, Gaziantep University, Gaziantep;(c)Department of Physics, Istanbul University, Istanbul; Türkiye.
[23](a)Facultad de Ciencias y Centro de Investigaciónes, Universidad Antonio Nariño, Bogotá;(b)Departamento de Física, Universidad Nacional de Colombia, Bogotá; Colombia.
[24](a)Dipartimento di Fisica e Astronomia A. Righi, Università di Bologna, Bologna;(b)INFN Sezione di Bologna; Italy.
[25]Physikalisches Institut, Universität Bonn, Bonn; Germany.

[26]Department of Physics, Boston University, Boston MA; United States of America.
[27]Department of Physics, Brandeis University, Waltham MA; United States of America.
[28][(a)]Transilvania University of Brasov, Brasov;[(b)]Horia Hulubei National Institute of Physics and Nuclear Engineering, Bucharest;[(c)]Department of Physics, Alexandru Ioan Cuza University of Iasi, Iasi;[(d)]National Institute for Research and Development of Isotopic and Molecular Technologies, Physics Department, Cluj-Napoca;[(e)]National University of Science and Technology Politechnica, Bucharest;[(f)]West University in Timisoara, Timisoara;[(g)]Faculty of Physics, University of Bucharest, Bucharest; Romania.
[29][(a)]Faculty of Mathematics, Physics and Informatics, Comenius University, Bratislava;[(b)]Department of Subnuclear Physics, Institute of Experimental Physics of the Slovak Academy of Sciences, Kosice; Slovak Republic.
[30]Physics Department, Brookhaven National Laboratory, Upton NY; United States of America.
[31]Universidad de Buenos Aires, Facultad de Ciencias Exactas y Naturales, Departamento de Física, y CONICET, Instituto de Física de Buenos Aires (IFIBA), Buenos Aires; Argentina.
[32]California State University, CA; United States of America.
[33]Cavendish Laboratory, University of Cambridge, Cambridge; United Kingdom.
[34][(a)]Department of Physics, University of Cape Town, Cape Town;[(b)]iThemba Labs, Western Cape;[(c)]Department of Mechanical Engineering Science, University of Johannesburg, Johannesburg;[(d)]National Institute of Physics, University of the Philippines Diliman (Philippines);[(e)]Department of Physics, Stellenbosch University, Matieland;[(f)]University of KwaZulu-Natal, School of Agriculture and Science, Mathematics, Westville;[(g)]University of South Africa, Department of Physics, Pretoria;[(h)]University of Pretoria, Department of Mechanical and Aeronautical Engineering, Pretoria;[(i)]University of Zululand, KwaDlangezwa;[(j)]School of Physics, University of the Witwatersrand, Johannesburg; South Africa.
[35]Department of Physics, Carleton University, Ottawa ON; Canada.
[36][(a)]Faculté des Sciences Ain Chock, Université Hassan II de Casablanca;[(b)]Faculté des Sciences, Université Ibn-Tofail, Kénitra;[(c)]Faculté des Sciences Semlalia, Université Cadi Ayyad, LPHEA-Marrakech;[(d)]LPMR, Faculté des Sciences, Université Mohamed Premier, Oujda;[(e)]Faculté des sciences, Université Mohammed V, Rabat;[(f)]Institute of Applied Physics, Mohammed VI Polytechnic University, Ben Guerir; Morocco.
[37]CERN, Geneva; Switzerland.
[38]Affiliated with an institute formerly covered by a cooperation agreement with CERN.
[39]Affiliated with an international laboratory covered by a cooperation agreement with CERN.
[40]Enrico Fermi Institute, University of Chicago, Chicago IL; United States of America.
[41]LPC, Université Clermont Auvergne, CNRS/IN2P3, Clermont-Ferrand; France.
[42]Nevis Laboratory, Columbia University, Irvington NY; United States of America.
[43]Niels Bohr Institute, University of Copenhagen, Copenhagen; Denmark.
[44][(a)]Dipartimento di Fisica, Università della Calabria, Rende;[(b)]INFN Gruppo Collegato di Cosenza, Laboratori Nazionali di Frascati; Italy.
[45]Physics Department, Southern Methodist University, Dallas TX; United States of America.
[46]National Centre for Scientific Research "Demokritos", Agia Paraskevi; Greece.
[47][(a)]Department of Physics, Stockholm University;[(b)]Oskar Klein Centre, Stockholm; Sweden.
[48]Deutsches Elektronen-Synchrotron DESY, Hamburg and Zeuthen; Germany.
[49]Fakultät Physik, Technische Universität Dortmund, Dortmund; Germany.
[50]Institut für Kern- und Teilchenphysik, Technische Universität Dresden, Dresden; Germany.
[51]Department of Physics, Duke University, Durham NC; United States of America.
[52]SUPA - School of Physics and Astronomy, University of Edinburgh, Edinburgh; United Kingdom.
[53]INFN e Laboratori Nazionali di Frascati, Frascati; Italy.

[54]Physikalisches Institut, Albert-Ludwigs-Universität Freiburg, Freiburg; Germany.
[55]II. Physikalisches Institut, Georg-August-Universität Göttingen, Göttingen; Germany.
[56]Département de Physique Nucléaire et Corpusculaire, Université de Genève, Genève; Switzerland.
[57(a)]Dipartimento di Fisica, Università di Genova, Genova;[(b)]INFN Sezione di Genova; Italy.
[58]II. Physikalisches Institut, Justus-Liebig-Universität Giessen, Giessen; Germany.
[59]SUPA - School of Physics and Astronomy, University of Glasgow, Glasgow; United Kingdom.
[60]LPSC, Université Grenoble Alpes, CNRS/IN2P3, Grenoble INP, Grenoble; France.
[61]Laboratory for Particle Physics and Cosmology, Harvard University, Cambridge MA; United States of America.
[62]Department of Modern Physics and State Key Laboratory of Particle Detection and Electronics, University of Science and Technology of China, Hefei; China.
[63(a)]Kirchhoff-Institut für Physik, Ruprecht-Karls-Universität Heidelberg, Heidelberg;[(b)]Physikalisches Institut, Ruprecht-Karls-Universität Heidelberg, Heidelberg; Germany.
[64(a)]Department of Physics, Chinese University of Hong Kong, Shatin, N.T., Hong Kong;[(b)]Department of Physics, University of Hong Kong, Hong Kong;[(c)]Department of Physics and Institute for Advanced Study, Hong Kong University of Science and Technology, Clear Water Bay, Kowloon, Hong Kong; China.
[65]Department of Physics, National Tsing Hua University, Hsinchu; Taiwan.
[66]IJCLab, Université Paris-Saclay, CNRS/IN2P3, 91405, Orsay; France.
[67]Centro Nacional de Microelectrónica (IMB-CNM-CSIC), Barcelona; Spain.
[68]Department of Physics, Indiana University, Bloomington IN; United States of America.
[69(a)]INFN Gruppo Collegato di Udine, Sezione di Trieste, Udine;[(b)]ICTP, Trieste;[(c)]Dipartimento Politecnico di Ingegneria e Architettura, Università di Udine, Udine; Italy.
[70(a)]INFN Sezione di Lecce;[(b)]Dipartimento di Matematica e Fisica, Università del Salento, Lecce; Italy.
[71(a)]INFN Sezione di Milano;[(b)]Dipartimento di Fisica, Università di Milano, Milano; Italy.
[72(a)]INFN Sezione di Napoli;[(b)]Dipartimento di Fisica, Università di Napoli, Napoli; Italy.
[73(a)]INFN Sezione di Pavia;[(b)]Dipartimento di Fisica, Università di Pavia, Pavia; Italy.
[74(a)]INFN Sezione di Pisa;[(b)]Dipartimento di Fisica E. Fermi, Università di Pisa, Pisa; Italy.
[75(a)]INFN Sezione di Roma;[(b)]Dipartimento di Fisica, Sapienza Università di Roma, Roma; Italy.
[76(a)]INFN Sezione di Roma Tor Vergata;[(b)]Dipartimento di Fisica, Università di Roma Tor Vergata, Roma; Italy.
[77(a)]INFN Sezione di Roma Tre;[(b)]Dipartimento di Matematica e Fisica, Università Roma Tre, Roma; Italy.
[78(a)]INFN-TIFPA;[(b)]Università degli Studi di Trento, Trento; Italy.
[79]Universität Innsbruck, Department of Astro and Particle Physics, Innsbruck; Austria.
[80]Department of Physics and Astronomy, Iowa State University, Ames IA; United States of America.
[81]Istinye University, Sariyer, Istanbul; Türkiye.
[82(a)]Departamento de Engenharia Elétrica, Universidade Federal de Juiz de Fora (UFJF), Juiz de Fora;[(b)]Universidade Federal do Rio De Janeiro COPPE/EE/IF, Rio de Janeiro;[(c)]Instituto de Física, Universidade de São Paulo, São Paulo;[(d)]Rio de Janeiro State University, Rio de Janeiro;[(e)]Federal University of Bahia, Bahia; Brazil.
[83]KEK, High Energy Accelerator Research Organization, Tsukuba; Japan.
[84(a)]Khalifa University of Science and Technology, Abu Dhabi;[(b)]University of Sharjah, Sharjah; United Arab Emirates.
[85]Graduate School of Science, Kobe University, Kobe; Japan.
[86(a)]AGH University of Krakow, Faculty of Physics and Applied Computer Science, Krakow;[(b)]Marian Smoluchowski Institute of Physics, Jagiellonian University, Krakow; Poland.
[87]Institute of Nuclear Physics Polish Academy of Sciences, Krakow; Poland.

[88]Faculty of Science, Kyoto University, Kyoto; Japan.
[89]Research Center for Advanced Particle Physics and Department of Physics, Kyushu University, Fukuoka ; Japan.
[90]L2IT, Université de Toulouse, CNRS/IN2P3, UPS, Toulouse; France.
[91]Instituto de Física La Plata, Universidad Nacional de La Plata and CONICET, La Plata; Argentina.
[92]Physics Department, Lancaster University, Lancaster; United Kingdom.
[93]Oliver Lodge Laboratory, University of Liverpool, Liverpool; United Kingdom.
[94]Department of Experimental Particle Physics, Jožef Stefan Institute and Department of Physics, University of Ljubljana, Ljubljana; Slovenia.
[95]Department of Physics and Astronomy, Queen Mary University of London, London; United Kingdom.
[96]Department of Physics, Royal Holloway University of London, Egham; United Kingdom.
[97]Department of Physics and Astronomy, University College London, London; United Kingdom.
[98]Louisiana Tech University, Ruston LA; United States of America.
[99]Fysiska institutionen, Lunds universitet, Lund; Sweden.
[100]Departamento de Física Teorica C-15 and CIAFF, Universidad Autónoma de Madrid, Madrid; Spain.
[101]Institut für Physik, Universität Mainz, Mainz; Germany.
[102]School of Physics and Astronomy, University of Manchester, Manchester; United Kingdom.
[103]CPPM, Aix-Marseille Université, CNRS/IN2P3, Marseille; France.
[104]Department of Physics, University of Massachusetts, Amherst MA; United States of America.
[105]Department of Physics, McGill University, Montreal QC; Canada.
[106]School of Physics, University of Melbourne, Victoria; Australia.
[107]Department of Physics, University of Michigan, Ann Arbor MI; United States of America.
[108]Department of Physics and Astronomy, Michigan State University, East Lansing MI; United States of America.
[109]Group of Particle Physics, University of Montreal, Montreal QC; Canada.
[110]Fakultät für Physik, Ludwig-Maximilians-Universität München, München; Germany.
[111]Max-Planck-Institut für Physik (Werner-Heisenberg-Institut), München; Germany.
[112]Graduate School of Science and Kobayashi-Maskawa Institute, Nagoya University, Nagoya; Japan.
[113(a)]Department of Physics, Nanjing University, Nanjing;[(b)]School of Science, Shenzhen Campus of Sun Yat-sen University;[(c)]University of Chinese Academy of Science (UCAS), Beijing; China.
[114]Department of Physics and Astronomy, University of New Mexico, Albuquerque NM; United States of America.
[115]Institute for Mathematics, Astrophysics and Particle Physics, Radboud University/Nikhef, Nijmegen; Netherlands.
[116]Nikhef National Institute for Subatomic Physics and University of Amsterdam, Amsterdam; Netherlands.
[117]Department of Physics, Northern Illinois University, DeKalb IL; United States of America.
[118(a)]New York University Abu Dhabi, Abu Dhabi;[(b)]United Arab Emirates University, Al Ain; United Arab Emirates.
[119]Department of Physics, New York University, New York NY; United States of America.
[120]Ochanomizu University, Otsuka, Bunkyo-ku, Tokyo; Japan.
[121]Ohio State University, Columbus OH; United States of America.
[122]Homer L. Dodge Department of Physics and Astronomy, University of Oklahoma, Norman OK; United States of America.
[123]Department of Physics, Oklahoma State University, Stillwater OK; United States of America.
[124]Palacký University, Joint Laboratory of Optics, Olomouc; Czech Republic.
[125]Institute for Fundamental Science, University of Oregon, Eugene, OR; United States of America.

[126]Graduate School of Science, University of Osaka, Osaka; Japan.
[127]Department of Physics, University of Oslo, Oslo; Norway.
[128]Department of Physics, Oxford University, Oxford; United Kingdom.
[129]LPNHE, Sorbonne Université, Université Paris Cité, CNRS/IN2P3, Paris; France.
[130]Department of Physics, University of Pennsylvania, Philadelphia PA; United States of America.
[131]Department of Physics and Astronomy, University of Pittsburgh, Pittsburgh PA; United States of America.
[132][(a)]Laboratório de Instrumentação e Física Experimental de Partículas - LIP, Lisboa;[(b)]Departamento de Física, Faculdade de Ciências, Universidade de Lisboa, Lisboa;[(c)]Departamento de Física, Universidade de Coimbra, Coimbra;[(d)]Centro de Física Nuclear da Universidade de Lisboa, Lisboa;[(e)]Departamento de Física, Escola de Ciências, Universidade do Minho, Braga;[(f)]Departamento de Física Teórica y del Cosmos, Universidad de Granada, Granada (Spain);[(g)]Departamento de Física, Instituto Superior Técnico, Universidade de Lisboa, Lisboa; Portugal.
[133]Institute of Physics of the Czech Academy of Sciences, Prague; Czech Republic.
[134]Czech Technical University in Prague, Prague; Czech Republic.
[135]Charles University, Faculty of Mathematics and Physics, Prague; Czech Republic.
[136]Particle Physics Department, Rutherford Appleton Laboratory, Didcot; United Kingdom.
[137]IRFU, CEA, Université Paris-Saclay, Gif-sur-Yvette; France.
[138]Santa Cruz Institute for Particle Physics, University of California Santa Cruz, Santa Cruz CA; United States of America.
[139][(a)]Departamento de Física, Pontificia Universidad Católica de Chile, Santiago;[(b)]Millennium Institute for Subatomic physics at high energy frontier (SAPHIR), Santiago;[(c)]Instituto de Investigación Multidisciplinario en Ciencia y Tecnología, y Departamento de Física, Universidad de La Serena;[(d)]Universidad Andres Bello, Department of Physics, Santiago;[(e)]Universidad San Sebastian, Recoleta;[(f)]Instituto de Alta Investigación, Universidad de Tarapacá, Arica;[(g)]Departamento de Física, Universidad Técnica Federico Santa María, Valparaíso; Chile.
[140]Department of Physics, Institute of Science, Tokyo; Japan.
[141]Department of Physics, University of Washington, Seattle WA; United States of America.
[142][(a)]Institute of Frontier and Interdisciplinary Science and Key Laboratory of Particle Physics and Particle Irradiation (MOE), Shandong University, Qingdao;[(b)]School of Physics, Zhengzhou University; China.
[143][(a)]State Key Laboratory of Dark Matter Physics, School of Physics and Astronomy, Shanghai Jiao Tong University, Key Laboratory for Particle Astrophysics and Cosmology (MOE), SKLPPC, Shanghai;[(b)]State Key Laboratory of Dark Matter Physics, Tsung-Dao Lee Institute, Shanghai Jiao Tong University, Shanghai; China.
[144]Department of Physics and Astronomy, University of Sheffield, Sheffield; United Kingdom.
[145]Department of Physics, Shinshu University, Nagano; Japan.
[146]Department Physik, Universität Siegen, Siegen; Germany.
[147]Department of Physics, Simon Fraser University, Burnaby BC; Canada.
[148]SLAC National Accelerator Laboratory, Stanford CA; United States of America.
[149]Department of Physics, Royal Institute of Technology, Stockholm; Sweden.
[150]Departments of Physics and Astronomy, Stony Brook University, Stony Brook NY; United States of America.
[151]Department of Physics and Astronomy, University of Sussex, Brighton; United Kingdom.
[152]School of Physics, University of Sydney, Sydney; Australia.
[153]Institute of Physics, Academia Sinica, Taipei; Taiwan.
[154][(a)]E. Andronikashvili Institute of Physics, Iv. Javakhishvili Tbilisi State University, Tbilisi;[(b)]High Energy Physics Institute, Tbilisi State University, Tbilisi;[(c)]University of Georgia, Tbilisi; Georgia.

[155]Department of Physics, Technion, Israel Institute of Technology, Haifa; Israel.
[156]Raymond and Beverly Sackler School of Physics and Astronomy, Tel Aviv University, Tel Aviv; Israel.
[157]Department of Physics, Aristotle University of Thessaloniki, Thessaloniki; Greece.
[158]International Center for Elementary Particle Physics and Department of Physics, University of Tokyo, Tokyo; Japan.
[159]Graduate School of Science and Technology, Tokyo Metropolitan University, Tokyo; Japan.
[160]Department of Physics, University of Toronto, Toronto ON; Canada.
[161] [(a)]TRIUMF, Vancouver BC; [(b)]Department of Physics and Astronomy, York University, Toronto ON; Canada.
[162]Division of Physics and Tomonaga Center for the History of the Universe, Faculty of Pure and Applied Sciences, University of Tsukuba, Tsukuba; Japan.
[163]Department of Physics and Astronomy, Tufts University, Medford MA; United States of America.
[164]Department of Physics and Astronomy, University of California Irvine, Irvine CA; United States of America.
[165]University of West Attica, Athens; Greece.
[166]Department of Physics and Astronomy, University of Uppsala, Uppsala; Sweden.
[167]Department of Physics, University of Illinois, Urbana IL; United States of America.
[168]Instituto de Física Corpuscular (IFIC), Centro Mixto Universidad de Valencia - CSIC, Valencia; Spain.
[169]Department of Physics, University of British Columbia, Vancouver BC; Canada.
[170]Department of Physics and Astronomy, University of Victoria, Victoria BC; Canada.
[171]Fakultät für Physik und Astronomie, Julius-Maximilians-Universität Würzburg, Würzburg; Germany.
[172]Department of Physics, University of Warwick, Coventry; United Kingdom.
[173]Waseda University, Tokyo; Japan.
[174]Department of Particle Physics and Astrophysics, Weizmann Institute of Science, Rehovot; Israel.
[175]Department of Physics, University of Wisconsin, Madison WI; United States of America.
[176]Fakultät für Mathematik und Naturwissenschaften, Fachgruppe Physik, Bergische Universität Wuppertal, Wuppertal; Germany.
[177]Department of Physics, Yale University, New Haven CT; United States of America.
[178]Yerevan Physics Institute, Yerevan; Armenia.
[a] Also at Affiliated with an institute formerly covered by a cooperation agreement with CERN.
[b] Also at An-Najah National University, Nablus; Palestine.
[c] Also at Borough of Manhattan Community College, City University of New York, New York NY; United States of America.
[d] Also at Center for Interdisciplinary Research and Innovation (CIRI-AUTH), Thessaloniki; Greece.
[e] Also at Centre of Physics of the Universities of Minho and Porto (CF-UM-UP); Portugal.
[f] Also at CERN, Geneva; Switzerland.
[g] Also at Département de Physique Nucléaire et Corpusculaire, Université de Genève, Genève; Switzerland.
[h] Also at Departament de Fisica de la Universitat Autonoma de Barcelona, Barcelona; Spain.
[i] Also at Department of Financial and Management Engineering, University of the Aegean, Chios; Greece.
[j] Also at Department of Modern Physics and State Key Laboratory of Particle Detection and Electronics, University of Science and Technology of China, Hefei; China.
[k] Also at Department of Physics, Ben Gurion University of the Negev, Beer Sheva; Israel.
[l] Also at Department of Physics, Bolu Abant Izzet Baysal University, Bolu; Türkiye.
[m] Also at Department of Physics, King's College London, London; United Kingdom.
[n] Also at Department of Physics, Stellenbosch University; South Africa.
[o] Also at Department of Physics, University of Fribourg, Fribourg; Switzerland.

[p] Also at Department of Physics, University of Thessaly; Greece.
[q] Also at Department of Physics, Westmont College, Santa Barbara; United States of America.
[r] Also at Faculty of Physics, Sofia University, 'St. Kliment Ohridski', Sofia; Bulgaria.
[s] Also at Faculty of Physics, University of Bucharest; Romania.
[t] Also at Hellenic Open University, Patras; Greece.
[u] Also at Henan University; China.
[v] Also at Imam Mohammad Ibn Saud Islamic University; Saudi Arabia.
[w] Also at Indian Institute of Technology (IIT), Jodhpur; India.
[x] Also at Institucio Catalana de Recerca i Estudis Avancats, ICREA, Barcelona; Spain.
[y] Also at Institut für Experimentalphysik, Universität Hamburg, Hamburg; Germany.
[z] Also at Institute for Nuclear Research and Nuclear Energy (INRNE) of the Bulgarian Academy of Sciences, Sofia; Bulgaria.
[aa] Also at Institute of Applied Physics, Mohammed VI Polytechnic University, Ben Guerir; Morocco.
[ab] Also at Institute of Particle Physics (IPP); Canada.
[ac] Also at Institute of Physics and Technology, Mongolian Academy of Sciences, Ulaanbaatar; Mongolia.
[ad] Also at Institute of Physics, Azerbaijan Academy of Sciences, Baku; Azerbaijan.
[ae] Also at Institute of Theoretical Physics, Ilia State University, Tbilisi; Georgia.
[af] Also at Millennium Institute for Subatomic physics at high energy frontier (SAPHIR), Santiago; Chile.
[ag] Also at National Institute of Physics, University of the Philippines Diliman (Philippines); Philippines.
[ah] Also at The Collaborative Innovation Center of Quantum Matter (CICQM), Beijing; China.
[ai] Also at TRIUMF, Vancouver BC; Canada.
[aj] Also at Università di Napoli Parthenope, Napoli; Italy.
[ak] Also at University of Chinese Academy of Sciences (UCAS), Beijing; China.
[al] Also at University of Colorado Boulder, Department of Physics, Colorado; United States of America.
[am] Also at University of Siena; Italy.
[an] Also at Washington College, Chestertown, MD; United States of America.
[ao] Also at Yeditepe University, Physics Department, Istanbul; Türkiye.
[*] Deceased